

# Heterogeneous Photochemistry in the Atmosphere

Christian George,<sup>\*,†,‡</sup> Markus Ammann,<sup>§</sup> Barbara D'Anna,<sup>†,‡</sup> D. J. Donaldson,<sup>||</sup>  
and Sergey A. Nizkorodov<sup>⊥</sup>

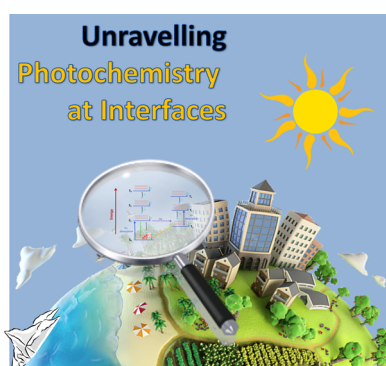
<sup>†</sup>Université de Lyon 1, Lyon F-69626, France

<sup>‡</sup>CNRS, UMR5256, IRCELYON, Institut de Recherches sur la Catalyse et l'Environnement de Lyon, Villeurbanne F-69626, France

<sup>§</sup>Laboratory of Radiochemistry and Environmental Chemistry, Paul Scherrer Institut, 5232 Villigen, Switzerland

<sup>||</sup>Department of Chemistry and Department of Physical & Environmental Sciences, University of Toronto, Toronto, Ontario M5S 3H6, Canada

<sup>⊥</sup>Department of Chemistry, University of California, Irvine, California 92697, United States



## CONTENTS

1. Background	4219	2.2.1. Pyruvic Acid	4228
1.1. Why Condensed Matter Matters: Types and Significance of Condensed Matter and Surfaces Encountered in the Atmospheric Environment	4219	2.2.2. Dicarbonyl Chemistry and Imidazole Production	4229
1.2. Principles of Atmospheric Photochemistry	4221	2.3. Humic-Like Substances (HULIS) of Primary and Secondary Origins	4229
1.2.1. Classification of Different Types of Photochemical Processes	4221	3. Mineral Dust	4230
1.2.2. Free Radicals and UV Radiation as the Primary Drivers of Chemistry in the Atmosphere	4221	3.1. Nitrogen Oxides	4230
1.2.3. Photosensitized Processes and Photochemistry Driven by Visible Radiation	4222	3.2. Gaseous H <sub>2</sub> O <sub>2</sub> /HO <sub>x</sub> Loss and Production	4231
1.2.4. Rates and Yields of Photochemical Reactions	4222	3.3. Sulfur Dioxide	4232
1.3. Gas Phase versus Condensed Phases	4223	3.4. Ozone Loss and Production	4232
1.3.1. The Importance of "Matrix Effects"	4223	3.5. Organic Compounds	4233
1.3.2. Diffusion and Transport Limitations	4224	3.6. Field Observations of Dust Photochemistry	4234
1.3.3. Influence of the Physical State and Viscosity	4224	4. Photophysical Processes at Liquid Interfaces	4235
1.3.4. Special Properties of Interfacial Regions between Different Phases	4225	5. Organic Aerosol Photochemistry	4236
2. Photophysical Properties of Observed Atmospheric Particles and Interfaces	4225	5.1. General Considerations	4236
2.1. Primary Chromophores	4225	5.2. Smog Chamber and Aerosol Flow Tube-Based Experiments	4238
2.1.1. Mineral Dust	4225	5.3. Photodegradation of Bulk Materials Mimicking Organic Aerosols	4239
2.1.2. Inorganic Anions	4226	5.3.1. Polycyclic Aromatic Compounds and Their Derivatives	4239
2.1.3. Hydrogen Peroxide	4227	5.3.2. Model HULIS Compounds	4242
2.1.4. Primary Organic Chromophores	4228	5.3.3. Organic Aerosols on Inert Substrates	4242
2.2. Secondary Organic Chromophores	4228	5.4. Photosensitized Reactions Involving Carbonyl Compounds	4243
		6. Heterogeneous Photochemistry at Ice Surfaces	4244
		6.1. Inorganic Chromophores	4245
		6.2. Photolysis of Organic Molecules	4246
		6.3. Photosensitized Chemistry with Organic Chromophores	4247
		6.4. Indirect Photochemistry Induced by Mineral Dust in Ice	4248
		7. Heterogeneous Photochemistry on Urban Surfaces	4248
		7.1. Outdoor Surfaces and Urban Grime	4248
		7.2. Indoor Surfaces	4249
		8. Looking Ahead	4249
		Author Information	4250
		Corresponding Author	4250
		Notes	4250

**Special Issue:** 2015 Chemistry in Climate

**Received:** November 14, 2014

**Published:** March 16, 2015

Biographies	4250
Acknowledgments	4251
Glossary	4251
References	4251

## 1. BACKGROUND

### 1.1. Why Condensed Matter Matters: Types and Significance of Condensed Matter and Surfaces Encountered in the Atmospheric Environment

The atmosphere is far from being a pure homogeneous gas, as is readily apparent on a rainy day! The air is in contact with airborne particulate matter (aerosol particles, cloud droplets, and ice particles) and ground surfaces. It was probably the German meteorologist August Schmauß who used for the first time the term “aerosol particles” in a scientific report by referring to the concept of air as a colloid.<sup>1</sup> Yet some of the impacts of aerosols were already known centuries ago when Leonardo da Vinci reported in ca. 1500 on the color of the sky: “...as I say, that the atmosphere assumes this azure hue by reason for the particles of moisture which catch the rays of the sun.”<sup>2</sup> Nowadays, atmospheric aerosols are defined as liquid or solid particles suspended in air for an atmospherically meaningful period of time, ranging from minutes to days for particles in the lower atmosphere to years for stratospheric aerosols. They are known to strongly influence many environmental processes because of their unusual physical and chemical properties.

As experienced by Da Vinci, aerosols scatter and absorb solar and terrestrial radiation, but are also the seeds on which clouds form, initially suggested to be water bubbles by Otto von Guericke (1602–1686). This idea was later shown to be incorrect by P. J. Coulier (1824–1890) and John Aitken (1839–1919) who demonstrated that dust particles are required for cloud formation to occur in the atmosphere. Binding these two aspects together resulted in the fact that aerosols markedly affect the radiative balance in the Earth’s atmosphere and play a central role in climate.

Despite their very small mass fraction in the air, which rarely exceeds  $10^{-5}$  wt %, even in polluted areas, aerosols do alter the chemical composition of the atmosphere by promoting specific chemical pathways that can only occur on surfaces or in condensed phases. One of the most dramatic examples for such effects can be found in the ozone hole chemistry where polar stratospheric clouds offer a surface on which stable HCl and ClONO<sub>2</sub> molecules are converted into the photochemically active Cl<sub>2</sub> under the cold and dark conditions of a polar night, leading to a massive ozone destruction upon sunrise.<sup>3</sup> Of course, other examples can also be found for the troposphere where, for instance, N<sub>2</sub>O<sub>5</sub> is readily taken up by most tropospheric aerosols resulting in a significant effect on the distribution of oxidized nitrogen compounds,<sup>4</sup> and sea-spray may act as a source of active bromine leading to ozone depletion events.<sup>3</sup>

Finally, since the reports on the killer fog in the Meuse valley in Belgium (1930), the Donora smog episode (1948), the great smog in London (1952), and other disastrous air pollution episodes, it is widely recognized that ambient aerosols do impact human health, with severe damaging effects on the respiratory and cardiovascular systems. The World Health Organization states that an estimated 3.7 million premature deaths resulted from air pollution worldwide in 2012.<sup>5</sup> The

level of air pollution in rapidly developing urban centers is especially problematic. Recently, the Organization for Economic Co-operation and Development made an environmental projection to 2050 and found that, if no new policies are implemented, urban air quality (typically governed by levels of particulate matter and ground level ozone) will continue to deteriorate globally, becoming by 2050 the top cause of environmentally related deaths worldwide.<sup>6</sup>

Despite the importance of aerosols in atmospheric chemistry, climate, and air pollution, our ability to assess the impact of aerosols on atmospheric physics and chemistry is still limited due to insufficient understanding of many processes associated with sources of particles (mechanisms of formation), their chemical composition and morphology, and evolution of their composition and properties during their atmospheric lifetime. Indeed, atmospheric aerosols can be viewed as a complex conglomerate of thousands of chemical compounds in a giant, strongly oxidizing chemical reactor of the Earth atmosphere. The complexity of chemical and physical processes involving aerosols is not yet fully assessed.

Atmospheric aerosols can be categorized into primary particles, which are directly emitted by their sources, and secondary particles, generated in the atmosphere from gaseous inorganic and organic precursors (Table 1). For example, atmospheric oxidation of sulfur containing compounds leads to sulfuric acid and its salts, which represent a major secondary inorganic component of atmospheric aerosols. Likewise, oxidation of nitrogen oxides leads to nitric acid or its salts, which are also abundant in aerosols. While there are only a few important inorganic precursors to secondary aerosols (SO<sub>2</sub>, NO<sub>2</sub>, NH<sub>3</sub>), there is a huge spectrum of volatile organic compounds (VOCs) that contribute to secondary organic aerosol (SOA) formation. It is estimated that  $10^4$ – $10^5$  different organic compounds have been measured in the atmosphere,<sup>7</sup> each of which can undergo a number of atmospheric degradation processes to produce a range of oxidized products, which may contribute to SOA formation and growth. In addition, a variety of organic compounds associated with particulate matter (PM) are emitted in the atmosphere directly in the form of primary organic aerosol (POA). This underlines the fact that aerosols may be produced by a huge variety of natural and anthropogenic processes, both chemically and mechanically (erosion, bubble-bursting, etc.). The erosion-driven processes are especially important for mineral dust aerosols emitted from arid regions such as the Sahara. Combustion of any type (fossil fuel or biomass) is also an important source of both primary particles and volatile organics that later form SOA. The distinction between the primary and secondary particles is blurred with time as particles are subjected to a battery of physical (gas-particle repartitioning, particle coagulation, water uptake by particles, phase transitions within particles, structural collapse of fractal particles such as soot, etc.) and chemical (reactive uptake of gases by particles, cloud/fog processing of particulate compounds, photochemistry, etc.) processes. All of these processes are collectively known as “aging” of aerosols, and photochemistry is at the core of many particle aging processes in the atmosphere.

Aerosols, fogs, and clouds offer to the surrounding gas a surface that may potentially favor surface-mediated chemical reactions (e.g., due to lower activation energies as in heterogeneous catalysis), and also a bulk condensed phase in which reactions can take place that are not possible in the gas phase (such as electron transfer, acid–base reactions,

Table 1. Approximate Classification of Atmospheric Aerosols by Their Sources

aerosol type	classification	examples
primary inorganic aerosol	directly emitted, typically by a mechanical action such as wind	mineral dust, open ocean sea-spray, volcanic ash, meteoritic fragments
primary organic aerosol (POA)	directly emitted, typically by combustion of fossil fuels and biomass or by mechanical processes	soot, smoke, tailpipe exhaust, coastal sea-spray
bioaerosol	directly emitted by the biosphere	airborne bacteria, pollen, spores and viruses, fungi
secondary inorganic aerosol	atmospheric oxidation of NO <sub>x</sub> , SO <sub>2</sub> , NH <sub>3</sub> in gaseous and aqueous phases	ammonium sulfate, ammonium nitrate
secondary organic aerosol (SOA)	atmospheric oxidation of VOCs in gas phase and water-soluble organics in aqueous phase	forest haze, photochemical smog
aged aerosol	complex chemical and physical transformations of pre-existing particles	oxidized smoke, aged mineral dust, residual particles left after fog/cloud evaporation, any of the above aerosols internally mixed together

hydrolysis, etc.). Because of the short diffusion time of products out of a small particle back to the gas phase, the effects of surface or condensed phase reactions may feed back into gas-phase composition. Of course airborne particles do not represent the only condensed phases in contact with the atmosphere that may offer a reactive surface: the natural ground (soil, ocean, rocks, sea ice, snow, etc.) and the built environment (glass, concrete, asphalt, urban grime, etc.) surfaces must also be considered. For instance, in the urban environment, depending on the height of the mixing layer, the overall external surface of buildings may be significantly larger than those of aerosols and therefore play a chemical role in controlling fluxes of various compounds. The ocean surface, which covers three-quarters of the planet, offers a remarkably dynamic and chemically complex surface for interfacial reactions in the marine boundary layer. The porous nature of permanent or perennial snowpacks adds a tremendous amount of surface area, with which the atmosphere interacts. This has dramatic consequences for the atmospheric chemistry in the shallow boundary layer of polar regions.<sup>8</sup> Table 2 provides approximate specific surface areas and surface area concentrations for environmental surfaces easily accessible to atmospheric gases, that is, the surfaces that are not buried in the bulk of the material.

Chemical reactions that occur rapidly upon mixing of two stable reactants are quite rare in the atmosphere, as very often the energy required to activate the reaction is considerably larger than the available thermal energy. In the troposphere and stratosphere, the available heat content is often not sufficient, and most atmospheric reaction cycles are initiated by solar irradiation. Light absorption creates a transient excited state that can fall apart (photodissociate), change to a new structure (photoisomerize), undergo various reactions (for example, via electron or H atom transfers), or transfer the excitation energy to other molecules.

In short, solar radiation can provide the energy to initiate reactions while atmospherically available surfaces or condensed phases may act to reduce the required energy for a given photochemical pathway, for instance, by allowing a longer wavelength for reaction of species associated with a surface or bulk phase environment. Altogether, heterogeneous or multiphase photochemistry has the potential to greatly facilitate atmospheric reactions. In contrast to the mature field of gas-phase photochemistry,<sup>3,12</sup> the level of understanding of photochemical processes involving aerosols and environmental surfaces is still very low. Our objective is to review recent advances in this emerging field and predict its future developments. We begin with an overview of fundamental concepts in photochemistry, followed by a discussion of the

Table 2. Typical Specific Surface Areas (Available Surface per Unit Mass of Material), Surface to Volume Ratios, and Surface Concentrations Offered by Aerosols, Clouds, and Other Environmental Surfaces for Atmospheric Heterogeneous Chemical and Photochemical Processes

	specific surface area (m <sup>2</sup> g <sup>-1</sup> )	surface to volume ratio of single particle (m <sup>-1</sup> )	effective surface concentration (m <sup>2</sup> m <sup>-3</sup> of air)
aerosol <sup>a</sup>	3–60	3 × 10 <sup>6</sup> to 6 × 10 <sup>7</sup>	6 × 10 <sup>-5</sup> to 1 × 10 <sup>-3</sup>
cloud/fog <sup>b</sup>	0.3	3 × 10 <sup>5</sup>	3 × 10 <sup>-2</sup> to 3 × 10 <sup>-1</sup>
snowpack <sup>c</sup>	0.006–0.06	600–6000	0.6–60
bulk materials <sup>d</sup>			
soil, rocks <sup>e</sup>	0.006	6000	6
urban built surfaces <sup>f</sup>	0–100	0 to 5 × 10 <sup>7</sup>	0.004–0.8
biosphere <sup>g</sup>	4–25		0.007–0.07
ocean, etc.			0.01

<sup>a</sup>Calculated for 20 μg/m<sup>3</sup> aerosol consisting of 0.05–5 μm spherical particles with unit density. The particles are being considered as homogeneous, without any internal porosity. <sup>b</sup>Calculated for 0.1–1 g/m<sup>3</sup> liquid water content and 10 μm spherical droplets. <sup>c</sup>Calculated for snow with an overall density ranging from 0.1 to 0.5 g/cm<sup>3</sup> and a specific surface area range as given, corresponding to an ensemble of effective cubic ice crystals with a grain size of 0.1–1 mm.<sup>9</sup> For the effective surface area to volume ratio, a boundary layer height of 100 m was assumed, and a thickness of 0.2 m of snow interacting with the air aloft. <sup>d</sup>For the effective surface area to volume ratio, a boundary layer height of 100 m was assumed, and a thickness of 0.01 m of material interacting with the air aloft. <sup>e</sup>Calculated for material with an overall density of 1 g/cm<sup>3</sup> and 1 mm cubic grains separated by a negligible amount of empty space. For the effective surface area to volume ratio, a boundary layer height of 100 m was assumed, and a thickness of 0.01 m of soil interacting with the air aloft. <sup>f</sup>Calculated for material with an overall density of 4 g/cm<sup>3</sup>. For the effective surface area to volume ratio, a boundary layer height of 100 m was assumed, and a thickness of 0.001 m of construction material interacting with the air aloft and an impervious surface index (ISI), accounting for the three-dimensional nature of the urban landscape, of 2 are assumed.<sup>10</sup> <sup>g</sup>Calculated with leaf area index in the range 0.7–7 m<sup>2</sup> m<sup>-2</sup>,<sup>11</sup> and an assumed boundary layer height of 100 m.

common types of photochemically active compounds existing in atmospheric condensed phases. We then provide a review of the current state of knowledge on photochemistry of mineral dust, aqueous surfaces, organic aerosols, ice, and urban grime. This Review will not cover photochemistry in liquid cloud droplets as this is treated in detail in another review by Herrmann et al. in this issue,<sup>13</sup> but it will include photochemical processes occurring at the liquid water–air interface and on/in atmospheric ices. The major challenges ahead will be discussed

and recommendations for future research directions proposed at the end of this Review.

## 1.2. Principles of Atmospheric Photochemistry

The atmosphere of Earth is predominantly made up of molecular nitrogen (~78% under dry conditions) and molecular oxygen (~21%), both of which are highly stable molecules. Consequently, oxidation in the atmosphere is achieved to a large extent by the highly efficient reactions of molecular oxygen and photochemically produced free radicals, with organic compounds, initiating an oxidation chain reaction sequence, which is ultimately responsible for their oxidation to CO<sub>2</sub> and H<sub>2</sub>O, either in the gas or in the aerosol phase.

**1.2.1. Classification of Different Types of Photochemical Processes.** When sufficient energy is supplied to a given molecule, for example, as a result of absorption of a UV photon, electrons can move from their ground state to an unoccupied or partially occupied molecular orbital of higher energy. Because the energy of UV light is of the same order as the enthalpies of covalent bonds, this additional energy can result in a bond cleavage splitting the excited-state molecule into two fragments, a process known as photolysis. However, excited states can also isomerize, react with surrounding molecules, lose energy by emission or relaxation, and undergo various other processes such as those described in Table 3 for an excited molecule A–B–C.<sup>14</sup>

**Table 3. Possible Photochemical Reactions for an Excited Molecule A–B–C\*, Adapted from Calvert and Pitts<sup>12</sup>**

reaction pathway	name
A–B–C* → A–B• + C•	bond cleavage (photolysis) into free radicals
A–B–C* → E + F	photoisomerization followed by decomposition into stable molecules
A–B–C* + RH → A–B–C–H + R•	H-abstraction from a neighboring molecule
A–B–C* + D → A–B–C + D*	photosensitization (energy transfer of all kinds)
A–B–C* + D → A–B–C <sup>+</sup> + D <sup>-</sup>	photosensitization (electron transfer)

For example, carbonyl compounds, such as aldehydes and ketones (ubiquitous in the troposphere), have a weak n → π\* transition around 280 nm. The photoexcited carbonyls are known to undergo a Norrish type I bond cleavage in which one of the α-carbon bonds on either side of the C=O group is broken, creating two free radical fragments (see Figure 1). For

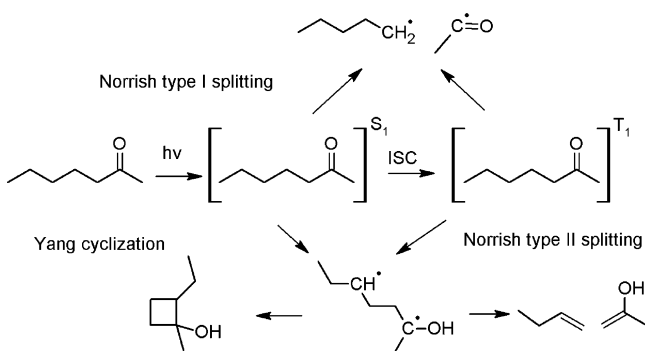
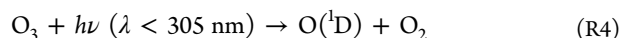


**Figure 1.** Photochemical processes that can occur in photolysis of carbonyls (using 2-heptanone as an example).

sufficiently large carbonyl compounds, Norrish type II splitting becomes an alternative pathway; in this case, the molecule splits into a smaller carbonyl and an alkene as a result of an intramolecular H atom transfer and bond cleavage (Figure 1). In addition to the Norrish type I and type II processes, a number of other reactions of photoexcited carbonyls are possible, such as Yang cyclization, also shown in Figure 1.

The initially excited S<sub>1</sub> or S<sub>2</sub> states in organic molecules may react immediately or, especially in the condensed phase, may quickly relax to the lower vibrational levels of the S<sub>1</sub> state due to interactions with the surrounding solvent species. The remaining excess energy is then dissipated by a variety of mechanisms, including photochemical reactions, and non-reactive processes such as fluorescence, internal conversion into the S<sub>0</sub> state, and intersystem crossing (ISC), in which the S<sub>1</sub> state decays to the lowest available triplet state T<sub>1</sub>. In situations when ISC is efficient, the T<sub>1</sub> state largely dominates photochemical processes as the triplet state lifetimes are long enough to allow chemical transformations to occur. Triplet state photochemistry in condensed media has been studied in detail for a number of organic molecules; this Review will only focus on selected examples of direct relevance to atmospheric heterogeneous photochemistry. One illustrative example of the important role of triplet states comes from a study of the photochemistry of aromatic ketones in water,<sup>15</sup> which showed that electronically excited carbonyls serve as important photooxidants in natural waters, reacting via a complex mechanism that does not necessarily involve singlet oxygen production, but rather electron transfer and H-abstraction processes as shown in Figure 2.

**1.2.2. Free Radicals and UV Radiation as the Primary Drivers of Chemistry in the Atmosphere.** Chemical bond enthalpies are typically in the 300–500 kJ mol<sup>-1</sup> range, equivalent to photon energies in the UV spectral region. In the atmospheric gas phase, free radicals are initially generated by short wavelength radiation photochemical reactions.<sup>12</sup> The radicals produced by the primary photolysis process often quickly transform to longer-lived radicals upon reactions with stable air components, such as in photolysis of formaldehyde yielding two HO<sub>2</sub> radicals (R1–R3) and in photolysis of ozone yielding two OH radicals (R4,R5):



Similar radical-generating pathways also exist in the atmospheric condensed phase (aerosols and clouds) where reactions initiated by UV light, such as those discussed above, produce dissolved free radicals or radical anions, such as OH, O<sub>2</sub><sup>•-</sup>, and SO<sub>4</sub><sup>•-</sup>.<sup>13</sup>

Probably the most important radical in the gas phase is OH, the hydroxyl radical. It is formed mostly via reaction R5, but other processes including HONO photolysis R9 and decomposition of Criegee intermediates of reactions of ozone with olefins also contribute.<sup>3</sup> The OH concentration is connected to that of the important NO<sub>x</sub> radical species (NO + NO<sub>2</sub>) through reactions such as

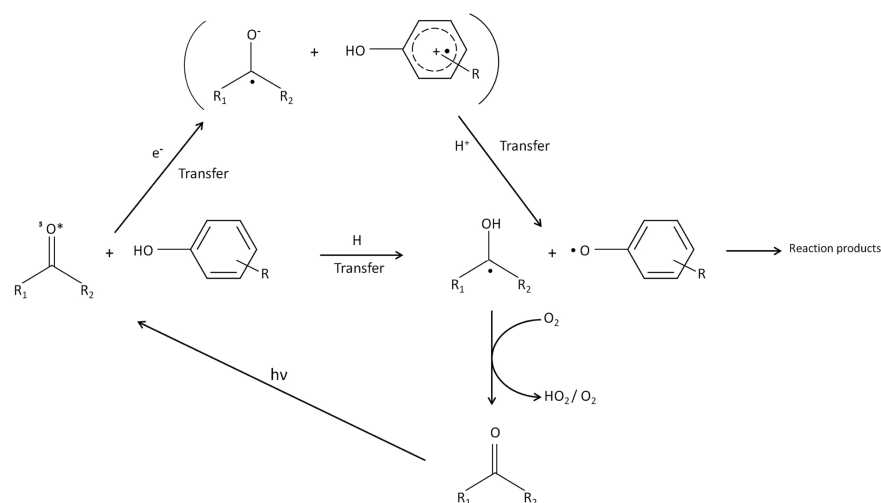
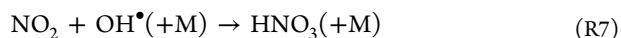


**Figure 2.** Catalytic oxidation reactions initiated by the triplet state of aqueous ketone molecules. Adapted with permission from ref 15a. Copyright 1995 American Chemical Society.



Reaction R6 has a critical importance in converting peroxy radicals, such as  $\text{HO}_2$ , into much more reactive  $\text{OH}$ , thus catalyzing photochemical oxidation processes leading to smog formation. Reaction R7 acts as a sink, at least in the troposphere, for both  $\text{OH}$  and  $\text{NO}_x$  species, while reaction R8 is easily reversed by the fast photolysis of  $\text{HONO}$  in reaction R9.

The gas-phase kinetic and photochemical parameters describing reactions R1–R9 are well-known.<sup>16</sup> In contrast, the processes generating free radicals in atmospheric condensed phases and on surfaces are poorly constrained. At least some fraction of the free radicals participating in heterogeneous photochemistry is initially created in gas-phase processes, and then transported to aerosol particles and surfaces. For example, most of the  $\text{OH}$  that drives aqueous photochemistry in cloud droplets is believed to be produced outside the droplets. However, as suggested above, free radicals can also be created, sometimes predominantly, directly in the condensed phase and on surfaces by various mechanisms.<sup>17</sup>

**1.2.3. Photosensitized Processes and Photochemistry Driven by Visible Radiation.** The processes discussed above are examples of direct photochemical reactions, in which the absorption of light by a molecule gives rise to a bond cleavage or rearrangement directly in that molecule. By contrast, indirect photochemical processes are those in which the initial absorption of light by some species gives rise to a chemical reaction involving a second species. For example, although reaction R4 is direct, its importance is to form a very short-lived intermediate,  $\text{O}(^1\text{D})$ , that essentially instantaneously produces the  $\text{OH}$  radical via R5. Thus,  $\text{OH}$  production by reactions R4 and R5 may be considered an example of indirect photochemistry. Photosensitized reactions also exhibit such indirect photochemistry. As listed in the final two lines of Table 3, absorption of light by a species  $\text{ABC}$  forms an excited species  $\text{ABC}^*$ , which then reacts with a second species,  $\text{D}$ , often

reforming  $\text{ABC}$  and/or generating excited or ionized states of  $\text{D}$  and other products. This is illustrated in Figure 2, which shows how carbonyl compounds may photosensitize reactions of phenols. The species  $\text{ABC}$  can reside in the same phase as  $\text{D}$ , or be just “visiting” an interface between two phases as a result of a gas–surface collision. Reactions in which gas-phase compounds react with electronically excited species on a particle surface fall into the category of heterogeneous photochemical processes.

As an interesting example, at saltwater surfaces in contact with the atmosphere, chlorophyll absorbs light and releases an electron, forming an electronically excited cation chlorophyll<sup>+</sup>. This species rapidly oxidizes halide anions such as  $\text{Cl}^-$ , forming highly reactive halogen atoms.<sup>18</sup> Thus, the photooxidation of chloride to chlorine is accomplished in the visible light region via the photosensitizing chlorophyll intermediate, even though chloride is transparent to radiation at those wavelengths. This is an important hallmark of photosensitized processes: they allow photoreaction to occur in wavelength regions in which the “target” molecule does not absorb. Thus, reactions that have modest energy requirements, in molecules with no long wavelength absorption features, may be induced via photosensitization. Of particular importance are photosensitized processes that can be initiated by visible radiation, which dominates the solar spectrum in the lowermost atmosphere.

**1.2.4. Rates and Yields of Photochemical Reactions.** Direct photochemical reactions, that is, those that involve photoreaction of the molecule initially excited, are considered to be pseudo first-order kinetic processes, with solar photons serving as an implicit excess reactant. The effective photochemical rate coefficient,  $J$ , depends upon the absorption cross-section  $\sigma(\lambda)$  of the absorbing compound, the quantum yield for the dissociation  $\phi(\lambda)$ , and the available spectral flux density  $I(\lambda)$ :

$$J = \int_{\lambda} \sigma(\lambda)\phi(\lambda)I(\lambda) d\lambda \quad (1)$$

The rate constants for other unimolecular processes, such as photoisomerization, can be defined in the same way, with the dissociation quantum yield replaced by the corresponding photochemical reaction yield. Encapsulated by  $J$  is the principle that a compound must absorb radiation in a wavelength region in which this photochemistry can and will occur, and that this

radiation must be available. As indicated by Figure 3, the intensity spectrum of available light in the atmosphere depends

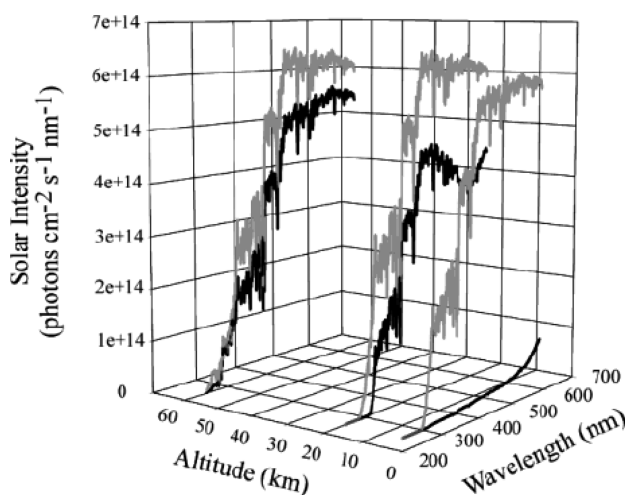


**Figure 3.** Altitude and solar zenith angle dependence of the solar actinic flux. The black lines show the solar spectrum at a zenith angle of  $90^\circ$  (i.e., with sun at the horizon); the gray lines show the actinic flux at a zenith angle of  $0^\circ$ . Reproduced with permission from ref 19. Copyright 2003 American Chemical Society.

on altitude, but also latitude, time of day, particle density, and cloud cover. Thus, even molecules with large absorption cross sections and unit dissociation quantum yields may not always be efficient at direct radical production.

The rate constants for processes involving bimolecular reactions, such as condensed phase reactions of triplet excited states with other molecules in the same particle, are more complicated and depend sensitively on the environmental conditions, but they are also proportional to the integrated overlap of the absorption cross sections of the primary absorber and spectral flux density.

Incorporation of heterogeneous photochemical reactions into atmospheric chemistry models requires suitable parametrization of such processes, similar to the one developed for gas-phase kinetics and for surface reactions.<sup>16</sup> While the rates of direct photolysis reactions can be calculated using eq 1, the description of the kinetics of photochemical processes that involve the loss of a trace gas species from the gas phase on a surface is slightly more complicated. It is commonly accepted to use the concept of the uptake coefficient,<sup>20</sup>  $\gamma$ , which is the net probability that a molecule X colliding with the surface is actually taken up at the surface.<sup>20,21</sup> This approach links the processes at the interface and beyond with an apparent first-order loss of X from the gas phase:

$$\frac{d[X]_g}{dt} = -k_p[X]_g = -\gamma \frac{\bar{c}}{4V} S [X]_g \quad (2)$$

$[X]_g$  denotes the concentration of X in the gas phase (molecules  $\text{cm}^{-3}$ ),  $S/V$  is the overall surface area of condensed phase per volume of atmosphere (generally in dimensions of  $\text{cm}^{-1}$ ), and  $\bar{c}$  is the mean thermal velocity of X ( $\text{cm s}^{-1}$ ). The uptake coefficient  $\gamma$  may be governed by varying kinetic regimes, for example, adsorption equilibration on the surface, reaction of the adsorbed trace gases with reactants on the surface, solubility equilibration, or reaction in the bulk of the particles, which all occur at different rates. It may also depend on the gas-phase concentration of X due to the possible

saturation of adsorption to the surface.<sup>22</sup> Finally, for photochemical reactions,  $\gamma$  will depend on the actinic flux. Therefore,  $\gamma$  is not a constant, and values reported from laboratory measurements should be taken with care when it comes to extrapolating them to atmospheric conditions. In many cases, the underlying elementary processes have been resolved allowing the usage of more detailed parametrizations for  $\gamma$ .<sup>21</sup> However, the knowledge in the context of heterogeneous photochemical processes is in its infancy, and detailed parametrizations have not yet been developed. Approaches developed for photocatalysis in engineering applications may be a good starting point.<sup>23</sup> Therefore, in several studies,  $\gamma$  has been parametrized by an empirical expression to describe its dependence on irradiance (see, for example, ref 24).

### 1.3. Gas Phase versus Condensed Phases

**1.3.1. The Importance of "Matrix Effects".** In this Review, we consider several categories of condensed phases interacting with the gas phase: aerosol particles, ocean surfaces, ice in airborne and ground forms, and urban ground surfaces. These categories by themselves are not unique phases but represent single or multiple (mixed) phase systems. Aerosol particles may be an internal mixture of solids or liquids, and the liquids may be either aqueous or organic or a mixture thereof. Ocean surface water may be enriched in nonsoluble or gel-type organics with specific physical properties.<sup>25</sup> Ice in the environment is always a complex multiphase system, most evident for sea ice (frozen seawater, a mixture of ice and brine), but even a cirrus ice particle in a clean environment is likely to contain the remnants of an aerosol particle that has acted as the original ice particle nucleus. In this section, we highlight the main features of these condensed phases as relevant for photochemistry.

Obviously, the main difference between a gas phase and a liquid is the presence of a solvent or, in the case of organic aerosols, a complex matrix, which could strongly alter any chemical pathway. However, it is important to mention a few main differences between the gas and condensed phases in the context of photochemical processes. For the remainder of this Review, the complex chemical matrix of condensed phases considered here is simply referred to as "the solvent", which certainly oversimplifies the picture, but facilitates the description of the possible interactions.

The impact of a solvent is manifold. First, the much higher density of the condensed phase environment means that reacting compounds interact strongly with the surrounding solvent molecules. For example, polar and ionic molecules in water are surrounded by a hydration shell composed of perhaps tens of water molecules. The level of solvation depends on the chemical nature of the solvent (as well as the solute) and exerts a direct influence on chemical rates and product yields. Furthermore, the solvent may reversibly react with the solute to form compounds with different properties; this happens, for example, in the conversion of aldehydes, which absorb radiation in the  $n \rightarrow \pi^*$  band associated with the  $\text{C}=\text{O}$  bond, into their *gem*-diol forms (in water) or into hemiacetals (in alcohols), which no longer possess the  $n \rightarrow \pi^*$  transition.

Such interactions may lower the activation energy for one chemical pathway, and thereby catalyze the reaction. For instance, both the hydrolysis of esters and the hydration of aldehydes (to form a *gem*-diol) are catalyzed by acidic solvents. Such catalysis may occur in one phase and would then correspond to homogeneous catalysis but may also occur at an

interface between two phases, corresponding to heterogeneous catalysis. For instance, Jang et al. showed that the participation of acidic seed aerosols can lead to an increase in SOA mass as compared to that obtained from neutral seed aerosols.<sup>26</sup> In this case, inorganic acids catalyze SOA formation by inducing complex oligomerization reactions between semivolatile organic compounds. In fact, it is now known that organic compounds containing carbonyl functions can be transformed to higher mass products (such as oligomers) through acid-catalyzed reactions.<sup>27</sup> These reactions are often discussed in the context of heterogeneous catalysis, but in many cases they actually correspond to homogeneous catalysis because the primary catalyzed step (i.e., starting with the protonation of the carbonyl function) takes place in the bulk of the particles.

In the troposphere, many condensed phases contain ions or polar compounds that influence the electrostatic forces between reacting compounds. While gas-phase reactions involving ions are rare at low altitudes, in liquids (and other water-rich matrixes, such as wetted aerosols) such reactions take place readily. Here, the ionic strength of the matrix is an important parameter for chemical kinetics, requiring knowledge of the activities of reacting species. Unfortunately, activity coefficients for molecules in complex environments such as aerosols are frequently unknown, although some methods for estimating the thermodynamic properties of soluble mixed inorganic/organic aerosols are available.<sup>28</sup> Water activity predictions from calculations using the UNIFAC (universal quasi-chemical functional-group activity coefficients) model were found to agree with the measured bulk water activity data to within 40% for most of the acids.<sup>29</sup> Using a global three-dimensional chemistry/transport model able to describe O<sub>3</sub>, NO<sub>x</sub>, VOCs, sulfur, and NH<sub>3</sub> chemistry, Tisgaridis and Kanakidou simulated the temporal and spatial distribution of primary and secondary carbonaceous aerosols in the troposphere focusing on SOA formation.<sup>30</sup> In their analysis of the uncertainties associated with the model results, the activity coefficient was one of the main identified uncertainty factors. Similar conclusions were made by Volkamer et al. in a study that identified glyoxal multiphase chemistry as the major source of organic aerosols in Mexico City, where an increased partitioning of glyoxal into aerosols, governed by activity coefficients, was required to match ambient observations.<sup>31</sup>

**1.3.2. Diffusion and Transport Limitations.** In a gas at atmospherically relevant pressures, molecules can be considered as being isolated, moving freely between collisions. In the condensed phase, the situation is totally different, as there is little free space between molecules, which are surrounded by a solvent cage, formed by the surrounding molecules. Because each reagent in a potential reaction has its own cage, there is a decreased mobility in solution-phase reactions as compared to that in the gas phase. A reactive encounter between two such reactants involves a melding of the individual solvent cages into a single one, which acts to “trap” them together for some time during which they could collide repeatedly and react with higher probability. In the context of photochemistry, one of the most important cage effects is the trapping of free radicals generated by photodissociation, thus facilitating their recombination. As an example of relevance to atmospheric photochemistry, Nissenon et al. studied the effect of a cage of water molecules on the photolysis quantum yields of nitrate, FeOH<sub>2</sub><sup>+</sup>, and H<sub>2</sub>O<sub>2</sub>.<sup>32</sup> They showed that the quantum yields for the photolysis of nitrate and FeOH<sub>2</sub><sup>+</sup> (but not that for H<sub>2</sub>O<sub>2</sub>) are decreased by the recombination of photofragments. Therefore,

the photolysis of nitrate and FeOH<sub>2</sub><sup>+</sup> could be enhanced if the cage of the solvent molecules is incomplete as is the case at the air water interface of atmospheric droplets.

Diffusion in condensed phases is much slower than that in the gas phase, meaning that otherwise fast reactions may be limited by the rate at which molecules are transported to encounter each other, that is, corresponding to diffusion-controlled reactions. Such limitations could be quite important for organic aerosols. For instance, Zhou et al. studied the effect of the bulk diffusivity of polycyclic aromatic hydrocarbons (PAHs) in SOA and its impact on the kinetics of the heterogeneous reaction of particle-borne benzo[*a*] pyrene (a common atmospheric PAH) with ozone.<sup>33</sup> They showed that on one hand, under dry conditions, diffusion of ozone through the SOA coating significantly hindered the kinetics, which approached those observed for the solid state. However, by increasing the relative humidity (RH), the viscosity of the chemical matrix was lowered, lifting the mass transfer constraint to the point where the kinetics were similar to results obtained without SOA coatings. This illustrates not only that viscosity affects diffusion and chemical rates but also that these are depending on environmental conditions such as RH and temperature.

### 1.3.3. Influence of the Physical State and Viscosity.

Another important attribute of atmospheric condensed phases is the physical phase (liquid or solid) of the particle. Inorganic salt particles are known to undergo deliquescence (transition from the solid state to a saturated solution) at an RH that depends on the chemical nature of the salt, or its mixing state with other inorganic or organic compounds. Thus, these particles may contain both phases depending on the ambient RH and also on the “history” of their air mass, because efflorescence (the reverse transition from the liquid state back to the solid phase) occurs typically at much lower RH than deliquescence.

Organic aerosols have been assumed to be mostly in a liquid state (potentially viscous); however, recently it has been suggested that biogenic SOA particles, formed from oxidation products of VOCs in plant chamber experiments and in boreal forests, could be in an amorphous solid, most probably glassy, state.<sup>34</sup> Koop et al. performed a systematic survey of a wide range of organic compounds and their amorphous properties, such as the glass transition temperature, and concluded that atmospheric SOA should be capable of forming glasses.<sup>35</sup> In a similar context, the morphology of particles could also alter their chemistry. Studying the mixing of primary and secondary organic particles and the adsorption of spectator organic gases during aerosol formation, Vaden et al. observed that hydrophilic SOA and hydrophobic dioctyl phthalate do not mix but instead form layered phases.<sup>36</sup> In addition, You et al., using optical and fluorescence microscopy, revealed the coexistence of two liquid phases in particles collected in Atlanta, GA, as well as for laboratory samples under simulated atmospheric conditions.<sup>37</sup> The existence of such morphologies in ambient particles will affect gas-particle partitioning, their light scattering and absorption properties, and finally the reactive uptake of atmospheric constituents. Furthermore, model laboratory systems may underestimate the true viscosity of ambient organic aerosol particles as a recent study of O'Brien et al. demonstrated.<sup>38</sup>

These observations, suggesting that SOA particles can exist in a highly viscous state, highlight the fact that slow water diffusion in the condensed aerosol phase will impact both

condensation and evaporation rates. The effects on the diffusion rates can be rather dramatic. For example, using coarse mode (3–4  $\mu\text{m}$  radius) ternary sucrose/sodium chloride/water droplets as a proxy for multicomponent ambient aerosol, Bones et al. demonstrated that the time scale for particle equilibration with the ambient gas phase correlates with bulk viscosity and can be in excess of  $10^3$  s.<sup>39</sup> The physical state and viscosity have the potential to strongly affect photochemical processes, especially the indirect ones, in which the long-lived excited molecules have to diffuse/appropriately orient themselves before the photochemical reaction.

**1.3.4. Special Properties of Interfacial Regions between Different Phases.** The phase boundary is a region characterized by a sharp change in density. For example, at an air–liquid interface, the density increases by a few orders of magnitude within a few angstroms distance across the interface. As a consequence, this region has special chemical and physical properties. The defining feature of an interface is that it can be regarded as two-dimensional (as its thickness is almost of molecular level), or, in other words, it is asymmetric with the geometrical arrangements of the molecules differing from the generally isotropic arrangement found in the bulk.<sup>40</sup> For instance, for solutes preferentially residing at the interface, the solvation shell is incomplete (as compared to bulk conditions) and depends on the location of the molecules with respect to the interface.<sup>41</sup> A first assessment of whether molecules at the interface are present in excess over their bulk concentration can be obtained from their ability to reduce surface tension.<sup>42</sup> However, a more detailed analysis of the atmospherically relevant case of halide ions indicates that they are significantly enhanced at the outermost boundary of air–water interface, despite the fact that the surface tension is increasing with increasing bulk halide concentration.<sup>43</sup> Molecular dynamics simulations and surface sensitive experiments of solutions containing  $\text{F}^-$ ,  $\text{Cl}^-$ ,  $\text{Br}^-$ , and  $\text{I}^-$  revealed that only the smallest halide  $\text{F}^-$  is preferably solvated in the bulk, while the larger halides have an increasing propensity, with increasing size, to be present at the interface, due to their increasing polarizability.<sup>43,44</sup> This changes the ionic environment at the interface of salt containing particles and, together with an incomplete solvation shell, facilitates potential surface reactions. Such surface involvement has been suspected for a number of reactions of oxidants with sea-salt solutions or (ice) particles and contributes to the release of molecular halogen compounds in marine environments.<sup>45</sup> Other reactive aerosol constituents also have a propensity to be enriched at the surface. For example, humic-like substances (HULIS), which are abundant in aerosol particles, are surface active and, as it will be discussed below, also offer photochemically interesting features.<sup>46</sup> Altogether, interfaces offer an environment that definitively favors unusual chemical interactions.<sup>47</sup> Despite the importance and widespread interest in the interfacial reactions, they remain understudied due to the difficulty of probing the chemistry and physics of interfaces, and in particular of gas–liquid interfaces.

An example of a special type of environmental interface is the ice–air interface. The surface of ice undergoes surface premelting at temperatures above about 230 K,<sup>48</sup> which is the result of the crystalline solid minimizing the surface energy in response to the asymmetric hydrogen-bonding environment at the ice–air interface. This is not unique to ice but a property of all atomic and molecular solids approaching their melting points.<sup>49</sup> Surface premelting results in a reduced ordering and changing orientation of the topmost water molecules,<sup>50</sup> the

extent of which steadily increases toward the melting point. This ice–air interfacial region has often been referred to as quasi-liquid layer. However, because this layer is a surface phenomenon and does not represent a thermodynamically stable liquid phase, but has distinct properties different from those of liquid water, we refer to it here as the disordered interface (DI).<sup>48,51</sup> This DI has unique properties and may provide an environment distinctly different from that on and in liquid water or on other solid surfaces. Soluble species may potentially experience incomplete solvation shells,<sup>52</sup> or the specific hydrogen-bonding environment may enable self-assembly of molecules.<sup>53</sup>

The role of the DI in determining the unique properties of the condensed phase–air interface is not only crucial for ice. For other solid materials, mainly mineral dust, hydroxylation of the surface oxides and adsorbed water layers enable the hydrogen-bonding environment for (partial) dissolution of soluble trace gases from the surrounding air,<sup>54</sup> for the dissolution of metal ions out of the mineral dust oxides,<sup>55</sup> or also for unexpected acid-catalyzed chemistry depending on the Lewis acidity of the substrate.<sup>56</sup>

We must also note that in frozen and other solid–liquid mixed phase systems, it is not only the condensed phase–air interface but also the solid–liquid, liquid–liquid, and solid–solid interface regions that possess special properties. For example, confinement within grain boundaries within polycrystalline ice may allow solutions to exist below the eutectic temperature.<sup>57</sup>

In summary, this section has highlighted a series of physical and chemical properties of interfaces that greatly differ from the homogeneous gas and aqueous phases. These special properties should be taken into account when describing, and studying, heterogeneous or multiphase photochemistry in the troposphere.

## 2. PHOTOPHYSICAL PROPERTIES OF OBSERVED ATMOSPHERIC PARTICLES AND INTERFACES

For photochemistry to take place, the incoming solar radiation first has to be absorbed by appropriate molecules at the interface or in the bulk of the condensed matter. As the actinic flux reaching lower altitudes generally possesses only wavelengths longer than 290–300 nm (Figure 3), for photochemistry to occur aerosol particles and ground surfaces need to contain appropriate chromophores, which may be of primary (directly emitted) or secondary (formed in situ) nature. This section will describe the basic types of important chromophores found across different atmospheric condensed phases and interfaces, including aerosol particles, urban surfaces, liquid droplets, and ice particles.

### 2.1. Primary Chromophores

**2.1.1. Mineral Dust.** Each year, massive amounts of mineral dust, 1500–2000 Tg,<sup>58</sup> are uplifted into the air from arid regions contributing significantly to the atmospheric particle loadings, with severe impacts on climate and air quality. Dust particles provide a surface on which a complex chemistry can take place as reviewed by Usher et al.<sup>54</sup> Dust particles' direct radiative forcing effect (due to scattering and absorption of incoming solar radiation) is accompanied by an indirect effect as clay and silica particles are effective cloud condensation and ice nuclei,<sup>59</sup> which can ultimately affect cloud structure and precipitation patterns.<sup>60</sup> Dust particles also deposit on snow and ice through wet and dry deposition, and substantially

modify the surface albedo of snow covered areas.<sup>61</sup> The optical properties of dust particles vary with size and mineralogical composition of the source region. Strongly absorbing minerals such as iron oxides predominantly influence the wavelength-dependent mass specific absorption cross section of naturally occurring mineral dusts in the visible spectral region.<sup>62</sup> Figure 4a shows a photograph of two parallel dust plumes, with one

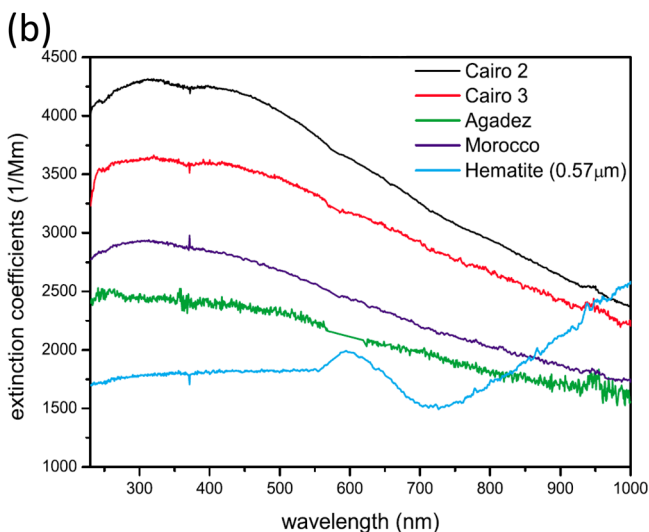


**Figure 4.** (a) A photograph of Western Sahara dust blowing across the Atlantic Ocean (the two shades of dust are two different material compositions (NASA/Jeff Schmaltz, MODIS Rapid Response Team, NASA-Goddard Space Flight Center); and (b) the extinction coefficients of various dust samples. Reproduced with permission from ref 63. Copyright 2006 European Geophysical Union - Copernicus Publications.

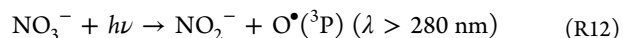
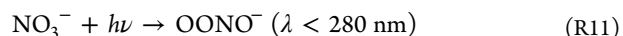
being substantially more absorbing (colored) than the other reflecting the difference in their sources. While Figure 4b shows the extinction coefficients for several common types of dust particles, the coefficients are large across the entire UV–visible range. The color of dust depends primarily on the content of iron oxides in the particles, a higher fraction of iron oxides resulting in the redder shades. For example, the dust outflows from Africa are more light-absorbing than Asian dust outflows due to the higher iron content in African soils.<sup>54</sup>

Dust particles may also contain other mineral components that absorb light and exhibit photocatalytic or photoreactive properties.<sup>64</sup> An example of a photocatalytic inclusion in dusts is titanium oxides (e.g.,  $\text{TiO}_2$ ), typically present in mass fractions ranging from 0 to 5 wt %. The role of  $\text{TiO}_2$  and other

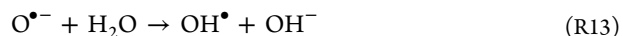
photocatalytic materials in dust particles has been recently reviewed by Chen et al.,<sup>65</sup> while photo-Fenton reactions involving iron oxides within the atmospheric condensed phase have been discussed by George et al.<sup>66</sup> When such a semiconducting metal oxide ( $\text{TiO}_2$ ,  $\text{ZnO}$ , iron oxides, etc.) is exposed to light carrying energy equal to or in excess of its band gap, the subsequent electron transition creates an electron–hole pair. The oxide may transfer its electron to any adsorbed electron acceptor molecule, thereby promoting its reduction, while the hole (or the electron vacancy) may accept an electron from an adsorbed donor molecule, promoting its oxidation. In case of an oxide exposed to ambient air, adsorbed oxygen ( $\text{O}_2$ ) will act as the dominant electron acceptor and produce the highly reactive superoxide radical anion ( $\text{O}_2^-$ ). Simultaneously, adsorbed water will be oxidized to hydroxyl radicals (OH), and adsorbed organics will be oxidized to a number of different products. In other words, illuminated mineral dust carrying such oxides will initiate very active redox chemistry on its surface.

**2.1.2. Inorganic Anions.** Nitrate anions ( $\text{NO}_3^-$ ) are ubiquitous in all types of ambient particles. The fractional amount of  $\text{NO}_3^-$  depends on the location and season. It is especially high in the vicinity of urban centers because  $\text{NO}_3^-$  is ultimately derived from anthropogenic emissions of  $\text{NO}_x$  via reaction R7, but it is also found as one of the major particulate constituents around the globe, including remote areas. For example, nitrate is a significant constituent in snow and ice in polar regions. In fact, its concentration and isotopic signature in ice cores is commonly used as a proxy to assess past environmental conditions.<sup>67</sup> Especially in snowpacks, photolysis of nitrate contributes a significant source of radicals and  $\text{NO}_x$  in polar regions.<sup>68</sup> The photolysis of nitrate anion has been reviewed by Mark and Bolton<sup>69</sup> and more recently revisited by Goldstein and Rabani.<sup>70</sup>

In dilute solutions, nitrate anions only weakly absorb light in the actinic region, as the absorption spectrum of  $\text{NO}_3^-$  shows only a weak  $n \rightarrow \pi^*$  band around 302 nm. Nitrate photolysis resulting from the  $n \rightarrow \pi^*$  excitation occurs through three possible channels:<sup>71</sup>



In water, reaction R10 is immediately followed by



Under typical tropospheric conditions, only the R10 and R12 channels are relevant, although their quantum yields around 300 nm are relatively small.<sup>70</sup> The importance of these pathways is that they produce the highly reactive OH radical, which can react with a broad range of organic compounds either in the condensed phase or after evaporation into the gas phase.

The nitrite radical produced by reaction R12 can also act as a chromophore. The extinction coefficient of  $\text{NO}_2^-$  at the peak of its  $n \rightarrow \pi^*$  band ( $\epsilon = 22.5 \text{ M}^{-1} \text{ cm}^{-1}$  at 360 nm) is only a little higher than that of  $\text{NO}_3^-$  ( $\epsilon = 7.2 \text{ M}^{-1} \text{ cm}^{-1}$  at 302 nm).



However, the photolysis rate of  $\text{NO}_2^-$  is significantly faster because it absorbs significantly all of the way to 400 nm, thus

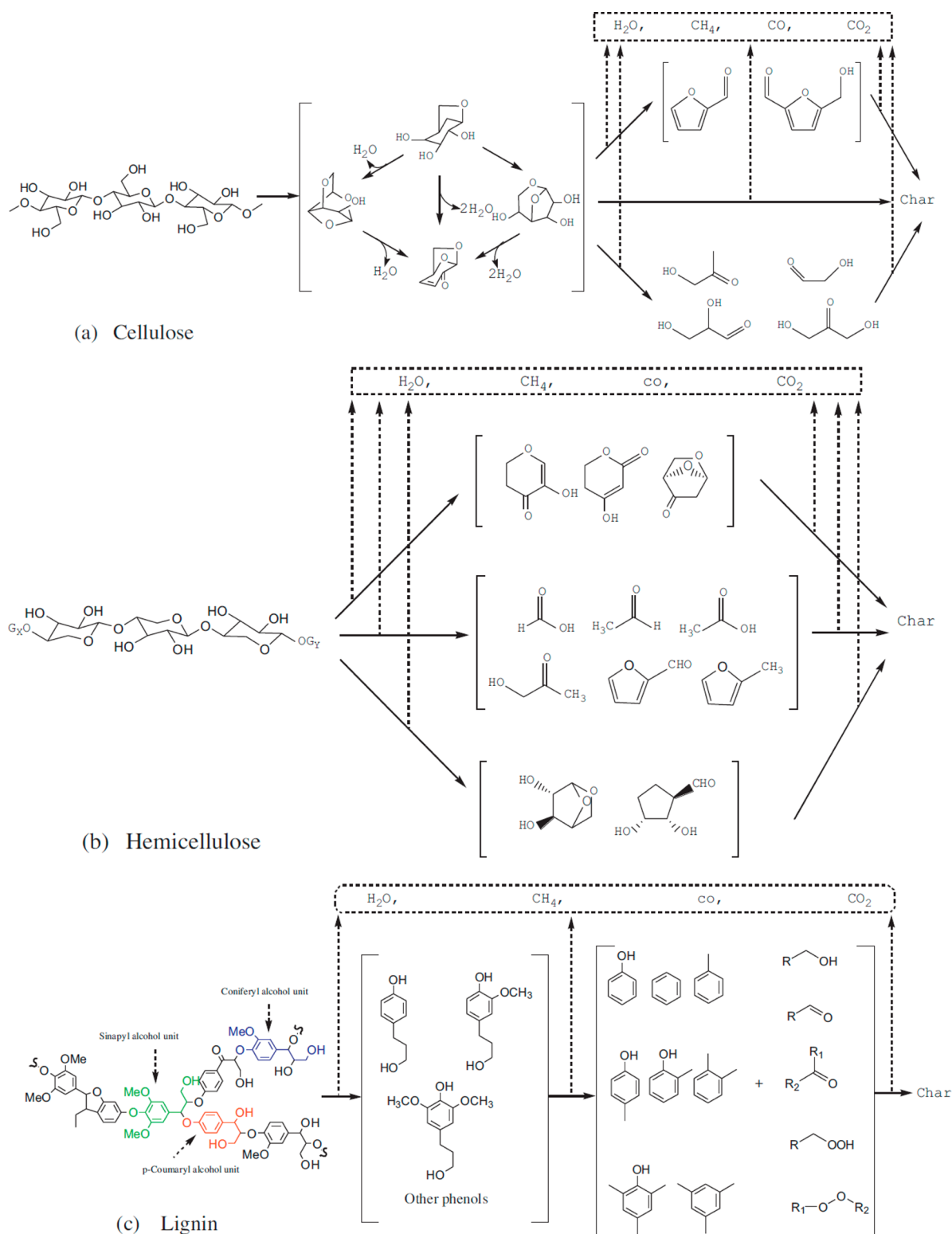


**Figure 5.** Reaction products of the pyrolysis of wood. Reproduced with permission from ref 85. Copyright 2013 Elsevier.

matching nicely the solar spectrum available in the troposphere. The photolysis of  $\text{NO}_2^-$  generates  $\text{NO}$  and  $\text{O}^-$  with a quantum yield of several percent, although measurements in different laboratories span a wide range.<sup>69</sup> In the presence of water,  $\text{O}^-$  is quickly converted into  $\text{OH}$  by reaction R13.

**2.1.3. Hydrogen Peroxide.** Another important inorganic chromophore is hydrogen peroxide.  $\text{H}_2\text{O}_2$  can directly oxidize certain atmospheric compounds (see Herrmann et al.<sup>13</sup> in this

issue), and it also serves as a source of  $\text{OH}$  radicals through photolysis of the weak  $\text{O}-\text{O}$  bond in the molecule:



Similar to nitrate, the absorption cross sections are low above 300 nm, but they drop off less steeply than those of nitrate toward 350 nm;<sup>72</sup> coupled with a high photolysis quantum yield, this makes R15 an important radical source.  $\text{H}_2\text{O}_2$  and

nitrate together account for a significant fraction of the UV light absorption in polar snow, depending on location.<sup>73</sup> Organic peroxides, ROOH, absorb radiation with similar efficiency, and can also produce OH, but their concentrations are typically much smaller than those of H<sub>2</sub>O<sub>2</sub>.

**2.1.4. Primary Organic Chromophores.** Combustion processes, both of biomass and fossil fuels, are substantial sources of black carbon (BC) and primary organic compounds, some of which are strongly light-absorbing.<sup>74</sup> Obviously, their exact chemical composition depends on the type of fuel and the combustion conditions.<sup>75</sup> As a consequence, combustion aerosols have a very complex chemical matrix, carrying thousands of different chemicals associated with complex aging processes that will not be reviewed here.<sup>76</sup>

Black carbon is the most obvious chromophore in atmospheric particles, and it has a direct impact on the radiative budget of the atmosphere. It is found everywhere in the atmosphere, but also deposited on snow and ice, where it significantly contributes to the surface albedo, similar to mineral dust.<sup>61a,77</sup> Absorption of solar radiation by BC has not been previously considered capable of initiating indirect photochemical processes, as it was assumed that all of the energy absorbed by BC is dissipated into heat. However, it is likely that its extended system of  $\pi$ -conjugation in aromatic, graphitic, and graphene type structures may serve to initiate indirect, photosensitized, photochemical processes.<sup>78</sup>

Indeed, with their large specific surface area on the order of 100 m<sup>2</sup> g<sup>-1</sup>, soot particles may represent an ideal substrate for certain heterogeneous reactions.<sup>79</sup> Several recent experiments revealed a significant importance of the presence of light during soot uptake experiments.<sup>79,80</sup> Ozone removal on soot surfaces was studied under dark conditions and in the presence of near-UV radiation on both fresh and passivated soot.<sup>80</sup> While hardly affecting the gas-phase composition, the ozone uptake under illumination showed a significant impact on the aging of soot itself: an enhanced oxidation with radical formation likely involving polymerization and volatilization was observed, a finding that was also confirmed by Han et al.<sup>81</sup> Contact angle measurements showed an increase in hydrophobicity and therefore supported the idea that particles remain with their more refractory and less hygroscopic components.<sup>80</sup> This is in some contrast to oxidative chemistry in the dark believed to make soot more hydrophilic.<sup>78b,82</sup> The strong radical induced oxidation initiated by indirect photochemistry obviously led to more fragmentation and thus volatilization of volatile oxidation products than functionalization observed, for example, in the ozonation studies in the dark. Monge et al. studied the reactivity of dry soot films toward NO<sub>2</sub> under illumination and reported a persistent reactivity and an enhanced emission of HONO and NO on soot films in the presence of artificial solar radiation.<sup>79</sup> Similar results have been reported by Han et al.<sup>83</sup> Using spectroscopic techniques, they identified nitro and oxygen-containing species among the reaction products adsorbed to the soot surface.<sup>83</sup> Organic compounds containing nitrogen were formed and readily photolyzed, releasing various carbonyl compounds, NO, and HONO in a subsequent experiment with no NO<sub>x</sub> present.<sup>79,83</sup> These observations suggest that soot transported away from a polluted urban environment might provide an active local photochemical source of NO and HONO.

From the huge amount of other combustion-derived primary organics, which to this day remains poorly characterized, only two families will be considered here, PAHs and aromatic

ketones. PAHs, organic compounds bearing several coupled aromatic rings, are ubiquitous in combustion aerosols as they are products of the incomplete combustion of organic matter; they form a specific class of compounds with many impacts, especially due to their mutagenicity and carcinogenicity.<sup>3</sup> Smaller PAHs (2–3 rings) are predominantly found in the troposphere as gases, while larger PAHs are partitioned between phases (3–5 rings) or may exist exclusively in or on condensed phases (5 or more rings). Larger PAHs are therefore accumulated in atmospheric particles and in polar and midlatitude snow.<sup>84</sup> The photochemistry and photodegradation of PAHs have been the focus of quite a number of studies to evaluate their impact on toxicity and aging of particles.<sup>3</sup> Their chemistry is complex and depends on the actual chemical structure of the PAH.

While PAHs are ubiquitous in all combustion particles, biomass burning also results in another important class of compounds, aromatic ketones. They are produced upon thermal degradation of cellulose, hemicellulose, and lignin, which are all present in biomass in massive amounts. Cellulose is a linear polymer of glucose, associated with hemicellulose, another polysaccharide, while lignin is an amorphous polymer built from the following monomeric aromatic building blocks: *p*-coumaryl, coniferyl, and sinapyl alcohols.<sup>85</sup> Burning of biomass will emit a large variety of organic compounds, depending on the exact nature and origin of the biomass, its water content, etc.<sup>75,85,86</sup> Figure 5 depicts schematically the type of expected products arising from cellulose, hemicellulose, and lignin in the case of pyrolysis. It can be seen that many of the products are oxygenated aromatics, unsaturated ketones, which are always found as tracers of biomass burning.<sup>75</sup>

The photochemistry of aromatic ketones has been intensively studied, especially with respect to the photodegradation of various organics, such as phenols, mediated by aromatic ketones.<sup>15a,87</sup> In this context, the H-abstraction reactions by photoexcited aromatic ketones have been the focus point of many studies.<sup>88</sup> Depending on the identity of the hydrogen atom donor, the overall mechanism may involve different pathways (see Figure 2). It may involve a direct H-abstraction pathway (the excited carbonyl acting as an alkoxyl radical, and abstracting a hydrogen atom) or be initiated by an electron transfer from the donor to the excited carbonyl function (as is observed with amines as reaction partners). In complex systems, it can also correspond to a mixture of both mechanisms, forming first an excited-state complex between the ketone and the donor, followed by an activation of the C–H bond by a charge transfer to the C=O function.<sup>88a</sup>

## 2.2. Secondary Organic Chromophores

The dominant fraction of organic compounds emitted to the atmosphere includes methane, isoprene, monoterpenes, small alcohols, saturated hydrocarbons, and other compounds that do not have suitable electronic transitions extending in the near-UV range ( $\lambda > 290$  nm).<sup>89</sup> However, some of their first- and later-generation oxidation products are photochemically active.

**2.2.1. Pyruvic Acid.** The chemistry and photochemistry of pyruvic acid (PA) has been the subject of a significant number of studies recently.<sup>90</sup> This  $\alpha$ -keto carboxylic acid is known to be present in aerosols (especially biogenic ones)<sup>91</sup> and polar ice.<sup>92</sup> It is produced via the aqueous-phase oxidation of methylglyoxal, a well-known oxidation product of isoprene<sup>93</sup> and aromatic compounds.<sup>94</sup> PA easily partitions into atmospheric aqueous phases and films because of its high solubility. The proximity of

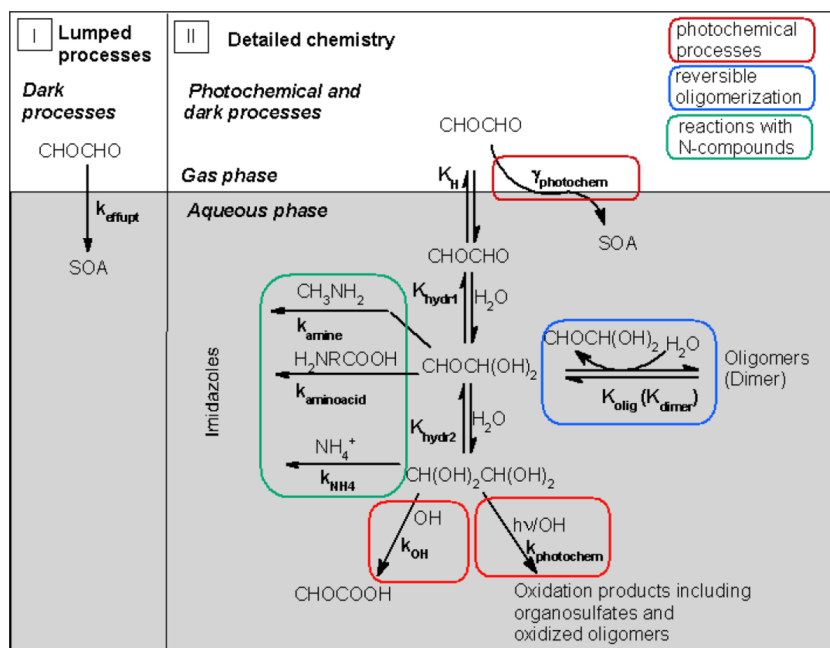


**Figure 6.** Schematic description of the condensed phase chemistry of glyoxal, showing different pathways, including the formation of imidazoles. Reprinted with permission from ref 97c. Copyright 2010 European Geophysical Union - Copernicus Publications.

the carboxyl and carbonyl groups in PA endows it with an enhanced absorption cross section relative to aliphatic carbonyls, as well as unique photochemical pathways. Indeed, out of more than 90 common carbonyls assessed in a study by Epstein et al., PA stood out as the most active in aqueous photochemistry.<sup>95</sup> PA is reversibly hydrated in aqueous solution to its *gem*-diol. The keto form can be excited in the near-UV (with light of  $\lambda > 300$  nm), promoting its photolysis and also the formation of a triplet state that is presumed to be involved in the aqueous phase photochemistry.<sup>90a</sup> Finally, PA has been shown to act as a photosensitizer and promote aqueous reactions of ozone with compounds it does not react with under dark conditions.<sup>96</sup>

**2.2.2. Dicarbonyl Chemistry and Imidazole Production.** Triggered by the suspected importance of glyoxal for SOA production,<sup>31</sup> a significant number of investigations have taken place to describe its multiphase chemistry, which has as products semivolatile, oligomeric products (see Figure 6).<sup>97</sup> The uptake of glyoxal into seed particles containing inorganic (e.g., ammonium (bi)sulfate) or organic solutes (e.g., fulvic acid, dicarboxylic acids, amines, amino acids) is followed by a complex chemistry, which is quite different from the one experienced by glyoxal in dilute solutions representative of cloud droplets. The transition between the two chemical regimes, that is, oxidation under dilute conditions and condensation at higher concentrations, potentially catalyzed by salts, has been clearly demonstrated.<sup>97a,b,98</sup>

More recently, it was shown that this chemistry gives rise to the production of light absorbing products, leading to the production of so-called brown carbon (BrC) in reactions between small water-soluble carbonyl compounds, including glyoxal and methyl glyoxal, and ubiquitous constituents of aerosols such as ammonium sulfate. The spectra of these light-absorbing products extend into the visible range, and may potentially influence absorption coefficients of aerosols containing these colored products.<sup>99</sup> Powelson et al. estimated an upper limit on the contribution of that chemistry of  $\leq 10\%$  of

global light absorption by BrC.<sup>99k</sup> More specifically, the absorbing species were observed to be N-containing compounds bearing an imidazole ring.<sup>99h,k,o,u</sup> The latter compounds were recently shown to act as efficient photosensitizers in organic aerosols; their photochemistry will be described in further detail in section 5.<sup>99l,100</sup>

### 2.3. Humic-Like Substances (HULIS) of Primary and Secondary Origins

It is now recognized that potentially all atmospheric condensed phases (i.e., fog,<sup>101</sup> cloud,<sup>102</sup> rainwater,<sup>103</sup> aerosol,<sup>104</sup> and snow)<sup>105</sup> contain a significant fraction of high molecular weight compounds, often termed HULIS, whose properties were reviewed recently by several authors.<sup>106</sup> This terminology arises from the comparison of HULIS to humic substances found in terrestrial and aquatic environments. Both families of compounds have rather complex molecular structures that defy complete molecular assignments with the currently existing analytical tools. Graber and Rudich reviewed the differences between humic substances and HULIS and described HULIS as being more surface active, less acidic, and having smaller molecular weight and lower degree of aromaticity than their terrestrial and aquatic counterparts.<sup>106a</sup> HULIS are produced by a variety of processes,<sup>106a</sup> including primary emissions (especially in the marine environment),<sup>107</sup> biomass burning, and a variety of heterogeneous or multiphase reactions. The impact of HULIS on cloud<sup>108</sup> and ice nucleation properties has been investigated.<sup>109</sup> For instance, Suwannee River standard fulvic acid, leonardite, and the corresponding O<sub>3</sub>-exposed HULIS particles nucleate ice via deposition mode at  $T \leq 231$  K, but for higher  $T_p$  water is taken up or ice nucleated either via deposition or via immersion mode.<sup>109</sup> HULIS species are also shown to be strongly linked to BrC,<sup>110</sup> and have photochemical properties matching those of humic acids,<sup>111</sup> which have been suggested to be a significant photochemical source of HONO.<sup>4b</sup> In snow and ice, HULIS compounds are a significant contributor to the absorbance by chromophoric dissolved organic matter (CDOM), which may

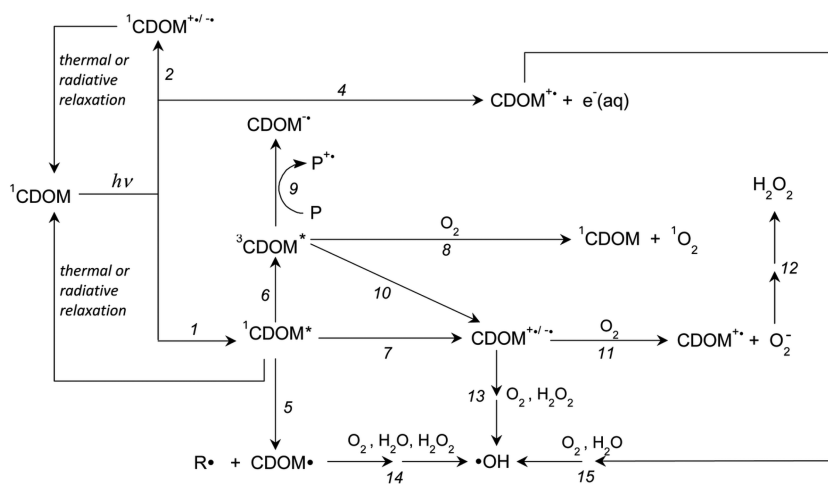


**Figure 7.** Dissolved organic matter photochemical properties. Reprinted with permission from ref 115. Copyright 2014 Royal Society of Chemistry.

make up a large fraction of the total absorbance by natural snow.<sup>84b,112</sup>

The photochemistry of CDOM has been the subject of intensive research as it controls, among other effects, the fate of a variety of organic aquatic pollutants.<sup>113</sup> Humic substances, split for operational purposes into humic acids (soluble above pH 2) and fulvic acids (soluble at all pH values), contribute significantly to the color of CDOM, which therefore comprises a large number of chemical functionalities such as carboxyl-rich alicyclic molecules and substituted phenols, ketones, or aldehydes.<sup>114</sup> The photochemistry of CDOM was recently reviewed by Sharpless and Blough,<sup>115</sup> who stressed the fact that both absorption, extending up to 500 nm, and other photochemical features are due to aromatic chromophores, but still inconsistent with the behavior of individual molecules. This prediction could also be the general case for particle phase chemistry in the troposphere, because particles contain complex matrixes of high molecular weight organic compounds, and their heterogeneous photochemistry could be more complex than that expected of isolated molecules.<sup>116</sup>

To explain the peculiar optical and photochemical properties of CDOM, it has been suggested that they arise, at least in part, through electronic interactions among various chromophores from partially oxidized oligomeric materials; electron donors could include phenols and/or methoxylated phenols, while acceptors could include quinones and/or (aromatic) ketones/aldehydes.<sup>115</sup> These interactions are of primary importance, as they contribute to the long-wavelength, near-UV, and visible absorption and emission properties of CDOM.

It has been known since the 1980s that illuminated CDOM is a photochemical source of singlet oxygen  $^1\text{O}_2$ ,<sup>117</sup> superoxide and hydrogen peroxide  $\text{O}_2^-/\text{H}_2\text{O}_2$ ,<sup>118</sup> solvated electron  $e^-_{\text{aq}}$ ,<sup>119</sup> and organic radicals.<sup>120</sup> More recently, the role of hydroxyl radical and excited triplet states as important photooxidants was discussed.<sup>15a,121</sup> The overall complexity of CDOM photochemistry is illustrated in Figure 7. We should note that a number of interesting questions remain about the comparison of photochemical activity in CDOM and atmospheric HULIS; for example, a recent study by Albinet et al. showed that dissolved organic matter in rainwater is considerably less active than CDOM found in surface waters.<sup>121b</sup>

### 3. MINERAL DUST

Atmospheric photocatalysis by  $\text{TiO}_2$  has been recently reviewed by Chen et al.,<sup>65,122</sup> and will therefore be only briefly addressed here. While photocatalysis is widely used in many engineered systems for water or air cleaning, its natural impact on the atmosphere has only received attention after the seminal suggestion by Parmon.<sup>123</sup>

As stated in section 2.1.1, the redox properties of photocatalytic dust are due to the formation of electron–hole pairs generating  $\text{O}_2^-$  and OH radicals. As a consequence, any adsorbed species that can act as electron acceptors or possess C–H bonds may react at the surface of illuminated dust. It follows that the rate at which these organic gases may be taken up by dust, the so-called uptake rate characterized by an uptake coefficient (eq 2),<sup>47</sup> could be significantly faster under illuminated conditions than in the dark. However, to have any atmospheric significance, the dark reactions have to be slow; any potential enhancement due to photocatalytic processes may not be measurable otherwise. For example, the dark uptake rate of nitric acid ( $\text{HNO}_3$ ) on dust is very fast, potentially approaching the gas-phase diffusion limit.<sup>124</sup> In this case, any additional photoinduced surface reaction would play only a marginal role in controlling the concentration of  $\text{HNO}_3$ . It should be noted that if the products of the photochemistry are different from those of the dark process, such chemistry could nevertheless be important in the atmosphere, for example, by changing the details of the surface composition. In general, however, to have any impact, the trace gas should have a tendency to adsorb to dust (e.g., be somehow polar) and have slow nonradical chemistry (e.g., not undergo efficient acid–base dissociation on the surface).

#### 3.1. Nitrogen Oxides

Interactions of nitrogen oxides ( $\text{NO}_x = \text{NO} + \text{NO}_2$ ) with  $\text{TiO}_2$  have been widely studied,<sup>65</sup> including the reactions occurring under simulated solar irradiation conditions. Only the later types of studies will be briefly described here.

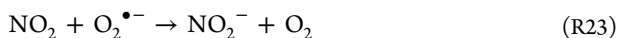
$\text{NO}_2$  has been shown to react heterogeneously on mineral dust in the dark, but at a very slow rate. For example, by means of a Knudsen cell reactor coupled to a quadrupole mass spectrometer, the initial dark uptake coefficient (i.e., interactions on a clean surface at reaction times approaching zero) of  $\text{NO}_2$  on pure  $\text{TiO}_2$  surfaces was measured to be around  $1 \times 10^{-7}$ . The subsequent uptake rapidly decreased to

almost unmeasurable values due to the passivation by adsorbed  $\text{NO}_2$ .<sup>54</sup> This led to the conclusion that  $\text{NO}_2$  dust interactions under dark conditions are not important in the troposphere, and an IUPAC recommended uptake coefficient for  $\text{NO}_2$  reacting on mineral dust surfaces of  $1.2 \times 10^{-8}$ .<sup>20</sup>

However, the steady-state  $\text{NO}_2$  uptake and gas-phase product formation have also been studied under dark and irradiated conditions on  $\text{TiO}_2$ ,  $\text{TiO}_2/\text{SiO}_2$  mixtures, and  $\text{TiO}_2$  containing authentic dust samples.<sup>125</sup> While the dark steady-state uptake coefficients were very small, of the order of  $10^{-9}$ – $10^{-8}$ , under irradiation they have been observed to drastically increase by almost 2 orders of magnitude, in excess of  $10^{-7}$ . The actual uptake coefficients could potentially be even larger because for these studies the entire BET surface was used to normalize the molecular surface collision rates. This photochemical enhancement was shown to be triggered by the  $\text{TiO}_2$  component of the dust studied, for both  $\text{NO}_2$  removal and product ( $\text{NO}$  and  $\text{HONO}$ ) formation.<sup>126</sup> With increasing  $\text{TiO}_2$  content,  $\text{NO}_2$  heterogeneous reactions were observed to proceed faster (i.e., the uptake coefficients increased), producing both  $\text{HONO}$  and  $\text{NO}$  at  $\text{TiO}_2$  amounts up to ca. 85 wt %. With higher  $\text{TiO}_2$  contents, only  $\text{NO}$  was detected as a product. In all cases, adsorbed nitrates were also produced. The  $\text{NO}_2$  uptake was observed to depend on RH, initially increasing at low RH and then decreasing above 20% RH to reach a minimum value at 80% RH,<sup>125a,c</sup> suggesting there is a competition between  $\text{NO}_2$  and  $\text{H}_2\text{O}$  molecules for adsorption sites. The proposed mechanism can be summarized as follows (subscripts vb and cb refer to valence band and conduction band in  $\text{TiO}_2$ , respectively):<sup>126,127</sup>



In the presence of molecular oxygen, there is an electron transfer to  $\text{O}_2$  that acts as the primary electron acceptor, leading to oxygen activated species, which can participate in the previous mechanism as follows:<sup>128</sup>



The production of  $\text{HO}_2^\bullet$  by reaction R24 leads to the formation of  $\text{H}_2\text{O}_2$ , which has been observed by Beaumont et al.<sup>129</sup> Indeed, no  $\text{H}_2\text{O}_2$  is detected in the absence of  $\text{O}_2$ .<sup>128b</sup> Gerischer and Heller have suggested that an electron transfer to  $\text{O}_2$  may be the rate-limiting step in semiconductor photocatalysis.<sup>130</sup> Hirakawa et al. proved that  $\text{O}_2^{\bullet-}$  participates in the decomposition of alcohols.<sup>131</sup> Also, Monge et al.<sup>126</sup> suspected that the formation of  $\text{N}_2\text{O}$  becomes possible at high  $\text{TiO}_2$  content, which was later confirmed by Bedjanian et al.<sup>127b</sup> The above mechanism clearly highlights the fact that the light

enhancement is not a simple acceleration of dark chemistry but rather corresponds to a fully different chemical pathway.

It is known that the chemical interactions between  $\text{NO}_x$  and certain  $\text{NO}_y$  compounds, such as  $\text{HNO}_3$  and  $\text{N}_2\text{O}_5$ , with mineral dust surfaces lead to the formation of adsorbed nitrate, an atmospheric sink for nitrogen oxides in the lower atmosphere with possible effect on the ozone budget, as initially discussed by Dentener et al.<sup>132</sup> Yet, if the dust surface is photocatalytically active, that is, sustaining redox chemistry, then surface nitrate may be reduced back to  $\text{NO}_x$  according to the following processes:<sup>133</sup>



The nitrate ion adsorbed at the oxide surface can react with the holes in the valence band to form a nitrate radical ( $\text{NO}_3$ ). The latter absorbs strongly in the visible range, and can subsequently be photolyzed to form  $\text{NO}$  and  $\text{NO}_2$  through reactions R27 and R28, respectively. This was indeed observed by Ndour et al., who suggested that reactions R26–R28 can serve as a potential renoxification process.<sup>133a</sup> These processes are then in competition with surface photolysis of nitrate anion, as described by Grassian and co-workers.<sup>122,133b,134</sup> Nanayakkara et al. studied the surface photochemistry of nitrate on hematite ( $\alpha\text{-Fe}_2\text{O}_3$ ) particles, identifying the binding process on these surfaces and the  $\text{NO}_2$ ,  $\text{NO}$ , and  $\text{N}_2\text{O}$  products arising from illumination.<sup>135</sup> Also, new surface bound species have been observed, but not conclusively identified.<sup>136</sup> Gankanda and Grassian investigated the photochemistry of nitrate adsorbed on mineral dust aerosol proxies, such as  $\text{Al}_2\text{O}_3$ ,  $\text{TiO}_2$ , and  $\text{NaY}$  zeolite, by means of FTIR spectroscopy, and reported the yield of gaseous  $\text{NO}_2$  production as a function of wavelength.<sup>137</sup> They in fact identified that the  $\text{NO}_2$  yield and the initial rate of production are highest on  $\text{TiO}_2$ , indicating that nitrate photochemistry is more efficient on photoactive oxides present in mineral dust and can then occur over a broader wavelength region of the solar spectrum as compared to nitrate ion in solution.<sup>137</sup> Therefore, dust particles can be regarded as a temporary reservoir of  $\text{NO}_x$  species in the atmosphere and not just a final sink for  $\text{NO}_y$ .

Monge et al. investigated the chemistry of  $\text{TiO}_2/\text{KNO}_3$  50% w/w surfaces (which are unrealistically high in nitrate but provide useful mechanistic insights) illuminated with near-UV irradiation (300–420 nm) in synthetic air and pure nitrogen at room temperature, and observed the formation of gaseous ozone, which is thought to be produced upon the recombination of surface-bound O atoms, produced on the photocatalyst.<sup>79</sup>

### 3.2. Gaseous $\text{H}_2\text{O}_2/\text{HO}_x$ Loss and Production

The uptake of  $\text{H}_2\text{O}_2$  on  $\text{TiO}_2$  surfaces has been studied in the dark on macroscopic surfaces,<sup>138</sup> as well as on aerosol particles as a function of RH.<sup>139</sup> The measured uptake coefficients ranged from ca.  $4 \times 10^{-3}$  under dry conditions to  $2 \times 10^{-4}$  at RH larger than 80%, exhibiting behavior of competitive adsorption of water and  $\text{H}_2\text{O}_2$  and a surface deactivation<sup>24a</sup> (see Figure 8).

The steady-state uptake coefficient of  $\text{H}_2\text{O}_2$  measured in a low pressure flow tube reactor on a UV-irradiated  $\text{TiO}_2$  surface was found to be independent of RH (see Figure 8) but inversely dependent on the initial  $\text{H}_2\text{O}_2$  concentration and

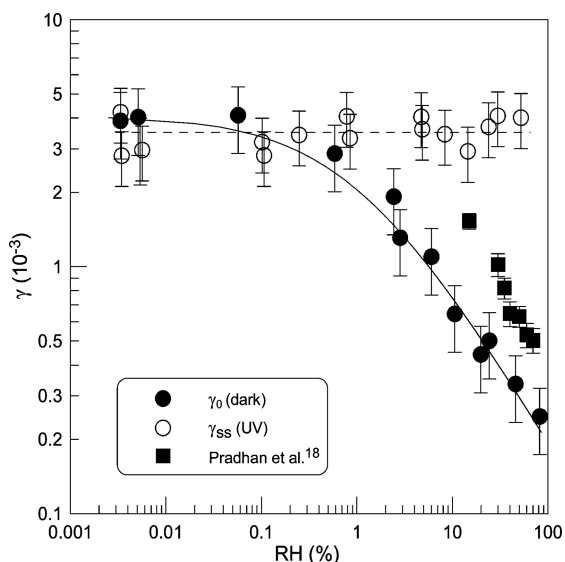
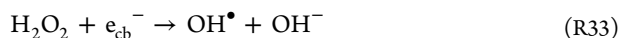
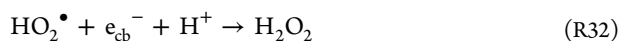
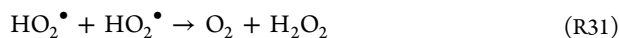
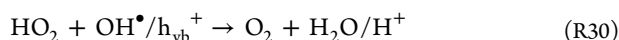
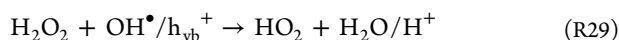


**Figure 8.** Evolution of the uptake coefficient of  $\text{H}_2\text{O}_2$  on dust surfaces as a function of relative humidity in the dark and under illumination, as measured by Romanias et al.<sup>24a</sup> Reprinted with permission from ref 24a. Copyright 2012 American Chemical Society.

increasing linearly with the photon flux.<sup>24a</sup> By adding NO to their reactor, Romanias et al. provided an indirect evidence for  $\text{HO}_2$  radical formation upon  $\text{H}_2\text{O}_2$  uptake.<sup>24a</sup> The production of gas-phase  $\text{HO}_2$  from the surface decomposition of  $\text{H}_2\text{O}_2$  on illuminated  $\text{TiO}_2$  films was directly monitored by means of cavity ring down spectroscopy (CRDS) by Yi et al., with yields depending on the actual nature of the surface (crystalline structure of  $\text{TiO}_2$ ).<sup>140</sup> On very reactive surfaces, such as Degussa P25, the  $\text{HO}_2$  radicals generated in situ seem to be rapidly degraded with little chance of desorption into the gas phase. The primary reaction steps that might be involved in the decomposition of  $\text{H}_2\text{O}_2$  on dust are summarized below (all species are adsorbed to the surface unless indicated otherwise):<sup>140</sup>



Desorption R36 is responsible for the observed production of gaseous  $\text{HO}_2$  radicals. The production of gaseous  $\text{H}_2\text{O}_2$  was also observed by Beaumont et al. in a  $\text{NO}_x$  containing system.<sup>129</sup> The formation of gaseous OH radicals from illuminated  $\text{TiO}_2$  surfaces, in the presence of water, was confirmed by laser-induced fluorescence experiments by Vincent et al., who also indirectly identified gaseous  $\text{H}_2\text{O}_2$ , as a byproduct.<sup>141</sup>

The isolated uptake of  $\text{HO}_2$  radicals on solid films of Arizona Test Dust was also investigated by Bedjanian et al. The uptake was shown to be independent of concentration, temperature, and UV irradiance intensity but to decrease with increasing RH. They reported an upper limit of 5% for the gaseous  $\text{H}_2\text{O}_2$ -forming pathway.<sup>142</sup>

### 3.3. Sulfur Dioxide

By studying the photochemical interactions of  $\text{SO}_2$  on Arizona Test Dust and iron oxide particles in an aerosol flow tube, Dupart et al. observed not only the uptake of  $\text{SO}_2$  onto the particles, but rather new particle formation, indirectly confirming the outgassing of OH radicals from these particles under UV irradiation.<sup>143</sup> It is well-known that under most conditions,  $\text{SO}_2$  heterogeneously reacts on dust surfaces producing particulate sulfate in the dark. However, metal oxides present in mineral dust act as atmospheric photocatalysts promoting the formation of gaseous OH radicals, which then initiate the conversion of  $\text{SO}_2$  to  $\text{H}_2\text{SO}_4$  in the vicinity of dust particles. Under low dust conditions, this process may lead to nucleation events in the atmosphere.<sup>143</sup>

### 3.4. Ozone Loss and Production

Ozone is known to react heterogeneously and irreversibly in the dark with many types of surfaces. The uptake of ozone was observed on authentic Saharan dust surfaces with possible surface passivation with time or  $\text{O}_3$  concentration.<sup>144</sup> This reaction is not very fast; the initial uptake coefficients are around  $10^{-5}$ ,<sup>144</sup> and the steady-state uptake coefficients may range between  $10^{-5}$  at low  $\text{O}_3$  concentration and below  $10^{-7}$  at high  $\text{O}_3$  concentration.<sup>20</sup> The origin of the inverse pressure dependence is likely the formation of a reversible charge transfer complex of  $\text{O}_3$  on the surface, as observed on  $\text{TiO}_2$  and  $\text{Fe}_2\text{O}_3$ .<sup>145</sup> Sample reactivation, over periods of hours, was found to take place after the exposure to  $\text{O}_3$  had ceased.<sup>146</sup>

In contrast to dark conditions, light greatly enhances the loss of  $\text{O}_3$  on authentic dust and on atmospherically relevant surfaces of  $\text{SiO}_2$  doped with traces of  $\text{TiO}_2$ .<sup>147</sup> This enhancement depends on the amount of semiconductor contained in the dust material, and there is no evidence of any surface saturation with time; that is, this photocatalytic pathway represents a sustained loss of  $\text{O}_3$  on dust. The photocatalytic loss of ozone was observed to increase with decreasing ozone concentration and exhibited a complex behavior as a function of RH.<sup>147a,b</sup> Initially, an RH increase results in a faster ozone decay, but further increases in RH yield a slower uptake. The different steps of this mechanism are summarized below:



According to the above sequence of reactions, ozone, which is a stronger oxidant than oxygen, can be reduced by the photogenerated electron producing an ozonide radical anion, which evolves rapidly in the presence of water and generates oxygen and hydroxyl radical. Another pathway for ozone

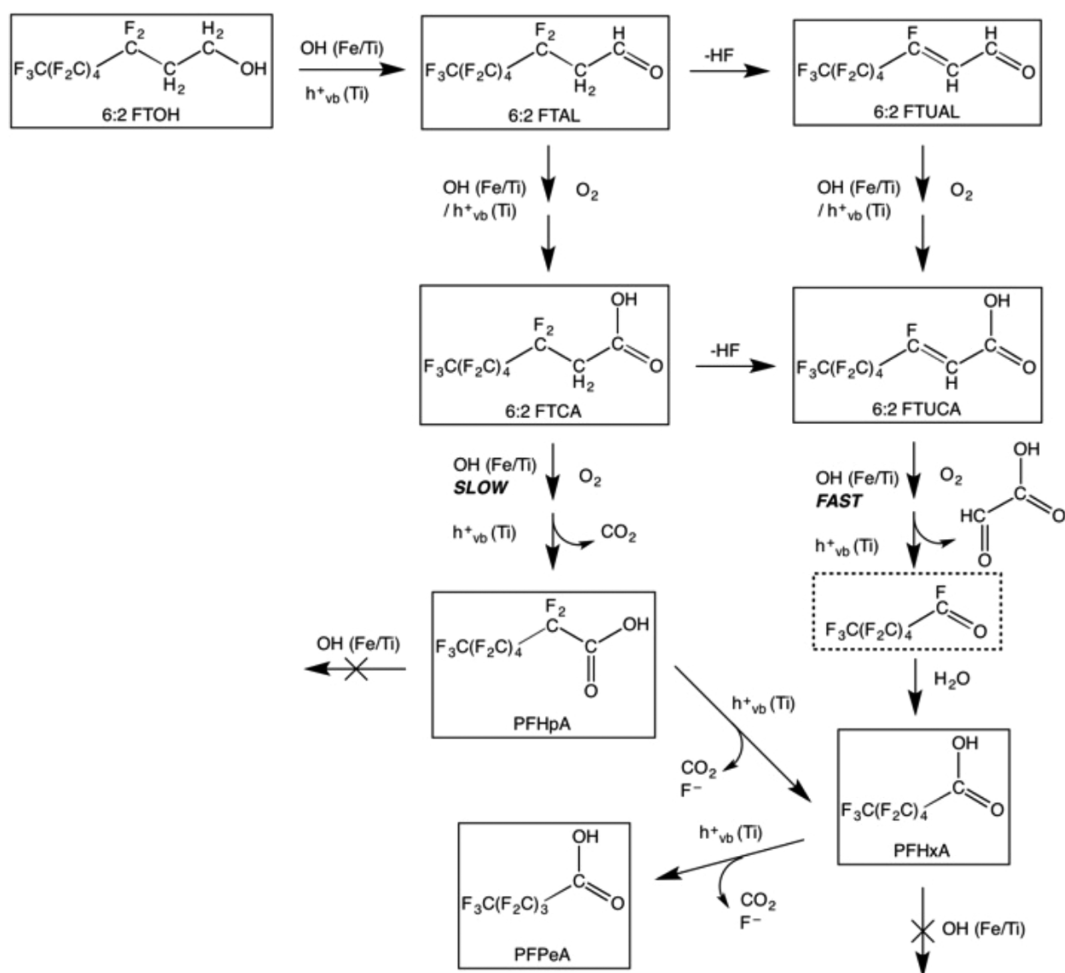


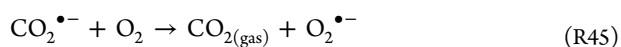
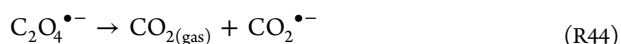
**Figure 9.** Proposed mechanism for surface photooxidation of fluorotelomer alcohols on mineral dust surfaces. Reproduced with permission from ref 149. Copyright 2013 American Chemical Society.

destruction involves the formation of superoxide radical anion, which can react with ozone.

### 3.5. Organic Compounds

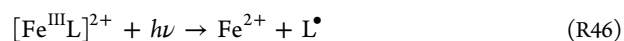
There are numerous studies that focused on the degradation of various VOCs on TiO<sub>2</sub> doped surfaces for understanding and describing air or water cleaning processes,<sup>65</sup> but only limited knowledge is available for these interactions on authentic dust surfaces and/or under atmospherically relevant concentration conditions.

Styler and Donaldson investigated oxalic acid photochemistry at the surface of Fe<sub>2</sub>O<sub>3</sub>, TiO<sub>2</sub>, Mauritanian sand, and Icelandic volcanic ash.<sup>148</sup> Illumination of these sample resulted in the production of gaseous CO<sub>2</sub> that scaled with the loss of surface oxalic acid. While the CO<sub>2</sub> yield followed the absorption spectrum of iron oxalate, suggesting an iron-mediated photochemistry, its variation with O<sub>2</sub> clearly showed that the chemistry is more complex and potentially involves Ti-mediated photochemistry:



Styler et al. further investigated the fate of fluorotelomer alcohols on similar surfaces, on illuminated TiO<sub>2</sub>, Fe<sub>2</sub>O<sub>3</sub>, Mauritanian sand, and Icelandic volcanic ash, and observed the rapid production and subsequent slow degradation of surface-adsorbed perfluorinated carboxylic acids, as well as the production of gas-phase aldehyde products.<sup>149</sup> Figure 9 illustrates the proposed mechanism for these transformations.

The presence of mobile iron in dust particles can have a dramatic effect on the photochemistry of particle-associated organics. The high photoreactivity of the Fe<sup>2+</sup>/Fe<sup>3+</sup> system in aqueous solutions is well-known. It appears that even traces of adsorbed water on particles can make iron accessible to photochemistry. For example, Wentworth and Al-Abadleh found that gallic acid, a trihydroxybenzoic acid hydrolysis product of tannic acid, is efficiently photooxidized in the presence of FeCl<sub>3</sub>, even under relatively dry conditions (1–30% RH).<sup>150</sup> As illustrated in Figure 10, the key photochemical processes involve generation of free radicals from complexes of Fe(III), where the ligand L<sup>-</sup> could be OH<sup>-</sup>, Cl<sup>-</sup>, or phenolate:



In the presence of H<sub>2</sub>O<sub>2</sub>, the Fe<sup>2+</sup> formed in R46 may undergo oxidation via a Fenton reaction, producing more OH radicals as products. Regardless of the way they are formed, the free radicals proceed to react with gallic acid generating a complex soup of products. Similar mechanisms were shown to be

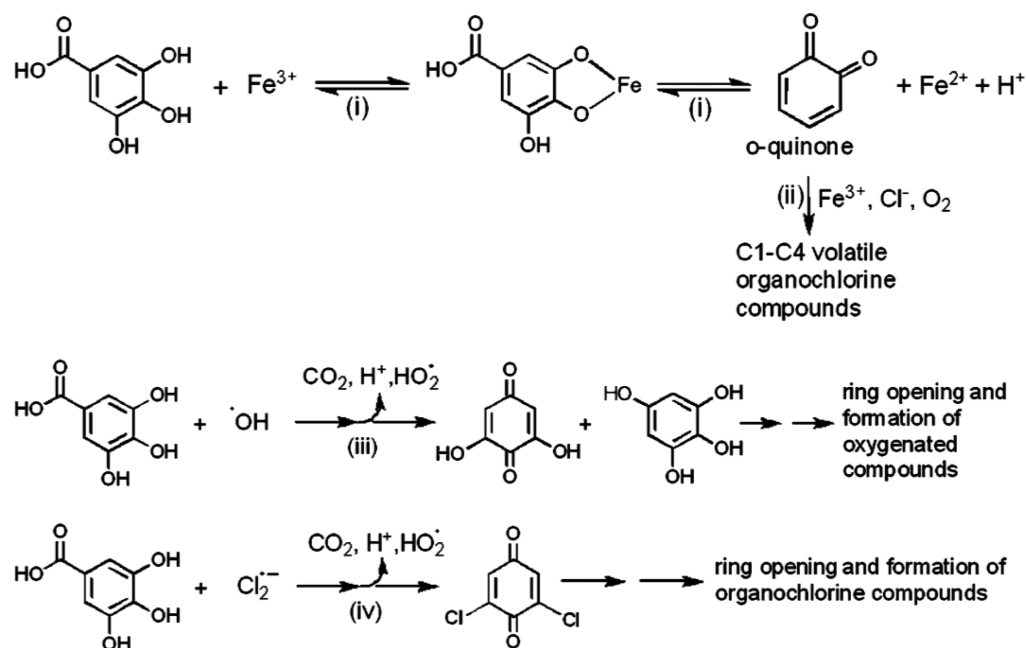


**Figure 10.** Mechanism of Fe(III) photosensitized oxidation of gallic acid. Reproduced with permission from ref 150. Copyright 2011 Royal Society of Chemistry.

operable in catechol adsorbed on  $\text{FeCl}_3$ , and they are likely to be broadly applicable to all organic aerosols containing soluble iron.<sup>151</sup>

Tofan-Lazar et al. investigated the uptake of catechol vapor on  $\text{FeCl}_3$  particles and photoreactivity of catechol-Fe complexes relative to dry conditions and no iron, along with the nature of the hydrogen-bonding network of adsorbed water.<sup>151</sup> They showed that surface water enhances the initial photodecay kinetics of catechol-Fe complexes by a factor of 10, pointing to the role of adsorbed water in enhancing ionic mobility and facilitating electron transfer upon light absorption. Moreover, difference spectra showed changes to the hydrogen-bonding network with irradiation time consistent with the mechanism where hydrated  $\text{Fe}^{3+}$  species photolyze, forming hydrated  $\text{Fe}^{2+}$  species according to the above equation. The generation of Cl radicals in these systems, as suggested by the mechanism shown above, can also lead to the heterogeneous chlorination of any organics present; this was calculated to shorten the organic lifetime by 3 orders of magnitude relative to homogeneous reactions.<sup>151</sup>

Bossan et al. investigated photolysis of several pesticides (Alachlor, Pendimethalin, Trifluralin, Malathion, Terbutylazine, Atrazine, Isoproturon, and Fenithrothion), adsorbed on kaolinite and fly ash particles.<sup>152</sup> They suggested that metals and metal oxides in fly ash particles were responsible for the rapid degradation of the first four compounds; no significant degradation was observed on kaolinite. Lackhoff et al. observed efficient photodegradation of Atrazine, a triazine herbicide, on synthetic and environmental particles.<sup>153</sup> Atrazine photodegraded efficiently on known photocatalysts, such as  $\text{TiO}_2$  and  $\text{ZnO}$ , and measurably on Fe, Ti, and Zn containing minerals. However, no significant activity was observed on soot, fly ash, sand, road dust, and volcanic ash. These studies, and many others, highlight the high sensitivity of the lifetimes of pesticides and herbicides to the kind of particles they are adsorbed to.

These types of processes are not limited to mineral dust and fly ash. Free radicals generated by any condensed-phase photochemical process in close proximity to an organic compound have the potential to indirectly photodegrade this compound. Both nitrate and nitrite are well-known OH radical sources in the presence of water. Karagulian et al. showed that irradiation of mixtures of  $\text{NO}_2^-$  with phospholipid 1-oleoyl-2-palmitoyl-*sn*-glycero-3-phosphocholine (OPPC), which by itself is photochemically stable, resulted in an efficient oxidation of OPPC “from the bottom up” at a typical ambient relative humidity ( $\sim 50\%$  RH), in the presence of just small amounts of adsorbed water.<sup>154</sup> The photooxidation remained efficient in the absence of water, with  $\text{O}^-$  acting as the main reactant. The important conclusion of this study was that organic coatings on particles can be photooxidized even in the absence of gas-phase oxidants by indirect condensed-phase photochemical mechanisms.

### 3.6. Field Observations of Dust Photochemistry

Photoinduced HONO formation was observed in the field during an intense Asian dust storm that originated from the Gobi Desert, captured at a mountain site (Mount Heng) in southern China by Nie et al. during April 2009. The collected dust particles exhibited a large enrichment in secondary species, and photoenhanced nitrite formation indicating photocatalytic HONO production under dust storm conditions.<sup>155</sup> The average nitrite concentration during the collected dust event was  $2.5 \mu\text{g m}^{-3}$ , much higher than that during the nondust days (the mean value =  $0.3 \mu\text{g m}^{-3}$ ), indicating an enhancement of nitrite formation on the dust particles. Furthermore, the enhanced nitrite formation during the dust event occurred only in the daytime samples.

The same group of researchers also presented<sup>156</sup> unique observational evidence of new particle formation and growth associated with mixed dust storm and anthropogenic plumes from North China during spring 2009, that is, a season with occasional dust events in Asia. Both the formation rates and the growth rates of nanoparticles were significantly enhanced

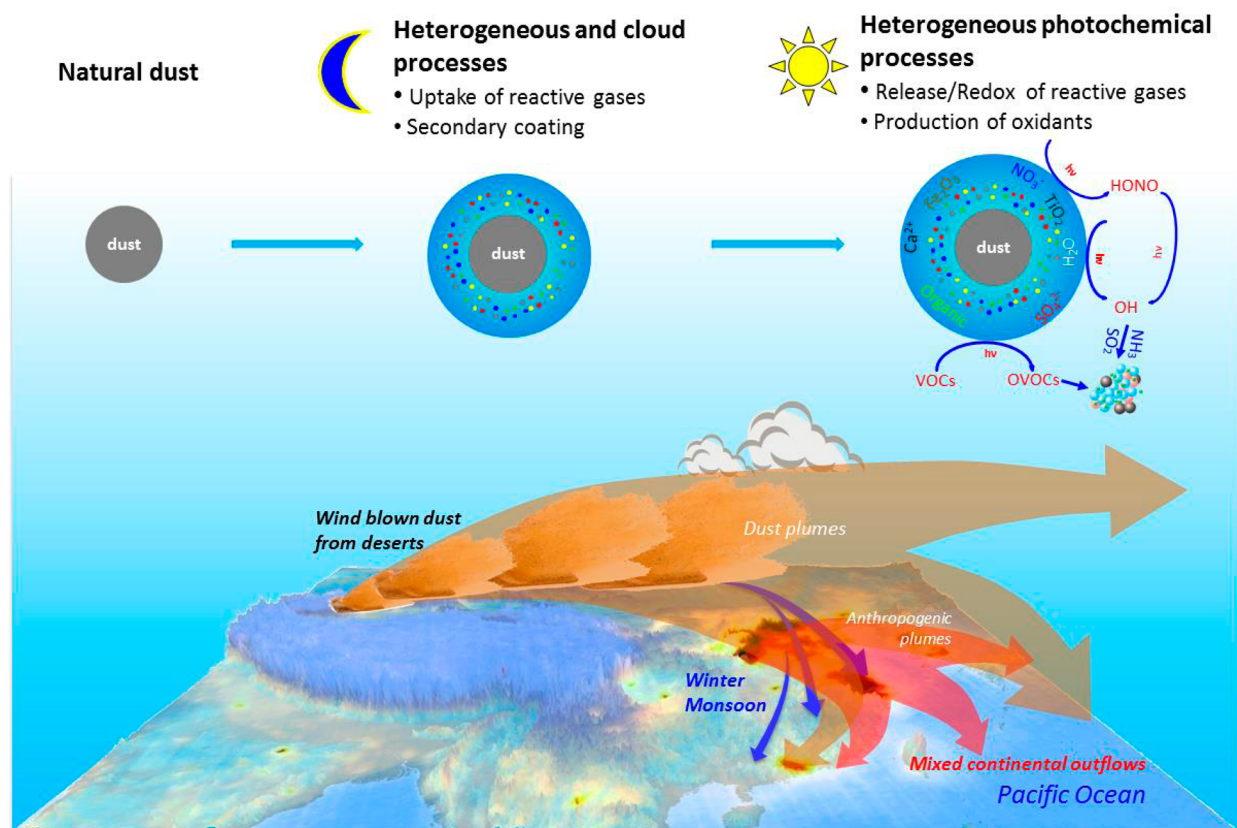


**Figure 11.** Schematic description of the heterogeneous photochemical processes involving Asian dusts during long-range transport in the atmosphere. Reprinted with permission from ref 156. Copyright 2014 Nature.

during dust event days, suggesting an important role of heterogeneous chemical processes, such as photo induced surface redox reactions and gaseous oxidants production, on aerosol formation that arises from the enhanced oxidation of gaseous  $\text{SO}_2$  (as shown in Figure 11).

Two episodes of very high aerosol loadings, with maximum  $\text{PM}_{10}$  mass concentrations of about 248 and  $911 \mu\text{g m}^{-3}$ , were observed associated with unexpectedly intense new particle formation and growth. The formation rates of new particles were slightly higher during dust days than during nondust days ( $0.27$  vs  $0.23 \text{ cm}^{-3} \text{ s}^{-1}$ ), and the highest rate ( $0.45 \text{ cm}^{-3} \text{ s}^{-1}$ ) was observed on the strongest dust day. The particle growth rates were considerably enhanced on dust days, especially in the diameter range 30–50 nm. The mean particle growth rate in this size range on dust days was  $14.3 \text{ nm h}^{-1}$ , more than twice the value on nondust days ( $6.6 \text{ nm h}^{-1}$ ).

#### 4. PHOTOPHYSICAL PROCESSES AT LIQUID INTERFACES

Interfacial dynamics at air/water interfaces have been studied, following the work of Eisenthal and co-workers using second-order nonlinear spectroscopic techniques.<sup>40b,157</sup> Yet reports of direct photochemical reactions at the air/liquid interface are still scarce, especially for atmospherically relevant conditions.<sup>158</sup> McArthur and Eisenthal studied electron-transfer reactions at the air/*N,N*-dimethylaniline (DMA) interface and monitored the buildup of  $\text{DMA}^{\bullet+}$  radical cation.<sup>159</sup> Unfortunately, no direct comparison with the same reaction in the bulk, either in pure DMA or in acetonitrile/DMA mixtures, was performed.

Hydrogen bonding is known to affect, in some cases, the nonradiative relaxation of excited molecules, shortening the

excited-state lifetime of molecules containing carbonyl and nitro groups.<sup>158</sup> For example, the  $S_1$  lifetime of eosin B could be as short as 4 ps in bulk water.<sup>160</sup> Yet the same molecule at a complex alkane/water interface exhibited much longer lifetimes than in the bulk solution, revealing that hydrogen-bond-assisted nonradiative deactivation is no longer or less operative at the interface.<sup>161</sup> Such a significant effect on the excited states at interfaces could potentially lead to enhanced interfacial photosensitized reactions.

Photoenhancement has been observed in some reactions taking place at the air–water interface. When adsorbed at this surface, both chlorophyll<sup>162</sup> and pyrene<sup>163</sup> react heterogeneously with ozone, showing a Langmuir–Hinshelwood kinetic mechanism. Under illumination, the reactions accelerate markedly,<sup>18b,164</sup> and the dependence on the gas-phase ozone concentration seems to change. In the case of chlorophyll, an action spectrum of the rate enhancement confirms that the enhancement is driven by an initial absorption by the chlorophyll chromophore. These observations have been interpreted as the result of electron transfer from the electronically excited organic compound at the interface to ozone, either a nearby gas-phase  $\text{O}_3$  molecule or one that has only recently adsorbed to the surface, followed by hydrolysis of the ozonide anion and reaction of the OH product of this hydrolysis. The new mechanism under illumination is thus similar to that suggested for enhanced ozone uptake on mineral dust surfaces, discussed in section 3. This in turn implies that such reactions at the water surface could give rise to the  $\text{NO}_2/\text{HONO}$  transformation that is observed on mineral dust and other photoactive interfaces. This idea has not yet been fully explored.

As mentioned in section 1.2, energy transfer is an important step in photosensitized reactions, which can be altered at interfaces due to competition between transfer into the bulk or in the two-dimensional interface. This competition is basically triggered by the relative distance between acceptor and donor molecules. This distance may vary if the molecules interact at the interface directly or between the interface and the underlying bulk phase.<sup>40b</sup> Sitzmann and Eisenthal identified, in the case of Rhodamine 6G as the donor and the 3,3-diethyloxadicyanin as the acceptor, considerably greater energy transfer at the interface, consistent with the shorter donor–acceptor distances at the interface (50–100 Å) as compared to bulk liquids (130 Å) and concluded that in this case transfer of energy between interface and bulk molecules can be neglected.<sup>165</sup>

An interface can act similarly to the solvent cage mentioned in section 2 by the recombination of molecules due to its asymmetry; that is, these compounds could be in distinct phases while still meeting at the interface. So far, such processes have only been studied at the liquid/liquid interface in the case of electron transfer between an organic electron donor phase and an aqueous acceptor.<sup>166</sup>

Although the photochemistry of nitrate ions in bulk aqueous solution is well-known (see section 2.1.2), there is experimental and theoretical evidence that it may be more efficient at liquid–gas interfaces, and that the presence of other ions in the liquid film may enhance interfacial reactivity (see ref 167 and references therein). Recent experiments on deliquesced thin films of mixed salts (halides and nitrates) revealed an enhanced photochemistry of nitrate in the presence of either chloride, bromide, or a mixture of the two.<sup>168</sup> This enhancement was explained by two combined effects: (a) an increased concentration of the halides closer to the air–water interface that attracts Na<sup>+</sup> cations, which in turn draw nitrate ions closer to the surface; and (b) by a reduced solvent cage effect of nitrate ions,<sup>168</sup> some enhancement could also be due to the reduction of the recombination reaction between the products of aqueous nitrate photolysis.<sup>169</sup> The same group showed that bromide anions had a higher propensity for the interface than chloride and, as consequence, showed a greater effect of nitrate photochemistry.<sup>168a–c</sup> When bromide was also present in the nitrate film, Br<sub>2</sub> was detected as a gas-phase product.<sup>168a,b</sup> Hong and co-workers<sup>170</sup> used glancing-angle Raman spectroscopy to measure nitrate concentrations at the air–aqueous interface, and observed an increase of nitrate at the air–water interface in bromide-containing solutions over those with nitrate alone, consistent with the MD simulations.<sup>167,168</sup> The enhanced photochemistry of nitrate at interfaces implies higher production of NO<sub>2</sub>, OH, and Br<sub>2</sub>, and such a process might have a potential impact at local and regional levels.<sup>168a–c</sup>

The enhancement of quantum yields at interfaces might have a number of other implications: if OH and O(<sup>3</sup>P) are formed at the surface of aerosols and films, their presence could enhance the reactivity of such surfaces toward adsorbed compounds (both organic and inorganic). Evidence of such a process has been reported for deliquesced films of NaNO<sub>3</sub> with gaseous  $\alpha$ -pinene. NO<sub>2</sub> was measured among the gaseous products together with pinonic acid, pinic acid, and *trans*-sorbrol and various hydroxy-aldehydes and organonitrates.<sup>171</sup>

The formation of oligomeric compounds in atmospheric aerosols is a subject of active discussion. Photopolymerization has been intensively studied due to the requirements of microelectronic surfaces in microlithography, as well as interest

in the fundamental science of polymerization in the restricted environment of an interface. For example, the photografting polymerization reactivity of various monomers that can undergo free-radical chain polymerization was examined by Yang et al., using benzophenone as the photoinitiator.<sup>172</sup> They showed that the surface reactivity in this system was governed by surface hydrogens and polarity. De Samaniego et al. showed that amphiphilic peptides comprising alternating hydrophilic and hydrophobic amino acid residues undergo fast UV-induced cross-linking at the air–water interface.<sup>173</sup> They also showed that the kinetics and extent of the reaction depend on the initial film organization, where a closer molecular packing leads to faster kinetics and more extensive network formation.

Are such processes also occurring under atmospherically relevant conditions, with enhanced oligomer formation at interfaces? This question remains open to future research.

## 5. ORGANIC AEROSOL PHOTOCHEMISTRY

### 5.1. General Considerations

The primary focus of this Review is heterogeneous photochemistry occurring at the atmospheric surface–air and other environmental interfaces. However, in many cases, the interfacial photochemical processes cannot be easily decoupled from the condensed-phase photochemistry occurring in the bulk of the material, as described, for example, in section 6 dealing with photochemistry on ice surfaces. This situation also applies to aqueous droplets and to aerosol particles that can be considered liquid in a sense that diffusion of molecules to and from the surface is faster than the photochemical reactions in the particle. In this section of this Review, we will discuss the bulk photochemical processes that take place in the “organic phase” associated with POA and SOA. The aqueous photochemical processes occurring in cloud droplets, fog droplets, and aerosol liquid water are thoroughly addressed by Herrmann et al.<sup>13</sup>

While the definitions of the atmospheric gaseous and aqueous phases are relatively straightforward, there is currently no accepted terminology to describe the phase(s) associated with particulate matter. By definition, an aerosol represents a colloidal suspension of particles in a gas, and it includes both particles and gases surrounding the particles. Therefore, the term “aerosol phase”, which is occasionally used to refer to solid or liquid states of individual particles in an aerosol, is ambiguous and should not be used without additional modifiers. The term “particle phase” also has disadvantages because atmospheric particles generally consist of multiple domains, which are easily observable in electron microscopy images of individual particles. We prefer to use the term “organic phase” or “aerosol organic phase” or simply “solvent” to refer to a homogeneous particle domain dominated by a mixture of organic compounds, which could be of primary or secondary origin. The related term “organic matrix” will be used to refer to the unique environment experienced by molecules in the organic phase in aerosols. The same terminology should be applicable to organic-rich domains in urban grime, which is discussed in section 8, and in other environmental surfaces. The organic phase may certainly contain water and inorganic compounds dispersed through the matrix. For example, particles of ammonium sulfate mixed with certain organic materials in the presence of water vapor consist of two liquid phases: a deliquesced ammonium sulfate core contaminated by dissolved organics, and an organic shell containing water.<sup>37</sup>

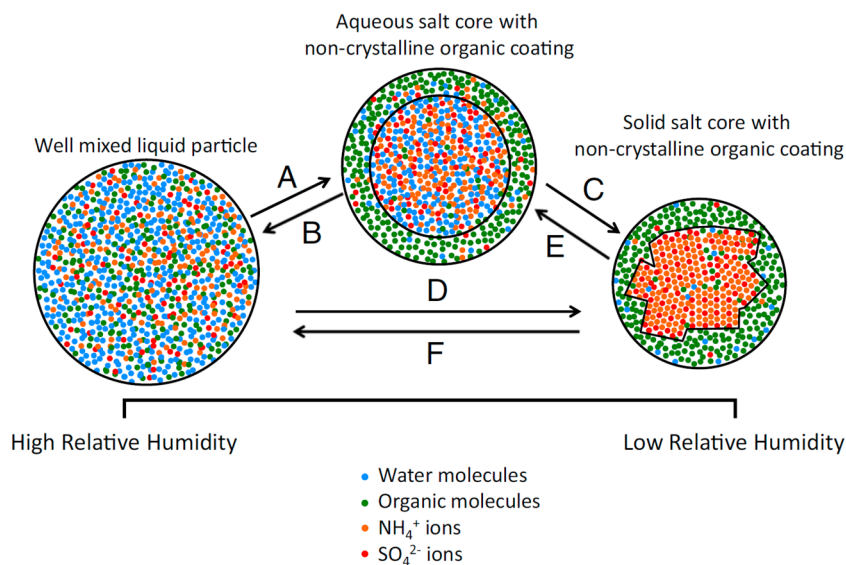


**Figure 12.** A representation of the possible phase transitions in mixed particles of oxygenated organics and ammonium sulfate. What is called “organic phase” in this Review corresponds to the green organic coatings on either solid or liquid core. Reproduced with permission from ref 37. Copyright 2012 National Academy of Sciences of the USA.

Figure 12 schematically illustrates possible phase transitions in such mixed particles.

In ambient particles, especially the highly aged ones, the organic phase typically appears attached to an inorganic domain (ammonium sulfate, mineral dust, soot, etc.). However, nearly purely organic “tar balls” have also been observed in field studies.<sup>174</sup> In a secondary organic aerosol generated in a smog chamber by homogeneous nucleation (without a seed aerosol), each particle will consist of more or less the same organic phase. When a sufficient amount of such particles are collected on a substrate, they can coalesce into a macroscopic amount of “secondary organic material” or SOM. With appropriate tools, this material can be prepared in a form of a homogeneous organic film, making it possible to study its physical properties.<sup>175</sup>

The organic phases in atmospheric aerosols can have an incredible level of molecular complexity, with thousands of molecules being simultaneously present in the same particle as revealed, for example, by high-resolution mass spectrometry analysis.<sup>176</sup> Furthermore, the particle composition does not remain constant during its atmospheric lifetime, which is typically several days. On this time scale, organic compounds in particles have been shown to undergo extensive chemical transformations, which affect their hygroscopic properties, optical properties, and toxicity.<sup>27,76a,108,177</sup> A significant fraction of these aging processes are driven, either directly or indirectly, by solar radiation. As already discussed above in the context of surface photochemistry, we can approximately classify the photochemical aging processes involving aerosols on the basis of their type and the media where the aging chemistry is taking place. This section specifically focuses on the following two photochemical aging processes: (i) The first is photosensitized and photocatalytic processes, in which primary absorbers, typically large organic molecules, metals, soot, or certain mineral dust components, create transient oxidants in the particle through various energy transfer processes.<sup>153,178</sup> The free radicals and other reactive species photochemically generated within the organic matrix then oxidize photochemically inert organic compounds that happen to be nearby.

Photosensitized photochemical processes are discussed in multiple sections of this Review, including this one, because of their pervasive nature in the environment. (ii) The second is photodegradation of organic compounds by direct photolysis, in which case the primary absorber of radiation breaks into fragments.

As compared to the much better studied aerosol aging mechanisms involving heterogeneous reaction of OH, O<sub>3</sub>, and other oxidants with particles, organic phase photochemistry is much less understood. For the organic phase photochemistry to have a significant effect on aging of aerosols, the following conditions must be satisfied: (i) organic aerosol compounds must have significant absorption cross sections in the tropospheric actinic window ( $\lambda > 300$  nm); (ii) the yield of photochemical reactions, such as photodissociation, photoisomerization, intermolecular hydrogen atom transfer, etc., must be large as compared to that for fluorescence, vibrational relaxation, geminate recombination, and other nonreactive processes. As discussed in the introduction, a number of primary and secondary organic compounds fit these criteria. For example, it has been known for some time that certain aromatic compounds associated with particulate matter undergo efficient photodegradation because of their large absorption cross sections and rich photochemistry.<sup>179</sup> However, photodegradation of SOM produced from biogenic, nonaromatic precursors has also been shown to be efficient,<sup>180</sup> suggesting that even the weakly absorbing carbonyl, peroxide, and organic nitrate compounds can photolyze on atmospherically relevant time scales. The mechanisms of direct photochemical aging of aerosols remain poorly constrained at present time. The field experiments on aerosol organic phase photochemistry are essentially nonexistent. To the best of our knowledge, none of the organic phase photochemical processes have been incorporated into air pollution models (only “back-of-the-envelope” types of modeling have been conducted so far).<sup>181</sup> However, the laboratory evidence for the importance of these processes is steadily growing, as discussed below, and we should anticipate the organic phase photochemistry in aerosols will soon find its way into atmospheric models.

It is important to acknowledge the vast amount of experimental data from the synthetic organic photochemistry research community, summarized in a number of books on this topic.<sup>182,183</sup> While this information is of critical importance for the fundamental understanding of photochemical processes in organic compounds, its applicability to organic aerosol chemistry is not straightforward for several reasons. First, the majority of synthetic organic photochemistry experiments rely on the 254 nm mercury line as the radiation source, a wavelength that is largely irrelevant for tropospheric photochemistry because it is fully attenuated by the stratospheric ozone layer. Second, most of these experiments have been carried out in inert solvents such as hexane, which is a poor model for the organic phase found in aerosols. This Review will primarily focus on bulk organic photochemistry experiments carried out with more relevant irradiation sources (with  $\lambda > 290$ ) and in more relevant solvents or in solvent mixtures attempting to more realistically mimic organic phases in aerosols.

## 5.2. Smog Chamber and Aerosol Flow Tube-Based Experiments

There is a rich history of studying SOA formation in photochemical smog chambers dating all the way back to the pioneering experiments of Haagen-Smit.<sup>184</sup> Because the smog chambers are equipped with UV radiation sources, one would think that organic phase photochemistry in SOA should have been a thoroughly known subject by now. However, observation of direct condensed-phase photochemical processes in chamber (and field) studies of SOA is quite challenging because of the lack of clean separation of aerosol formation/growth resulting from gas-phase reactions from the concurrent organic phase processes. The chamber content is normally exposed to actinic radiation to produce free radicals needed for SOA formation, growth, and aging. The direct condensed-phase photochemistry always has to compete with the heterogeneous oxidation of particles by photochemically generated gas-phase free radicals and oxidants.

Despite these complications, it has been possible to discern the effects of UV irradiation on the yields and composition of SOA in several smog chamber studies. For example, UV irradiation during ozonolysis of  $\alpha$ -pinene decreased the SOA yield by as much as 20–40%, most likely due to a shift in the product volatility distribution to higher volatility species resulting from a combination of gas-phase and particle-phase photolysis processes.<sup>185</sup> Similar observations of the suppression of SOA yield were made for limonene SOA under UV illumination.<sup>186</sup> More recently, Henry and Donahue examined the competing effect of photolysis and OH exposure on  $\alpha$ -pinene ozonolysis SOA by cleverly manipulating the mechanisms of OH generation in the chamber.<sup>187</sup> Exposure of SOA to OH generated by a dark reaction (no UV radiation present) between ozone and tetramethylethene increased the aerosol mass concentration. However, under irradiated conditions, the SOA growth slowed, or even reversed, because of photofragmentation of highly functionalized organic molecules that would otherwise end up in particles. Because of the chamber design of the experiments, it was not possible to say with certainty whether the photofragmentation occurred in the gas phase or organic phase. SOA formed by photochemical oxidation of isoprene was found to be susceptible to photodegradation as well. For example, Kroll et al. observed initial SOA growth during the irradiation of a mixture of

isoprene and hydrogen peroxide under low-NO<sub>x</sub> conditions, followed by a decrease in particle size as the SOA mixture was continuously irradiated.<sup>188</sup> Surratt et al. detected similar decreases in the particle size of low-NO<sub>x</sub> isoprene SOA upon irradiation.<sup>189</sup> The fraction of condensable peroxides<sup>189</sup> and the effective yield<sup>190</sup> of SOA particles prepared by photooxidation of isoprene decreased with irradiation time, implying that photochemical aging was occurring after the initial particle formation.

The effect of condensed-phase photolysis is not limited to the highly oxidized organic compounds associated with SOA; compounds found in POA may be susceptible to condensed-phase photochemistry as well. For example, Leskinen et al. studied POA from wood chip combustion in an outdoor chamber, and concluded that heavier aerosol compounds may be degrading into lighter ones in particles.<sup>191</sup> Zhong and Jang examined biomass-burning aerosols, also in an outdoor chamber, and concluded that there is a competition between production of larger chromophoric compounds and photodegradation of these chromophores that occur on comparable time scales of hours.<sup>192</sup>

The above-mentioned studies could not fully decouple the relative importance of gas-phase and condensed-phase processes. Several experimental approaches have attempted to overcome the complications arising from the simultaneous presence of photolyzable organic vapors and particles in chamber studies. In one approach, a tracer molecule of interest was added to a chamber containing particles, and the tracer molecule decay was observed in both the particle and the gas phase. The caveat of this method is that the tracer must be of sufficient volatility to allow it being injected into the chamber in measurable amounts, but it should also be of sufficiently low volatility to ensure that it resides predominantly in the particle phase; otherwise it will be difficult to separate particle-phase processes from gas-phase chemistry followed by repartitioning of the products. Fan et al. used this approach to investigate photodegradation of deuterated (so that they can be easily tracked) PAH and nitro-PAH compounds on diesel exhaust and wood smoke particles in an outdoor chamber.<sup>179a</sup> They found that 1-nitropyrene, 2-nitropyrene, 1-nitrofluoranthene, 3-nitrofluoranthene, and 8-nitrofluoranthene efficiently photodegraded in the presence of soot particles with the condensed-phase photolysis acting as the main loss pathway. They concluded that photodegradation of nitro-PAH was strongly dependent on the chemical and physical properties of the particles with which the nitro-PAH were associated.

In another approach,  $\alpha$ -pinene ozonolysis aerosol created in a chamber was collected, re-aerosolized in a separate chamber by atomization, and photolyzed.<sup>193</sup> The particle size distribution shifted to lower masses as a result of photolysis inside the particles leading to a loss of volatile products. A significant change in the particle composition was observed with an aerosol mass spectrometer. The efficiency of photolysis appeared to increase at higher RH levels, suggesting that the presence of water in particles accelerates their photolysis, likely due to moisture-induced changes in the organic phase. In a related approach,  $\alpha$ -pinene ozonolysis aerosol produced in a chamber was drawn in a photolysis flow tube through a set of denuders.<sup>194</sup> The denuders stripped most of the remaining oxidants and most volatile organic compounds from the particles, allowing only for the low-volatility particulate compounds to come through. Exposure of the residual particles in a flow cell to UV radiation produced a small change in

particle size distribution but a significant change in chemical composition. Most significantly, the peroxide compounds were degraded with an effective atmospheric photolysis lifetime on the order of several days (which is of the same order of magnitude as the lifetime of particles with respect to their removal by wet and dry deposition). It is worthy of note that experiments with and without the denuders showed the same trends, implying that condensed-phase processes possibly dominated over gas-particle reactions. The applicability of this result to other SOA systems will need to be verified in future experiments, but it is likely that other biogenic and anthropogenic SOA will similarly respond to condensed-phase photolysis by shedding volatile photolysis products and thereby changing the particle composition on atmospherically relevant time scales.

A number of relevant experiments have been carried out by aerosolizing suitably chosen mimics of POA or SOA and exposing them to UV or visible radiation in a flow tube. For example, Sareen et al.<sup>99m</sup> examined photolysis and ozone oxidation of organic material resulting from aqueous reactions between methylglyoxal with ammonium ( $\text{NH}_4^+$ ), which is known to produce model imidazole-based brown carbon (BrC) compounds.<sup>99o,u</sup> As discussed in a separate review in this issue,<sup>195</sup> BrC is a carbonaceous aerosol that absorbs near-UV and visible radiation with a much steeper wavelength dependence than observed for black carbon (soot) dominated aerosols.<sup>74a</sup> BrC can contribute significantly to the light absorption by aerosols, but to have any measurable effect on climate, BrC has to be photochemically stable with respect to photobleaching.<sup>196</sup> Sareen et al. data suggest that the primary absorbers in the methylglyoxal +  $\text{NH}_4^+$  brown carbon undergo remarkably rapid photolysis on a time scale of minutes leading to small volatile photooxidation products including formic acid, acetic acid, and glyoxylic acid.<sup>99m</sup> We note that BrC produced by other mechanisms, such as photooxidation of naphthalene, is considerably more resilient to solar radiation.<sup>197</sup>

### 5.3. Photodegradation of Bulk Materials Mimicking Organic Aerosols

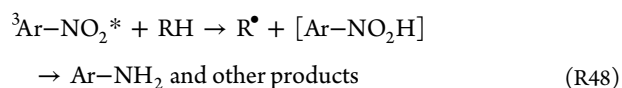
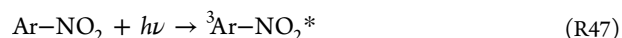
Experiments on photodegradation of suitable organic compounds or mixtures of organic compounds mimicking a given type of POA or SOA have a long history. An organic solution or film is irradiated with a suitable light source in a photoreactor, and the composition of the material and/or volatile photolysis products probed with sensitive analytical methods. This bulk photochemistry approach eliminates the interference from gas-phase oxidants and volatiles present in the smog chamber studies discussed above, but it makes it challenging to extrapolate the results to the behavior of atmospheric aerosols because of the mass-transfer and various other limitations associated with bulk materials. For example, dissolved molecular oxygen may not be able to enter and volatile products may not be able to escape from the bulk organic material as quickly as they would from an aerosolized material. In addition, the surface effects are amplified considerably in an aerosol as compared to the bulk solution. For example, the photolysis yield of  $\text{Fe}^{2+}$  from 300 nm ferrioxalate ( $[\text{Fe}(\text{C}_2\text{O}_4)_3]^{3-}$ ) photolysis was found to be increased in an aqueous aerosol by a factor of  $\sim 50$  relative to the bulk solution because ferrioxalate was enhanced on the surface where the electromagnetic radiation was amplified.<sup>198</sup> Nevertheless, a number of important insights have been obtained from bulk

photochemical experiments. Several important examples will be mentioned below; this is by no means a comprehensive list.

**5.3.1. Polycyclic Aromatic Compounds and Their Derivatives.** In a series of studies, McDow et al. investigated the effect of the organic matrix on the PAH photodegradation rates.<sup>179b,c,199</sup> They used a liquid-phase photoreactor to photolyze benz[*a*]anthracene, benzo[*a*]pyrene, and other PAH compounds dissolved in toluene in the presence of different classes of organic compounds associated with aerosols. The PAH removal rate was found to depend sensitively on the added solutes. This study showed that methoxyphenols, aromatic ketones, quinones, furans, and substituted benzaldehydes were efficient promoters of the PAH photodegradation, while carboxylic acids and carbohydrates had no significant effect. Several competing mechanisms were implicated, such as free-radical reactions initiated by abstraction of hydrogen atoms from the solvent by the photo excited molecules, reactions from the triplet state, and reactions involving singlet oxygen.

A number of studies compared photodegradation of bulk PAH films adsorbed on environmentally relevant surfaces with photochemistry of the same PAH in dilute organic solutions. Because of space constraints, only selected examples are mentioned here. Sotero and Arce examined 320–580 nm irradiation of perylene adsorbed on silica gel, as a model of particulate matter.<sup>200</sup> The major observed products were 1,12-perylenedione and 3,10-perylenedione. Their results suggested two mechanisms of photodegradation operating in parallel, one involving singlet oxygen ( $^1\text{O}_2$ ) produced by energy transfer from the photoexcited perylene, and one involving perylene radical-cation. The latter mechanism was not observed in dilute solutions, and appears to be unique to adsorbed perylene. Similar conclusions were reached by Fioressi and Arce for photodegradation of benzo[*e*]pyrene; the major dione, diol, and hydroxy photoproducts were formed in the film but not in a hexane solution.<sup>201</sup> These results highlight the sensitivity of the PAH photodegradation mechanism to the surrounding matrix. The involvement of the PAH radical-cations was also observed, for example, by Reyes et al. in 300 nm photodegradation of pyrene on activated silica surfaces.<sup>202</sup> The main photoproducts were 1,6- and 1,8-dihydroxypyrene, as illustrated in Figure 13.

Feilberg and Nielsen carried out experiments on the photodegradation of nitro-PAH in viscous organic media, in glycerine as a model of polar organic phase in SOA and diisooctyl phthalate as a model for the organic phase of combustion particles.<sup>179d,e</sup> The nitro-PAH ( $\text{Ar}-\text{NO}_2$ ) were shown to undergo photoreduction to amino-PAH ( $\text{Ar}-\text{NH}_2$ ) resulting from the excited-state reactions of nitro-PAH with the solvent molecules.



Although the photoreduction of nitro-PAH to amino-PAH in the presence of alcohols is well documented in the organic photochemistry literature,<sup>203</sup> the Feilberg and Nielsen study was done in more atmospherically relevant solvents. The photodegradation was strongly accelerated by the presence of anthraquinone (AQ), which acted as a photosensitizer giving rise to additional free radical chain reactions.

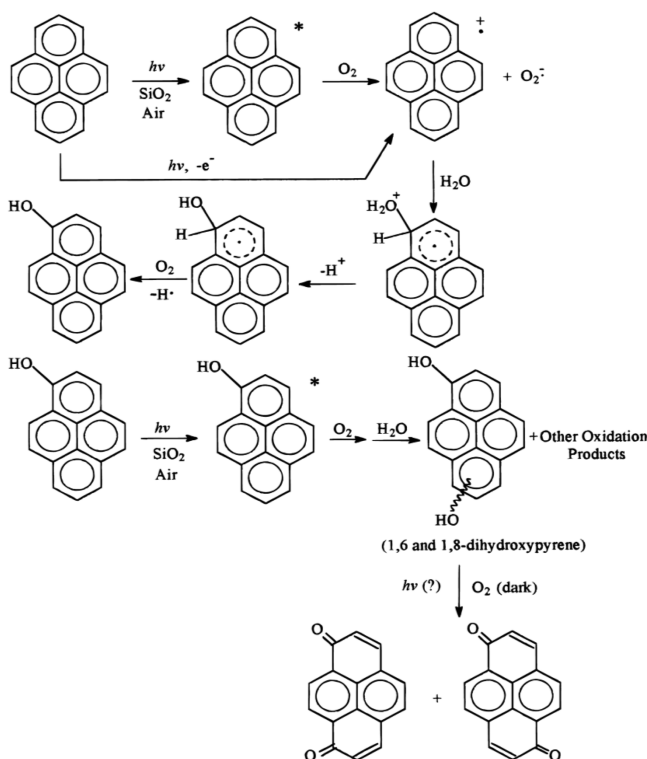


**Figure 13.** Schematic mechanism illustrating the involvement of radical-cations (produced either directly or in reactions with singlet oxygen) in photodegradation of adsorbed pyrene. Similar mechanisms likely operate in other adsorbed PAH compounds. Reproduced with permission from ref 202. Copyright 1999 American Chemical Society.



The authors concluded that viscosity of the matrix does not serve as a major impediment to nitro-PAH photodegradation in aerosols by either of these two mechanisms; if anything, the effect of AQ was more pronounced in a viscous solvent.

Garcia-Berrios and Arce published a thorough study of the mechanism of 300–420 nm photodegradation of 1-nitropyrene in various organic solvents (alcohols, benzene, toluene, saturated hydrocarbons, tetrachloromethane, and acetonitrile).<sup>204</sup> In solvents with easily abstractable hydrogen atoms, such as alcohols, the main products were 1-hydroxypyrene and 1-hydroxy-2-nitropyrene (the migration of the  $-\text{NO}_2$  group was explained by a cage effect, see Figure 14). The measured photodegradation quantum yield was of the order of  $\sim 10^{-3}$  in toluene, benzene, and polar protic solvents; it decreased to  $\sim 10^{-4}$  in saturated hydrocarbon solvents. The presence of molecular oxygen decreased the yield, and so did the presence of water (when added to acetonitrile). However, phenolic compounds increased the photodegradation yield. No significant effect of the solvent viscosity between hexane and hexadecane was observed on the photodegradation.

Dolinová et al. studied the photochemistry of model organic pollutants in waxy matrixes representative of organic aerosols, in paraffin and spruce wax.<sup>205</sup> They examined intramolecular rearrangements of valerophenone and 2-nitrobenzaldehyde (the latter is a common actinometer),<sup>206</sup> hydrogen atom abstraction between excited benzophenone and the paraffin/wax hydrocarbon chains, and photochemistry of common chlorinated pollutants. They intentionally picked the systems that were believed to be sensitive to confining restraints of the

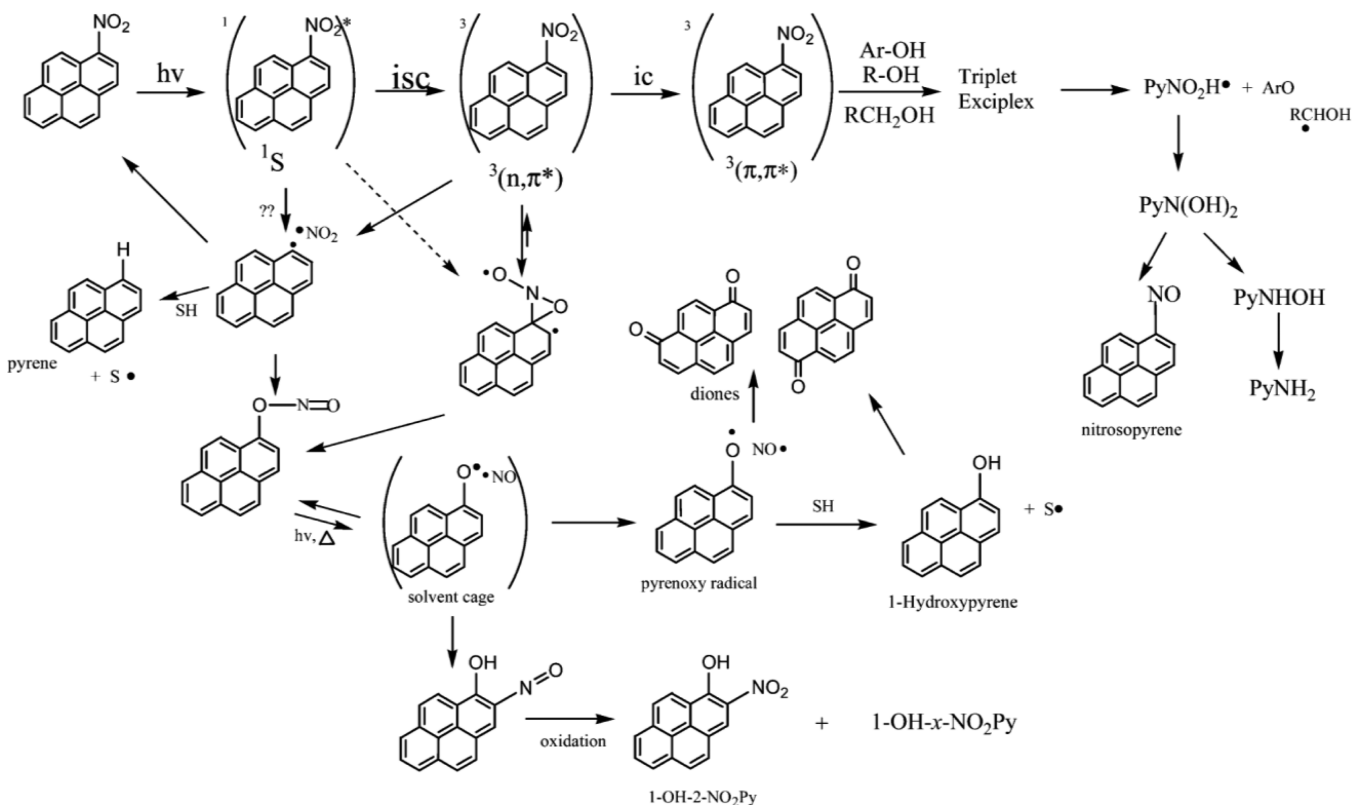


**Figure 14.** Mechanism of photodegradation on nitropyrene. Reproduced with permission from ref 204. Copyright 2012 American Chemical Society.

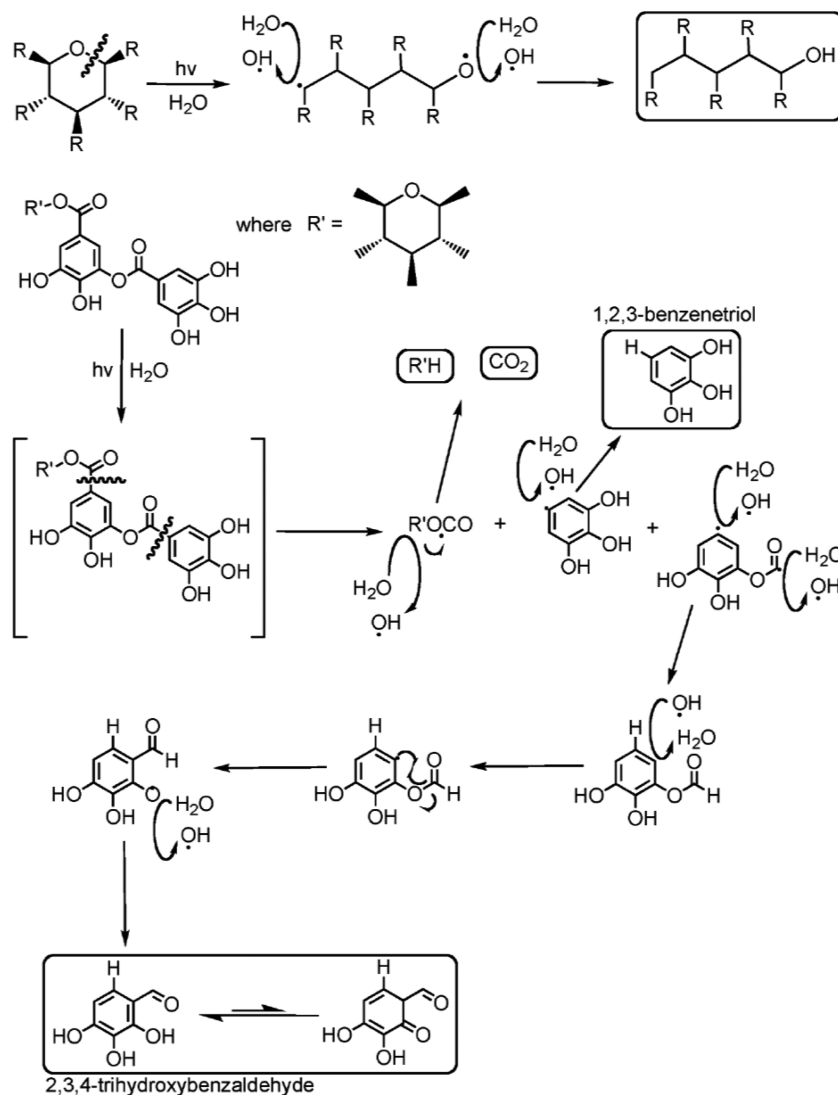


**Figure 15.** Proposed mechanism of photodegradation of tannic acid. Reproduced with permission from ref 212. Copyright 2009 Royal Society of Chemistry.

surrounding matrix.<sup>207</sup> They noted that the viscous nature of the organic matrix presented certain restrictions for the bimolecular reactions, such as hydrogen atom transfer, but did not fully impede photochemistry.

The perception by the atmospheric chemistry community of the true viscosity of natural organic aerosols has changed significantly in recent years.<sup>35,208</sup> As mentioned in the introduction section, there is strong evidence that materials in the organic particles are far more viscous than any of the reaction media discussed above, and may even adopt a “glassy” state, in which physical diffusion, chemical reactions, and photochemistry are strongly suppressed. To investigate the potential role of the high organic phase viscosity on photochemistry, Lignell et al. studied the effect of the environment on the rate of photolysis of 2,4-dinitrophenol (24-DNP).<sup>209</sup> Despite the high viscosity of the SOM produced by ozonolysis of  $\alpha$ -pinene,<sup>210</sup> the room-temperature photolysis rate of 24-DNP embedded in SOM was considerably higher than that for 24-DNP dissolved in 1-octanol or water. Although the detailed mechanism is still not known, the efficient photolysis in SOM was attributed to the large number of easily abstractable H atoms in the SOM molecules, which could

transfer to the triplet state of 24-DNP. However, lowering the temperature decreased the photolysis rate of 24-DNP in SOM much more significantly than that of 24-DNP in octanol. This was explained by constraining the motion of 24-DNP in the matrix, thus preventing it from abstracting an H atom. The Lignell et al. study was the first demonstration of a significant effect of the matrix, and possibly viscosity, on the rate of an atmospheric photochemical reaction within the particle.

There is a significant body of literature on the photodegradation of pesticides, fungicides, insecticides, and related compounds. These compounds and their photodegradation products can be transported with wind-blown dust, and present a significant health risk far away from the point of the initial application. Therefore, it is important to understand the rates and mechanisms by which these compounds photodegrade in particulate matter. Both direct and photosensitized processes appear to contribute to the photodegradation. For example, Samsonov found that photodegradation of pesticide propiconazole (commercial formulation Tilt) is driven entirely by photosensitization, while photodegradation of haloxyfop-ethoxyethyl (Zellek) proceeds by a combination of direct and photosensitized reactions.<sup>211</sup> Segal-Rosenheimer and Dubowski

examined direct photolysis as well as heterogeneous oxidation by ozone of thin films of insecticides methyl-parathion and cypermethrin. Photodegradation of adsorbed cypermethrin was shown to be a major outdoor sink for cypermethrin, with quantum yields that were as high as 0.41 and 0.25 under 254 and 310 nm irradiation, respectively.<sup>211a,b</sup> The quantum yields for the photodegradation of methyl-parathion were smaller, but the thin film photolysis was found to yield more toxic products than photolysis in a solution.

**5.3.2. Model HULIS Compounds.** The importance of HULIS in aerosols was briefly discussed above and reviewed in detail by Graber and Rudich.<sup>106a</sup> HULIS do not have a well-defined chemical structure, and it is common to use simplified models with known structural elements of HULIS to study mechanisms of chemical and photochemical transformations in HULIS. Cowen and Al-Abadleh investigated photodegradation of tannic acid as a model for HULIS in atmospheric aerosols using diffuse reflectance Fourier transform spectroscopy.<sup>212</sup> The spectra were consistent with a destruction of carbohydrate moieties, aromatic rings, and ester linkages in tannic acid, and formation of aliphatic alcohols and unconjugated carbonyls. Figure 15 shows the mechanism they proposed. An important result of their work was an observation of a significant increase in the photodegradation rate as the relative humidity increased from 5% to 30%, which implies that adsorbed water is needed for the photodegradation of HULIS in aerosols. In addition to directly participating in photochemical reactions, water can act as a plasticizer that softens the organic matrix and accelerates reactions occurring in the matrix.

Humic acids, which are ubiquitously found on ground surfaces (soils), are known photosensitizers, and their photochemistry has been extensively studied in aqueous solution and water waste treatments. Some recent works suggest that they could play an important role not only in the aquatic medium but also in the atmospheric context. Stemmler et al. investigated the light-induced uptake of NO<sub>2</sub> on dry films of humic acid and soil dust and found that the rate of the photosensitized conversion of NO<sub>2</sub> to HONO was sufficient to explain the high daytime concentrations of HONO observed in the near ground levels of the troposphere.<sup>24b</sup> The same group investigated humic acid aerosols used as proxy of HULIS and showed that the light-induced NO<sub>2</sub> uptake was able to release more HONO than under dark conditions; however, the photochemical process on organic aerosol was not efficient enough to provide a significant air-borne source of HONO in the boundary layer.<sup>213</sup>

Sosedova et al. investigated photoenhanced HONO formation resulting from an exposure of tannic acid to NO<sub>2</sub>. On one hand, NO<sub>2</sub> can initiate dark nitration of the gallic acid subunits, which then photolyze under UV light to yield HONO at photolysis rates comparable to those of nitrophenols in aqueous solution.<sup>214</sup> On the other hand, a direct photo-enhanced HONO formation was also observed, possibly photosensitized by partially oxidized tannic acid residues that promote direct electron transfer to NO<sub>2</sub>. Aging of the tannic acid prior to the experiment led to some visible light photosensitization with reactivity comparable to that observed in the presence of added methylene blue, further confirming that the photooxidation of tannic acid may generate products with photosensitizing ability.

The photoenhanced reactivity of ozone with humic substances (aerosol and solid films) was investigated by D'Anna et al. The authors concluded that the photoinduced

process could contribute to daytime ozone deposition on natural and agricultural soil providing an alternative chemical mechanism, in addition to stomatal uptake, for ozone removal near the Earth surface.<sup>215</sup> Although the photosensitized ozone uptake on humic acid aerosols is not fast enough to affect gas-phase concentration of ozone in the troposphere,<sup>215</sup> the amount of ozone reacted could be significant for the aerosol aging because of the OH radical production upon electron transfer from the organic substrate to ozone.<sup>216</sup> In addition, the light-induced ozone uptake to these humic acid films was a source of oxygenated VOC species with yields ranging between 1% and 7% of ozone taken up.<sup>215</sup> Photoenhanced ozone loss on HULIS extracts from winter filters collected in Chamonix, France, was also explored, and the results indicate a higher photoinduced reactivity on the HULIS films extracted from wood burning than with films of pure humic acids.<sup>111</sup>

**5.3.3. Organic Aerosols on Inert Substrates.** In these experiments, a sufficient quantity of organic particles is deposited on an inert substrate from a chamber or from ambient air, the collected particles are flushed with clean air until all of their volatile components are removed, and the sample is photolyzed. The amount of the material available for the experiments is typically very small, but the material more closely approximates the type of the organic matrix found in ambient aerosols. Only a few experiments of this type have appeared in the literature so far. One approach was to photolyze a SOA sample on a filter or an optical window with monochromatic radiation and to observe volatile photolysis products by infrared CRDS,<sup>180c,d</sup> chemical ionization mass spectrometry (CIMS),<sup>217</sup> gas chromatography (GC),<sup>180b</sup> or another suitable technique. The wavelength dependence of the photolysis product yields (a photolysis action spectrum) carries information about the mechanism and efficiency of photolysis. Another approach was to track changes in the film itself, for example, with attenuated total reflection Fourier transform infrared spectroscopy (ATR-FTIR).<sup>180e</sup>

Walser et al. examined the photolysis of SOA material produced by the ozonolysis of *d*-limonene.<sup>180c</sup> Two major volatile products, formic acid and formaldehyde, were detected by IR CRDS. The shape of the photolysis action spectrum for production of HCOOH (Figure 16b) implied that the most photochemically active species in SOA were organic peroxides, which are highly abundant in monoterpene ozonolysis SOA.<sup>218</sup> Mang et al. relied on the infrared CRDS detection of CO and GC detection of small hydrocarbons (methane, ethane, ethane, etc.) as tracers for carbonyl photochemistry in the SOA material, which was also produced by ozonolysis of *d*-limonene. In addition to comparing the CO<sup>180b</sup> and HCOOH photolysis action spectra,<sup>180c</sup> Figure 16 shows that a diverse spectrum of VOC can be produced by SOA photolysis. This work demonstrated that direct photolysis of carbonyl functional groups represents a significant sink for monoterpene SOA compounds in the troposphere and occurs on atmospherically relevant time scales of hours. The mechanism of photolysis of carbonyls in organic phase was studied theoretically by Shemesh et al., who demonstrated the prevalence of free-radical driven secondary processes in such systems.<sup>219</sup> Pan et al.<sup>180a</sup> examined photodegradation of limonene ozonolysis SOA with a related action spectroscopy approach, which relied on the detection of volatile photoproducts with CIMS as a function of the UV irradiation wavelength. The observed photoproducts were dominated by oxygenated C1–C3 compounds such as methanol, formic acid, acetaldehyde, acetic

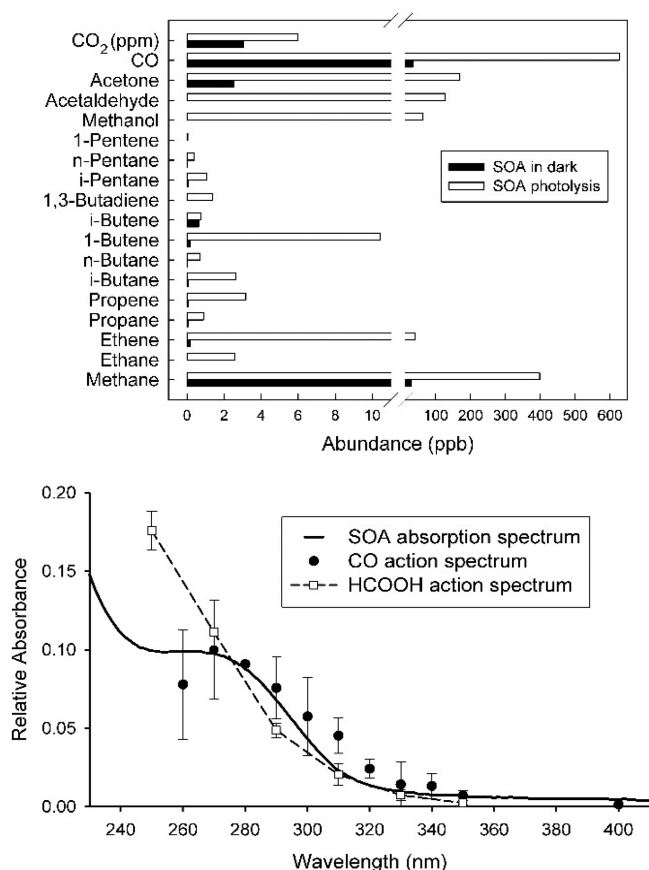


**Figure 16.** Top: Sample GC measurement of gaseous products of limonene SOA photolysis. Filled bars, no radiation present; open bars, after 10 min of photolysis. The CO<sub>2</sub> mixing ratio is in ppm; other mixing ratios are in ppb. Bottom: Comparison of the absorption spectrum, CO action spectrum, and HCOOH action spectrum for limonene SOA obtained with the infrared CRDS instrument. Reproduced with permission from ref 180b. Copyright 2008 American Chemical Society.

acid, and acetone. Pan et al. used kinetic modeling to show that similar photodegradation processes should readily occur in realistic SOA produced by OH- or O<sub>3</sub>-initiated oxidation of biogenic volatile organic compounds in clean air.

Hung et al. used ATR-FTIR to investigate aging of thin films of SOA produced by OH oxidation of isoprene and by ozone oxidation of  $\alpha$ -pinene.<sup>180e</sup> The IR spectra suggested that hydroxyl compounds dominated in the isoprene + OH SOA, whereas the  $\alpha$ -pinene + O<sub>3</sub> SOA was rich in carbonyl compounds (carbonyls are commonly produced in ozonolysis of olefins). Neither SOA showed significant reactivity toward ozone. However, an exposure to 254 nm radiation caused significant degradation in the film with the steady reduction in the intensities of the O–H, C–H, and C–O vibrational bands, and more complicated changes in the intensity of the carbonyl/carboxyl C=O band. Similar to the limonene SOA case,<sup>180c</sup> organic peroxides were implicated as photochemically active SOA compounds. As mentioned above, 254 nm is not a relevant irradiation wavelength for tropospheric photochemistry; it would be desirable to carry out similar experiments at longer irradiation wavelengths.

Gomez et al. described a mechanistic study of ozonolysis and the subsequent photolysis of thin films of undecylenic acid.<sup>220</sup> Fatty acids, which are commonly found in primary aerosols, are

stable with respect to photolysis in the tropospheric actinic window ( $\lambda > 290$  nm). However, when undecylenic acid was oxidized by ozone, the resulting products were photolabile, with organic peroxides and carbonyls being the most photochemically active. Photolysis of the preoxidized undecylenic acid film led to evolution of formaldehyde and formic acid. Park et al. observed similar photolysis processes in alkene-terminated self-assembled monolayers (SAM) that were oxidized by ozone.<sup>217</sup> These two studies concluded that photolysis should serve an important additional aging mechanism for aerosols containing unsaturated fatty acids, and more generally primary organics, once they are sufficiently oxidized.

#### 5.4. Photosensitized Reactions Involving Carbonyl Compounds

The photochemistry of aromatic ketones in the environment has been extensively studied, especially with respect to the photodegradation of various organics (see section 2.2.2).<sup>15a,b,87,221</sup> De Laurentis et al. recently showed enhanced degradation of 4-phenoxyphenol in the presence of 4-carboxybenzophenone through formation of phenoxy radical. The reduced sensitizer could be regenerated through reaction with oxygen, or by undergoing possible further transformation both in solution and in deliquesced particles.<sup>221</sup> Other recent studies on photochemistry of model compounds such as catechol, 4-phenoxyphenol, and phenol in the presence of aromatic ketones and aldehydes showed a significantly enhanced reactivity toward ozone when exposed to UV and/or visible radiation as compared to dark conditions.<sup>178b,222</sup> The photosensitized reaction mechanism expected for such type of systems is presented in section 2 and Figure 2, and the additional electron transfer reaction to ozone with formation of an ozonide anion (O<sub>3</sub><sup>-</sup>) that can further react to generate a hydroxyl radical.<sup>222a</sup> The presence of OH radicals was confirmed by the work of Net et al.,<sup>223</sup> who identified several reaction products arising from the OH-addition to 4-phenoxyphenol. Upon exposure of the dry film to ozone and simulated solar radiation, a red-shift of the absorption spectra for the benzophenone-phenol and for 4-phenoxyphenol-4-carboxyphenone systems was observed.<sup>222a,224</sup> The same authors reported a concomitant decrease of the surface wettability probed by contact angle measurements.<sup>222a,224</sup> Both observations have a number of other implications with respect to both direct and indirect climate effects of aerosols containing phenolic compounds and traces of photosensitizer.

Forrester et al. studied the photoinduced (UV-A and visible) uptake of O<sub>3</sub> on two molecular markers of hemicellulose combustion, levoglucosan and 5-nitroguaiacol, in the presence of Pahokee Peat used as photosensitizer.<sup>225</sup> While the presence of Pahokee Peat did not change the photouptake of ozone on levoglucosan, its presence clearly enhanced ozone uptake on 5-nitroguaiacol both in the UV-A and in the visible region.<sup>225</sup> Estimated 5-nitroguaiacol particle lifetimes indicate that some BBA markers can undergo significant degradation during typical atmospheric transport times of up to 1 week, and therefore care should be taken if these markers are used in source apportionment studies.<sup>225</sup>

Degradation of particulate organic compounds in irradiated aerosols is not the only possible outcome of organic phase photochemistry. A recent study by Monge et al. suggested that particles containing organic photosensitizers can efficiently oxidize gaseous organic compounds leading to an increase in the particle mass.<sup>178h</sup> They observed a large reactive uptake of

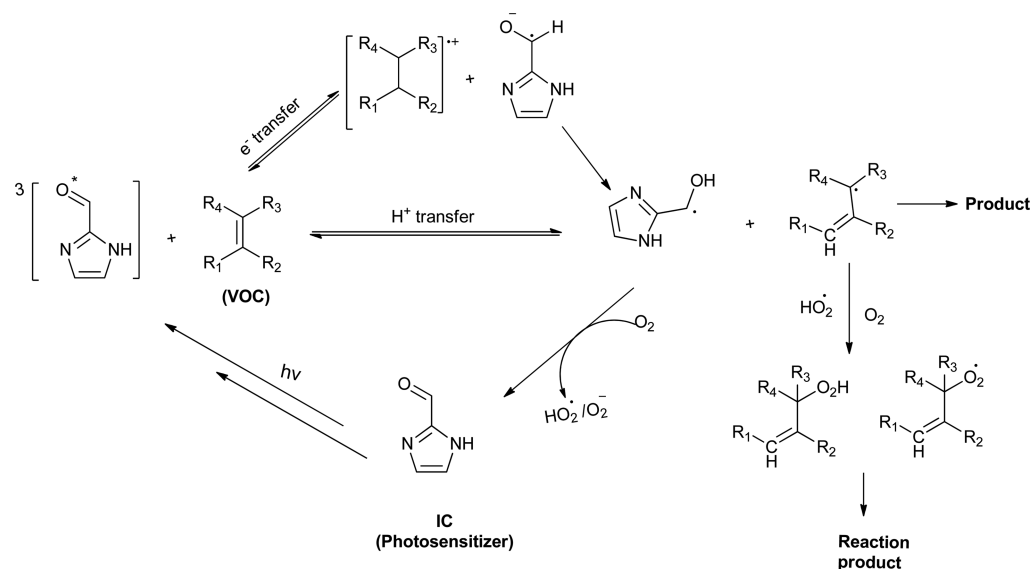


**Figure 17.** Possible/proposed mechanism for the photoinduced oxidation of VOC by imidazole-2-carboxaldehyde (IC) as a particle-bound photosensitizer. Reproduced with permission from ref 100. Copyright 2013 Royal Society of Chemistry.

limonene and isoprene upon exposure of particles containing humic acid or 4-(benzoyl)benzoic acid (an efficient photosensitizer) to 300–420 nm radiation. The estimated particle growth rates ( $\sim 5$  nm/h) were within the range of the observed growth rates (1–20 nm/h) for ambient particles, implying that the photoinduced processes can serve as a pathway for atmospheric particle growth. The presence of a photosensitizer in the particle is a key for this mechanism; for example, the  $\alpha$ -pinene ozonolysis aerosol, which presumably lacks molecules with strong photosensitizing abilities, did not increase in particle size in the presence of VOC and radiation.<sup>194</sup> In contrast, aerosols produced in the reaction of glyoxal and ammonium sulfate were shown to be highly efficient in photoenhanced aerosol particle growth because of the presence of a small amount of imidazole-2-carboxaldehyde (IC), an unusually effective photosensitizer.<sup>99,100</sup> The proposed mechanism for the reactions of electronically excited IC with VOCs is shown in Figure 17. High-resolution mass spectrometry of the IC-mediated products of oxidation of limonene showed that this free-radical driven mechanism can result in highly oxidized compounds including  $C_{10}H_{16}O_n$  with up to  $n = 6$  atoms of oxygen incorporated into the limonene ( $C_{10}H_{16}$ ) frame, as well as C9 and C8 products with a fragmented limonene skeleton, and nitrogen-containing products of association between IC and limonene oxidation products.<sup>99</sup> In these experiments and those of Monge et al.,<sup>178h</sup> the gas-phase concentration of limonene was very high but performed with very short time scales; if extrapolated to atmospheric VOC doses (i.e., concentration  $\times$  time), it leads to growth rates comparable to those observed in the field of a few nanometers per hour.

## 6. HETEROGENEOUS PHOTOCHEMISTRY AT ICE SURFACES

Photochemical processes associated with ice in the environment are most relevant in those areas of the atmosphere where the magnitude of air–ice exchange fluxes directly affects the concentration of trace gases in the air, or where the formation or degradation of species associated with ice affects their fate in a relevant way. These types of processes are especially important in polar areas for several reasons. First, snow packs

in general have a very high effective surface area concentration (see Table 2) when compared, for example, to cirrus clouds. Second, for a good part of the year, the lowermost atmosphere in the polar regions is characterized by a shallow boundary layer, so the production and loss of species through photochemical processes in the snow has a large impact due to the reduced mixing with the free tropospheric air masses. Third, as local sources of short-lived trace gases are scarce, any photochemical sources or sinks of species work against a small background. In combination, these three aspects explain why photochemical processes may significantly affect the oxidation capacity, the nitrogen oxide, and the halogen budgets in these regions.<sup>68,226</sup> The question whether a species (e.g.,  $HNO_3$ ) previously lost to an ice particle and thereby taken out of the oxidation cycles may be recycled back to the gas phase may be very relevant. Another important consideration is that long-lived photochemical precursors can be transported over long distances into these pristine and remote areas, where their recycling into short-lived or mobile products can have a larger impact than at the point of their emission. This aspect explains the vivid interest in the fate of persistent organic compounds (POPs),<sup>84b</sup> and mercury,<sup>227</sup> which interact with the local ecosystems, for example, via entering the food web upon snowmelt. An additional topic of interest is how both primary and secondary chemical species are stored in ice archives (both in polar and in midlatitude sites), from which information about past environmental conditions is retrieved. The photochemical processes occurring in ice may play a significant role in determining the transfer function between the atmospheric composition and the resulting concentrations in the ice, and knowledge of these photochemical processes is required to correctly interpret these ice archives.<sup>228</sup> A series of reviews to address the features of air–ice chemical interactions have recently been published in a special issue of *Atmospheric Chemistry and Physics*.<sup>229</sup>

Ice by itself is a high temperature material in the sense that under typical atmospheric conditions it is within not more than 50 K from its melting point, making it quite different from other common solid materials that have a considerably wider gap between the melting point and the ambient temperature.<sup>48</sup>

The relatively weak hydrogen bonds that are responsible for the solid hexagonal ice phase prevalent in the environment lead to its characteristic high vapor pressure. In combination, this results in a high dynamic character of ice, meaning that ice particles in a cirrus cloud quickly respond to changes in relative humidity or temperature, or that ice in snow strongly responds to temperature gradients to undergo substantial mass transport within a snowpack called metamorphosis.<sup>230</sup>

Ice in the environment hosts a vast amount of chemicals that originate from the ice nucleating agent in the atmosphere, from precipitation scavenging in the case of snow, or from the seawater from which it has been frozen in the case of sea ice. On the other hand, it remains in or gets into contact with its surrounding medium, which has substantial impacts on the latter, for example, fractionation processes between sea ice and seawater,<sup>231</sup> exchange of gases between snow and the air aloft,<sup>232</sup> or partitioning of gases to ice in cirrus clouds.<sup>233</sup> Partitioning of volatile organic and inorganic compounds to ice can be reasonably well explained by a Langmuir-type adsorption.<sup>20,84b,234</sup> Air–snow exchange can then be estimated through the concept of effective diffusivity.<sup>235</sup> For a few species, formation of a solid solution in crystalline ice is relevant, for example, for formaldehyde.<sup>236</sup>

Under most atmospherically relevant circumstances, ice is in a local equilibrium with the gas phase and other solid and liquid phases present in its vicinity. This means that to a first approximation, photochemical processes in environmental ices can be divided into two categories: (i) photochemistry of solutes in the crystalline ice matrix, for which their reduced mobility in ice is an important aspect; and (ii) photochemistry of condensed material phase separated from but in equilibrium with ice, where the concept of photochemistry with the same materials at the same water activity will apply (given by the vapor pressure of ice at that temperature). This second aspect is the origin of the well-known and well-characterized freeze concentration effect that explains many of the observations of enhanced rates of chemical reactions in frozen solutions in comparison to their parent solutions.<sup>51a</sup> This concentration effect also affects acid–base equilibria because excess protons are concentrated in the remaining aqueous phase upon ice formation, which enables acid-catalyzed (photo)chemistry in a way similar to that in aerosol particles, which also contain concentrated acids.

As mentioned above, ice represents a dynamic multiphase medium engaged in a continuous exchange of matter with the air, with highly concentrated solutions between ice crystals and with solid inclusions inside them. Photochemical processes initiated by chromophores, both direct and indirect, occurring in these other phases are comparable to those discussed in the context of aqueous or organic aerosol particles or dust, except that there is a difference in temperature. Many essential photochemical processes associated with soluble species present in ice or snow can be reasonably well assessed through this approach. Many of these processes have been described either in the preceding sections or in a separate review on aqueous phase photochemical processes (Herrmann et al.,<sup>13</sup> this issue). Several other recent reviews have discussed these in the context of snow chemistry.<sup>51a,68,84b</sup> We only briefly address some of them in this section, and concentrate on indirect photochemical processes, for which the specific environment in an ice matrix or the disordered interface (DI, see section 1.3.4) at the ice–air boundary or within ice grain boundaries is essential.

## 6.1. Inorganic Chromophores

Pure ice is not a chromophore by itself in the wavelength range reaching the lower atmosphere, because its absorption coefficient has a minimum between 200 and 400 nm.<sup>237</sup> In this and following subsections, we will address only photochemical processes initiated by chromophores present in the ice or its surface as contaminants. The main inorganic chromophores relevant in the environment, H<sub>2</sub>O<sub>2</sub>, HNO<sub>3</sub>/nitrate, and nitrite/HONO/H<sub>2</sub>ONO<sup>+</sup>, show comparable photochemistry in frozen and aqueous solution.<sup>238</sup> Nevertheless, several complications arise from examination of experiments that try to address photolysis of these species when they reside predominantly in one of the conceivable compartments: the disordered interface (DI), a liquid brine, or a crystalline ice matrix.

H<sub>2</sub>O<sub>2</sub> is a significant OH source in all environmental ices. It has also been used as a proxy to assess atmospheric oxidation capacity in past climates from its concentration in ice cores.<sup>239</sup> Chu and Anastasio studied the photolysis of H<sub>2</sub>O<sub>2</sub> in ice samples that were made from slowly frozen solutions, which resulted in photolysis behavior similar to that in aqueous solution.<sup>238b,240</sup> They also studied H<sub>2</sub>O<sub>2</sub> photolysis in ice samples prepared by flash freezing very dilute aqueous solutions to avoid H<sub>2</sub>O<sub>2</sub> being excluded from ice into a brine or the DI, but rather to keep it in the ice matrix. On the basis of the initial rates of H<sub>2</sub>O<sub>2</sub> photolysis, they found quantum yields for OH formation up to 50% smaller than for the slowly frozen solution at temperatures between 238 and 265 K. This indicates that H<sub>2</sub>O<sub>2</sub>, which has reasonable solubility in crystalline ice, may undergo slower photolysis possibly due to larger recombination of radical pairs in the complete cage of crystalline ice.

Photolysis of nitrate and HNO<sub>3</sub> in snow is one of the main drivers of photochemistry in snowpacks by providing a direct source of NO<sub>x</sub> to the air in contact with the snowpack and by providing a direct source of OH to the local environment, for example, to initiate the oxidation of organic species contained in the snow nearby. A large body of literature covering laboratory, field, and modeling studies exists and has been reviewed recently.<sup>51a,68</sup> We only address a few studies on the subject that highlight some of the molecular level details and open issues of the subject.

Chu and Anastasio measured the formation of OH from the photolysis of nitrate in frozen solutions using benzoic acid as an OH scavenger and probe.<sup>238a</sup> Their results indicate that in the temperature range 239–270 K, photolysis of nitrate in such frozen solutions behaves largely as expected for solutions of composition expected for equilibrium thermodynamics. This concerns the quantum yield of OH, the molar absorptivity, and its temperature dependence. This study refined earlier experiments based on the detection of the NO<sub>2</sub> photolysis product that were complicated by secondary NO<sub>x</sub> chemistry,<sup>241</sup> as also discussed by Boxe et al.<sup>242</sup> Chu and Anastasio observed a reduction in quantum yield at lower pH of the parent solution, which remained unexplained.<sup>238a</sup> The question may arise as to whether the partitioning of some of the nitrate or HNO<sub>3</sub> to the DI may play a role. Krepelova et al. concluded from a surface-sensitive photoelectron spectroscopy experiment that the local environment of HNO<sub>3</sub> or nitrate is similar to that at an aqueous nitrate solution–air interface, even though they would have probably lacked the sensitivity to differentiate HNO<sub>3</sub> from nitrate or partial from full solvation of the two.<sup>243</sup> The DI on ice seems to provide sufficient hydrogen-bonding options for efficient ionization of HNO<sub>3</sub>, indicated by both

more recent spectroscopy experiments<sup>244</sup> and theory<sup>245</sup> (and references therein). However, the question, whether HNO<sub>3</sub> or nitrate at the DI may experience only partial solvation that would offer room for higher quantum yields, remains open. Zhu et al. studied photolysis of HNO<sub>3</sub> on ice by directly detecting NO<sub>2</sub>\* from the OH forming channel.<sup>246</sup> They found even larger absorption coefficients than those for gas-phase HNO<sub>3</sub>. Wren and Donaldson, using glancing angle Raman spectroscopy, measured the exclusion of nitrate to the air–ice interface during freezing of nitrate solutions.<sup>247</sup> Although exclusion was clearly demonstrated, there was less nitrate present at the frozen solution–air interface than expected from bulk thermochemical models, suggesting that some nitrate is retained within liquid pockets in the ice matrix. Overall, quantitative conclusions should be taken with care, because the HNO<sub>3</sub>/nitrate/DI/ice system is rather complex. This concerns both the absorption coefficient and the quantum yields for the two product channels (O<sup>-</sup> + NO<sub>2</sub>; NO<sub>2</sub><sup>-</sup> + O). Different amounts of nitrate with respect to the available ice volume and ice surface area lead to different partitioning to the various compartments in different laboratory experiments performed with frozen solutions, with polycrystalline ice films, or with amorphous ice films at low temperature, so that the extraction of quantitative information for one specific compartment remains difficult.<sup>51a,248</sup>

## 6.2. Photolysis of Organic Molecules

Perhaps the smallest organic molecule that can conceivably participate in photochemical processes in ice is methyl hydroperoxide (CH<sub>3</sub>OOH), the smallest organic peroxide found in environmental waters and ices.<sup>249</sup> Its photolysis was recently investigated by both experimental and theoretical methods. Epstein et al. showed that molar extinction coefficients and photolysis quantum yields of CH<sub>3</sub>OOH do not significantly change upon freezing.<sup>250</sup> Just like in the case of H<sub>2</sub>O<sub>2</sub>, which is known to freeze into a two-phase system with solid water and a liquid water–peroxide solution, CH<sub>3</sub>OOH was likely excluded in the liquid phase explaining the lack of significant freezing effects on its photophysics in the Epstein et al. experiments. The structure adopted by CH<sub>3</sub>OOH adsorbed to a surface of large ice clusters was investigated by DFT methods.<sup>251</sup> On-the-fly ab initio molecular dynamics simulations for a CH<sub>3</sub>OOH molecule on a surface of a smaller ice cluster consisting of 20 water molecules predicted large sensitivity in the absorption spectrum of truly frozen CH<sub>3</sub>OOH to temperature,<sup>250</sup> with the spectrum narrowing and shifting to the blue under cryogenic conditions because of constrained dihedral motion around the OO bond. Calculations on the dynamics of CH<sub>3</sub>OOH photolysis in ice predict that ice catalyzes the deactivation of CH<sub>3</sub>OOH from the excited state to the ground state on the femtosecond time scale,<sup>252</sup> followed by dissociation into primary fragments OH and CH<sub>3</sub>O, which promptly react to form formaldehyde and other secondary products.<sup>253</sup> Despite the theoretical interest in CH<sub>3</sub>OOH, its ice photochemistry may be too slow to affect the polar environments. For example, Hamer et al. modeled photochemical production of formaldehyde in a snowpack from a variety of different sources, and concluded that CH<sub>3</sub>OOH photolysis is a relatively minor source of formaldehyde.<sup>254</sup>

Many of the larger organic molecules that are of interest in the environmental chemistry of ice and snow absorb actinic radiation in the wavelength region reaching the ice at ground level and may therefore participate in direct photochemical

degradation or may initiate indirect photochemistry by acting as photosensitizers. For some smaller oxygenated VOCs, the absorption properties depend strongly on their precise phase behavior once in contact with ice. For example, as mentioned in the introduction, carbonyls absorb UV-A radiation in the gas phase, while their fully hydrated counterparts, *gem*-diols, do not absorb appreciably above 200 nm. Therefore, the nature of oxygenated VOC species at the ice DI is crucial to understand their ability to participate in photochemistry. Another example is the case of aromatic molecules: there is convincing evidence from experiments and theory that the interplay between intermolecular interactions and the specific hydrogen-bonding environment offered at the ice DI leads to self-association of phenol derivatives,<sup>255</sup> benzene,<sup>256</sup> naphthalene,<sup>257</sup> anthracene,<sup>258</sup> 4-methylbenzylketone,<sup>259</sup> and methylene blue.<sup>53a</sup> This self-association generally leads to a red shift of the absorption, allowing photochemistry at wavelengths where higher intensity is available at ground surfaces.

Under the earlier assumption that photochemical degradation of organic compounds in environmental ices is mainly driven by the major inorganic chromophores nitrate, nitrite, and H<sub>2</sub>O<sub>2</sub> as OH sources, many studies have looked at the photochemistry in frozen aqueous solutions of the target organic compounds in mixtures with these inorganic chromophores. Often, behavior comparable to that of aqueous solutions was found, but also indications for the involvement of more radical coupling reactions due to the higher local concentrations.<sup>255,260</sup> We concentrate here on cases where the specific effects of the local conditions at ice surface play an important role.

Kahan et al. studied the photolysis of harmine, an aromatic fluorescent probe molecule at the air interface of frozen freshwater and salt water (NaBr, NaCl) solutions.<sup>261</sup> Similar to their earlier results on other aromatics,<sup>53b,256</sup> the photolysis loss rate at the frozen freshwater–air interface was observed to be markedly faster than that observed in aqueous solution. However, at the air interface of the frozen salt solutions, the rate was seen to decrease as the concentration of salt in the prefreezing solution was raised, in accord with the increasing amount of liquid brine expected to be present due to freeze exclusion. At a fairly low prefreezing salt concentration (the exact value depending on the temperature and the identity of the salt, as expected from the freezing phase diagram), the photolysis rate became equivalent to that observed in solution. The more rapid photolysis rates observed on the freshwater ice surface were seen to be related to the surface-to-volume ratio of the illuminated sample,<sup>53b,258,261</sup> being fastest at the air–ice interface and becoming equal to the solution rate for bulk ice samples. This observation may explain the different results reported by Ram and Anastasio, who found the degradation rates of phenanthrene, pyrene, and fluoranthene within frozen samples (but not measured at their interface to air) to be consistent with those determined in aqueous solution.<sup>262</sup> Thus, the location of the organic chromophore on or within the ice, as well as the presence or absence of a brine controlled by other solutes, plays a key role in the photodegradation rate.

Along similar lines, differences in the initial photolysis quantum yields between aqueous solution and ice observed by Weber et al.<sup>263</sup> for the insecticides fenitrothion and methylparathion, as well as the amounts of later generation photodegradation products observed, could be characteristic of these competing mechanisms: solution-like photolysis in freeze concentrated brines versus photolysis at the ice DI where

intermolecular interactions (such as the self-association mentioned above) and incomplete hydrogen bonding may allow locally more efficient photolysis and different degradation pathways. Another suggestion that photolysis kinetics might be affected by different phases present in natural snow and ice samples is given by Domine et al.<sup>264</sup> These authors propose that SOA and other (including nonchromophoric) organic matrixes deposited to ice surfaces may alter the photochemistry of organic chromophores present thereby creating a different environment (an organic phase) into which the chromophores may partition. This effect has recently been demonstrated in the laboratory, where the photolysis kinetics of anthracene, pyrene, and phenanthrene in ice samples were slowed substantially in the presence of trace amounts of nonchromophoric organics.<sup>265</sup>

Photolysis of halobenzenes gave predominantly dehalogenation, coupling, and rearrangement products, rather than photosolvolysis products.<sup>260c,266</sup> This was attributed mainly to the freeze concentration effect and could, in retrospect, be rationalized in terms of the relative roles of brine versus DI specific effects discussed above. One aspect controlling such mechanisms is the specific hydrogen-bonding environment encountered at the DI in comparison to a concentrated brine. Heger and Klan<sup>267</sup> used frozen solutions containing hydrogen donor and hydrogen acceptor probes to show that hydrogen-bond and electron-pair donating interactions were substantially larger than those measured in liquid aqueous solutions and relatively insensitive to the sample temperature.

### 6.3. Photosensitized Chemistry with Organic Chromophores

Taking the example of several PCBs (polychlorinated biphenyls) in frozen solution, Matykiewiczova et al.<sup>268</sup> observed reductive dehalogenation as the main photochemical pathway and found photosolvolysis products to be absent, just as in the case of the halobenzenes<sup>260c,266</sup> mentioned before. However, in the specific case of PCBs, the authors could argue that adventitious organic contaminants acted as hydrogen donors for the reductive dehalogenation, thus a clear case of indirect photochemistry. Proof was provided by adding deuterated ethanol and tetrahydrofuran. A similar conclusion was drawn by Rowland et al.<sup>269</sup> from an investigation of photodegradation of insecticides aldrin and dieldrin, where tiny amounts of organic chromophores must have induced indirect degradation comparable to that induced by substantial amounts of H<sub>2</sub>O<sub>2</sub>.

As discussed in section 2, such indirect photochemical processes involve electron, energy, and hydrogen atom transfer. Of course the question arises whether such processes are feasible in environmental ices. In comparison to liquid solutions, the mobility of intermediates is strongly reduced in ice or frozen systems, leading to different quenching conditions. The question arises again, whether chemistry evolves mainly within the brines in equilibrium with ice and as expected from the corresponding behavior in aqueous or organic aerosol particles discussed in section 5.

Some detailed insight into the photophysics of photosensitized processes in ice can be obtained from the case of pyruvic acid, already discussed in section 2 in the context of aqueous phase photochemistry. As mentioned there, the primary excitation of PA that leads to an initial radical pair is followed by electron transfer to neighboring carbonyl acceptors, finally leading to decarboxylation.<sup>270</sup> Guzman et al. found that CO<sub>2</sub> was also promptly released from frozen PA/H<sub>2</sub>O films upon illumination, even down to a temperature of 140 K,

indicating that the radical–radical reactions involved are also operating in ice, although at a slower rate.<sup>271</sup> The overall quantum yield of CO<sub>2</sub> production at 313 nm in a 250 K ice was approximately 60% of that in water at 293 K. The temperature-dependent study also allowed the authors to estimate that radical pairs escaped the solvent cage above 190 K. Similar conclusions were drawn by Ruzicka et al., who studied Norrish type I reactions of dibenzyl ketone (DBK) and 4-methyldibenzyl ketone (MeDBK) in frozen aqueous solutions down to 190 K.<sup>272</sup> Diffusion of the benzyl radicals to produce recombination products was efficient still at temperatures below 220 K. Also using MeDBK photolysis, Kurkova et al.<sup>259</sup> found that the efficiency of out-of-cage reactions decreased at much higher temperatures for spray produced artificial snow with a higher surface to volume ratio and lower MeDBK surface coverage than those determined for frozen solutions by Ruzicka et al.<sup>272</sup> This indicates that for indirect processes that involve electron or energy transfer, the degree of partitioning among the compartments (brine, DI) also plays a decisive role. As a side note, the PA case also demonstrates that in-ice electron transfer reactions among organic molecules are feasible and that these also induce polymerization reactions similar to those leading to HULIS in the atmosphere.

Returning our attention back to the more complex cases, Grannas et al. used aldrin as a probe molecule and investigated its photosensitized degradation with various proxies of dissolved organic matter (DOM) considered as photosensitizers or building blocks thereof in aquatic photochemistry.<sup>273</sup> While in principle the photosensitized degradation followed the expected behavior for the concentrated brines in frozen solutions, the detailed picture again gains in complexity, because the distribution of DOM between brine and the DI may be affected by a possible phase separation. Grannas et al. illustrated this by showing the different relative importance of OH-induced degradation between liquid and frozen solutions.<sup>273</sup> The same holds for the importance of singlet oxygen pathways, where the differentiation between the hydrophilic and hydrophobic singlet oxygen scavengers prompted a conclusion that singlet oxygen production occurs in different compartments. Related to this point, Bower and Anastasio provided a careful analysis of the temperature and solute content dependence of the enhancement of singlet oxygen production by Rose Bengal in frozen solutions.<sup>274</sup> They pointed out the changing relative importance of liquid water as the main singlet oxygen scavenger: while the concentration of the <sup>1</sup>O<sub>2</sub> source, Rose Bengal, increases due to the freeze concentration effect (controlled by different solutes in this study), the rate of singlet oxygen quenching by water remains constant. This is different from the role of OH radicals where the ratio of source strength (e.g., photolysis of H<sub>2</sub>O<sub>2</sub>) and sink (e.g., another solute) remains constant upon freezing. These examples emphasize the picture of ice as a multiphase medium, which complicates the understanding of indirect photochemical processes substantially.

Photosensitized chemistry in ice is not limited to organic acceptor molecules, similar to those in aqueous aerosol particles. Bartels-Rausch et al. showed that photosensitized reduction of NO<sub>2</sub> to HONO occurred in humic acid doped ice films in the temperature range 215–260 K.<sup>275</sup> The HONO production rate was linearly related to irradiation and, at low humic acid contents, to the humic acid concentration. At these low concentrations, on a per mass basis, the HONO production rate was consistent with that observed earlier on pure humic

acid films under comparable irradiation conditions.<sup>24b,213</sup> At higher concentrations, the HONO production rate was lower. This is likely attributable to different partitioning of humic acid to brine or separate organic phases and the DI, each with different abilities to promote energy and electron transfer processes, similar to effects found by Kurkova et al. for the indirect MeDBK photochemical degradation pathways.<sup>259</sup> Bartels-Rausch et al. found the photosensitized HONO production to saturate at high NO<sub>2</sub> concentration.<sup>275</sup> Whether this should be attributed to an adsorbed precursor as electron acceptor or to a competing process quenching one of the photochemical intermediates remained open.

The same group investigated the photolytic reduction of Hg(II) to elemental mercury Hg(0) in the presence of benzophenone in ice films frozen from solutions containing benzophenone and Hg(II) and various cosolutes.<sup>276</sup> Substantial conversion of Hg(II) to Hg(0) was observed. Because the addition of 2,6-dimethoxyphenol (expected to act as an electron donor) suppressed rather than enhanced Hg(0) emission, the authors concluded that Hg(II) reduction was driven by an energy transfer and not by an electron transfer from benzophenone. Again, different partitioning behavior of the species present could have been the origin of this behavior rather than the absence of electron transfer. Experiments with ice frozen from solutions with different pH indicated that the process involved Hg(I) complexes with OH<sup>-</sup> as intermediates. In the presence of chloride, the yield of Hg(0) was suppressed, probably due to oxidation of Hg(I) by Cl<sub>2</sub><sup>•-</sup>, which is formed as a result of the photosensitized reduction of chloride.<sup>277</sup>

#### 6.4. Indirect Photochemistry Induced by Mineral Dust in Ice

Finally, we briefly address the option of semiconductor metal oxide induced redox chemistry in ice. Kim et al.<sup>278</sup> found significant enhanced photoreductive dissolution of iron oxides in frozen solutions containing various nanoparticulate iron oxides (hematite, maghemite, and goethite) and different electron donors (organic acids) to yield Fe(II) in these matrixes under both UV and visible light irradiation. While the results could be qualitatively explained by the freeze concentration effect, agglomeration of the nanoparticles in the vein structure of the polycrystalline matrix allowed electron hopping through the interconnected grain boundaries of iron oxide particles to facilitate the separation of photoinduced charge pairs. Comparable effects were observed with frozen solutions containing MnO<sub>2</sub><sup>279</sup> and solutions containing Cr(VI), in combination either with organic acid electron donors or with As(III) to build corresponding redox couples.<sup>280</sup>

## 7. HETEROGENEOUS PHOTOCHEMISTRY ON URBAN SURFACES

### 7.1. Outdoor Surfaces and Urban Grime

The existence and growth of a deposit on surfaces exposed to the urban atmosphere is commonplace, and has spurred the formulation of window cleansers and the appearance of an industry devoted to cleaning outside surfaces of office buildings. Recently, some makers of window glass have incorporated TiO<sub>2</sub> into the glass matrix, in an effort to develop “self-cleaning” windows, via photocatalytic degradation of the deposited material. Despite the obvious interest in maintaining clean windows, it is only very recently that any work has been done to investigate the chemical properties of the deposit, which we will call “urban grime” in what follows. Here, we present briefly

what is known about the chemical composition, and summarize the very small number of studies (to date) on the chemistry and photochemistry of this new environmental compartment.

The group of Miriam Diamond at the University of Toronto was the first to suggest that urban grime could act as a separate environmental compartment.<sup>281</sup> Their work,<sup>282,283</sup> augmented by that of others,<sup>284</sup> has established that the grime consists of a rich mixture of chemical compounds, no more than about 25 wt % of which are organic. Nitrate, sulfate, and carbonate are important anions balanced by ammonium, sodium, and calcium as counterions. A host of trace elements, including metals,<sup>285</sup> is also present, at least in some samples and reports. There is a fair mass fraction of elemental carbon reported as well in the analyses. A recent study has also reported the presence of significant amounts of water associated with grime films;<sup>286</sup> this appears to be in fairly rapid equilibrium with ambient atmospheric water vapor. Within the organic fraction, fatty acids, long-chain aliphatic compounds, PAHs, PCBs, and polybrominated biphenyls have been identified.<sup>281c,282,283,287,288</sup>

The presence of toxic compounds such as PAHs and PCBs has motivated work to explore whether urban grime may act as a passive sampler for urban atmospheric pollution.<sup>281c,289</sup> It seems there is some relationship between the partitioning behavior of organic compounds from the air phase to the grime and the partitioning of the same compounds to 1-octanol (quantified by the octanol–water partitioning coefficient) or to ethylene vinyl acetate.<sup>290</sup> This suggests that the presence of the organic component may act to draw other organic compounds to the grime film as well (much in the same way as the apparent yield of SOA in smog chamber experiments increases with the total amount of available condensed phase organics). It remains unclear how or whether the large nonorganic fraction may influence this partitioning behavior. Nevertheless, it seems that models that treat the grime as an urban environmental compartment, and treat partitioning in a manner similar to that of gas–aerosol partitioning, may provide useful insights into the nonchemical lifetimes and fates of organic compounds associated with the grime.

There have been no field measurements reported of chemistry that takes place associated with grime surfaces. However, Stutz and co-workers<sup>291</sup> have shown that, in an urban setting, there is a photochemical source of HONO that is associated with fixed (as opposed to aerosol) surfaces. During a field campaign in downtown Houston, they used a fine gridded multialtitude model to assign this source to photochemistry of NO<sub>2</sub> deposited to the ground, which they defined as being the lowest 20 m. This is in keeping with earlier work that demonstrated that such NO<sub>2</sub>–HONO photoconversion could be very important on humic substances and other soil materials.<sup>24b,125a,213</sup> Other recent studies in suburban Paris,<sup>292</sup> and Beijing,<sup>293</sup> came to essentially the same conclusion: there is an important heterogeneous photochemical source of HONO in the urban environment. Michoud et al.<sup>292</sup> also associated this source with the ground surface, based on the relationship of the HONO source strength to soil moisture. However, the possible involvement of building surfaces with their attendant nitrate loading within the grime was not considered. Given recent laboratory results, this source could also play an important role in urban photochemical renoxification.

There is only one report (to our knowledge) of a laboratory measurement of photochemistry involving real urban grime. Following an earlier study using proxies for urban grime,<sup>294</sup> Baergen and Donaldson<sup>286</sup> collected real grime from Toronto

air over the course of 1–3 weeks on an ATR-FTIR crystal, and measured nitrate loss kinetics following illumination in a solar simulator. Very short photochemical lifetimes were obtained for the nitrate associated with real grime samples. Under artificial solar illumination, the grime-associated nitrate was removed 3–4 orders of magnitude faster than aqueous nitrate photolysis would predict. This finding was true for both the “native” nitrate, deposited from the urban atmosphere, as well as extra nitrate, deposited by exposing the grime-coated ATR crystal to gas-phase nitric acid. It is not clear at this time whether the enhanced photolysis rate is a consequence of decrease solvent caging in the grime matrix, different absorption cross sections and/or quantum yields (perhaps due to symmetry breaking in the nitrate anion), or some other reason. The observed rapid loss of nitrate is in line with previous studies using nitric acid deposited onto glass and leaf surfaces, where the nitrate lifetime under actinic illumination is very much shorter than that in solution.<sup>286</sup>

Chabas and co-workers have studied the efficacy of “self-cleaning” glasses at reducing grime buildup (and consequent visibility reduction).<sup>295</sup> Samples of ordinary and self-cleaning glasses were left outdoors for many months, and the grime remaining at the end of this time was analyzed for its overall organic content, as well as for several key ions. Here, the nitrate associated with the TiO<sub>2</sub>-impregnated samples was found to be lower than that of the ordinary glass, consistent with a photocatalytic removal of nitrate. As discussed in section 3, such photochemistry has been reported by George and co-workers for nitrate anion adsorbed onto TiO<sub>2</sub>, as well as onto mineral dust samples containing TiO<sub>2</sub>.<sup>126,133a</sup> In both cases, HONO is observed as a major product.

There have been a small number of laboratory photochemical studies using proxies for urban grime. As mentioned above, Handley et al.<sup>294</sup> measured the loss of nitrate following illumination of octanol films (as proxies for the complex organic fraction in the grime) that had been exposed to gas-phase nitric acid. The loss seemed to be somewhat enhanced when a photosensitizer, acridine, was also present in the film. Likewise, Baergen and Donaldson reported a photochemical loss rate of nitrate from proxy films (in this case Apiezon N vacuum grease) similar to that from actual urban grime samples following the exposure of each to gas-phase nitric acid.<sup>286</sup> Such studies seem to justify the use of organic films as reasonable proxies for the real urban grime sample.

Other laboratory studies of urban grime photochemistry using proxies have recognized the photoactive nature of many of the organic compounds identified in real samples. A significant photoenhancement is observed for the uptake of gas-phase NO<sub>2</sub> by solid films of pyrene,<sup>296</sup> fluoranthene,<sup>297</sup> soot,<sup>298</sup> humic acids,<sup>24b</sup> and several partially oxidized aromatics,<sup>299</sup> which are possible constituents of the organic portion of urban grimes. HONO(g) is observed to be a major product of the photochemistry. The kinetic mechanism is well described as a Langmuir–Hinshelwood type, following that of the corresponding (much slower) dark reaction. In the presence of added nitrate salt, the NO<sub>2</sub> uptake is significantly reduced, but photochemical HONO production is observed, even in the absence of gas-phase NO<sub>2</sub>.<sup>299</sup> A generally similar photoenhancement in the uptake of gas-phase ozone by illuminated solid organic films (PAHs and soot) is also observed in laboratory studies.<sup>79,164</sup> Interestingly, in a complementary set of experiments that measured the loss kinetics of the pyrene due to heterogeneous reaction with gas-

phase ozone, although a photoenhancement was observed for solid pyrene film (consistent with the enhanced ozone uptake), no enhancement was measured for pyrene present in an octanol film, at either high or low concentration.<sup>300</sup> Spectroscopic measurements confirm that the (collective) electronic structure of the solid films is different from that of isolated PAH molecules, clearly giving rise to the different photoenhancement effects observed. What this means in the context of real urban grime films remains unclear at this time.

## 7.2. Indoor Surfaces

The indoor environment is rarely discussed in the context of atmospheric photochemistry because the intensity of actinic radiation produced by indoor lighting and penetrating through windows is quite low. However, important photochemical reactions have been shown to occur both in indoor air and on indoor surfaces, and affect the oxidative capacity of the indoor environment.<sup>301</sup> Gómez Alvarez et al.<sup>302</sup> observed unexpectedly high concentrations of OH in an indoor environment shown to be a result of indoor photolysis of HONO. The latter was shown to be efficiently produced on indoor surfaces through both dark and photoinduced reactions of NO<sub>2</sub>.<sup>303</sup> The observed NO<sub>2</sub> to HONO conversion was enhanced by the presence of sunlight with wavelengths in excess of about 340 nm on white wall paint and on indoor surfaces coated with various household chemicals. The exact nature of the chemicals responsible for this photosensitized reaction is unclear, but the resulting fluxes of HONO are relevant.

## 8. LOOKING AHEAD

Despite the amount of work described in this Review, photochemistry or photosensitized processes at interfaces of atmospheric relevance still represent a “terra incognita”. It should be obvious now to the reader that both interfaces and appropriate light-absorbing materials are widespread in the troposphere, with solar radiation driving a number of surface and bulk photochemical processes on urban surfaces exposed to outdoor air, on ice and snow, in airborne particles, on the ocean surface, on vegetation and soils, etc. These processes have the potential to alter not only the chemical composition and properties of the irradiated surfaces, but also in some cases of the air surrounding them. While a number of key experimental and theoretical advances have been made in recent years, especially in the photoenhanced uptake of gases on surfaces or the production of radical precursors, significant gaps in our understanding of heterogeneous photochemistry still remain. Future work should progress from the fundamental aspects of heterogeneous photochemistry to their potential impacts at various scales.

From the fundamental perspectives, there is a clear requirement to bridge the physical properties of an interface, especially the air/water one, with chemical features. For instance, while it has been known for decades that organic molecules can alter surface energy (or surface tension), the consequence of this in terms of photochemical processing is unknown. Does a surfactant consequently also alter the concentration of various photochemical reactants, for instance, by increasing local (surface) concentrations of similar species? Can such a local increase introduce or promote intermolecular interactions, which could enhance photochemistry at interfaces (as observed in the bulk for humic acids)? Triplet lifetimes have been observed to be extended at the interface; how does this translate into photoreactivity at the interface? Overall, there is

simply the need and space for basic photochemical investigation of such processes; most of the heterogeneous photochemical processes discussed in this Review were studied under a much more limited set of experimental conditions, that is, using a single wavelength or a broadband radiation source, and at a single or limited range of temperatures. We are not suggesting that comprehensive measurements should be done for all conceivable heterogeneous photochemical processes. However, a wider range of environmental conditions and excitation wavelengths should be probed in future experiments for processes that have the potential to have a dramatic effect on the chemical composition. This suggestion is especially relevant in view of the ongoing climate change, which may lead to a large enough change in ambient conditions to affect the rates of photochemical processes.

As outlined in the introductory sections, the physical state of organic material is an important aspect for the description of the dynamic response of aerosol particles to a changing environment both in physical and in chemical terms. While the impact of high viscosity on reaction rates and gas–condensed phase equilibria has become an emerging focus of research, the effects in the context of photochemistry should now be an important new field for future investigation. Charge, energy, and hydrogen transfer are likely to change in a high viscosity environment, leading to changes to both rates and quantum yields, and possibly also leading to new pathways or shutting them down.

Understanding the fundamentals basis of heterogeneous photochemistry will allow us to assess their atmospheric relevance. Such processes have already been found in daytime production of HONO or dust-induced nucleation events. Yet how widespread are these phenomena? Where is the next big surprise to be found? Perhaps they will be confined to local environments, for example, in urban grime chemistry? The built environment offers in cities a huge surface/interface on which photochemistry may take place (see above), but its impact remains still largely unassessed. It is likely that further surprises await at large scales, at the air/sea interface where all ingredients are present for a rich chemistry.

Previous experiments have amply demonstrated a large impact of heterogeneous photochemistry on concentrations of important atmospheric air pollutants such as NO<sub>2</sub> and O<sub>3</sub>. However, the impact of heterogeneous photochemistry on the toxicity of particulate matter remains much less explored. The effects of heterogeneous photochemical processes can potentially be quite significant because such processes are known to transform various organic compounds, such as mutagenic and carcinogenic nitro-PAH discussed in section 5, into other products with different levels of toxicity. In addition, photochemical processes may create long-lived reactive intermediates similar to those generated by exposure of particles to ozone.<sup>304</sup> Therefore, the effect of irradiation on toxicity of different particulate matter should be more systematically investigated in future work.

A concise and simple conclusion is that we are only just starting to explore the fundamentals and the atmospheric consequences of photochemistry at interfaces.

## AUTHOR INFORMATION

### Corresponding Author

\*Phone: +33-4-72431489. E-mail: christian.george@ircelyon.univ-lyon1.fr.

## Notes

The authors declare no competing financial interest.

## Biographies



Dr. Christian George was the head of the Air Cleaning, Gas Treatment, Atmospheric Chemistry research team at the Institute of Research on Catalysis and Environment at Lyon ([www.ircelyon.univ-lyon1.fr](http://www.ircelyon.univ-lyon1.fr)). He obtained his Ph.D. (1993) from the University Louis Pasteur at Strasbourg, working on mass transfer processes at gas/liquid interfaces with Professor Philippe Mirabel. He was a postdoc with Professor Cornelius Zetzsch at Hannover (1994–1995) and a Centre National de la Recherche Scientifique (CNRS) researcher at the research center on surface geochemistry at Strasbourg (1995–2000). Since 2013, he has been a visiting professor at Fudan (Shanghai), Shandong (Jinan) Universities. His research aims at a better understanding of heterogeneous chemistry in the troposphere by means of laboratory studies.



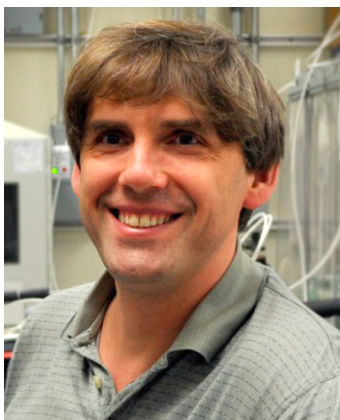
Markus Ammann received his diploma in physical chemistry and solid-state physics from ETH Zürich, Switzerland, in 1988, with a thesis on gas adsorption on nanoparticles in gas suspension. He got his Ph.D. in 1992 from ETH with a thesis on ultrafine particles in volcanic gases. After postdoctoral stays at Paul Scherrer Institute and University of Bern, he joined the Laboratory of Radiochemistry and Environmental Chemistry at Paul Scherrer Institute in 1996. Since 1997 he has been head of the Surface Chemistry group. In 2005 he joined the University of California, Irvine (UCI) as a visiting scientist. Since 2008 he has been a lecturer at ETH Zürich at the Institute of Atmospheric and Climate Sciences, and since 2014 he has been an adjunct professor at the same institute. The work of his group is focused on the kinetics, thermodynamics, and mechanisms of heterogeneous chemical processes on aerosol particles and ice under atmospheric conditions, by means of laboratory studies based on flow tube techniques and, recently, surface sensitive spectroscopy.



Barbara D'Anna received her undergraduate degree in industrial chemistry from University of Turin, Italy in 1996 with a thesis on EPR study of peroxy radical species in Na<sup>+</sup>/Y zeolites. She then received her Ph.D. in 2001 from University of Oslo, Norway, with a thesis on degradation of carbonyl compounds in the atmosphere. She did her postdoctoral research in marine aerosol measurements at Queensland University of Technology, Australia, in 2004 and in aerosol photochemistry at UCI, U.S. in 2005. She then joined the CNRS as senior researcher in 2006. She teaches atmospheric chemistry courses and does research on aerosol photochemistry, and particulate matter measurements in ambient air and in indoor environments.



James Donaldson received his B.Sc. and Ph.D. degrees from Carleton University in Ottawa, ON. Following postdoctoral work in Boulder, CO, he joined the University of Toronto in 1988, where he is now a Professor of Chemistry. His original research interests in detailed studies of photodissociation and reaction dynamics have evolved to predominantly involve studies of heterogeneous and interfacial processes of importance to atmospheric chemistry.



Sergey Nizkorodov received his undergraduate degree in biochemistry from Novosibirsk State University, Russia, in 1993 and graduate degree in chemical physics from Basel University, Switzerland, in 1997. After doing his postdoctoral research in chemical kinetics and reaction dynamics at the University of Colorado at Boulder, and in atmospheric chemistry at the California Institute of Technology, he joined the faculty of the Department of Chemistry, UCI, in 2002. He teaches analytical, physical, and atmospheric chemistry courses, and does research on chemistry of particulate matter in the ambient atmosphere and in indoor environments using state-of-the art spectroscopic and mass-spectrometric techniques. His primary areas of expertise are molecular spectroscopy, high-resolution mass spectrometry, chemical reaction dynamics, and photochemistry.

## ACKNOWLEDGMENTS

S.A.N. acknowledges support from the U.S. National Science Foundation grant AGS-1227579. C.G. acknowledges funding from the European Research Council under the European Union's Seventh Framework Programme (FP/2007-2013)/ERC Grant Agreement 290852 - AIRSEA. D.J.D. acknowledges ongoing financial support from NSERC (Canada). M.A. acknowledges support by the Swiss National Science Foundation (grant no. 149492).

## GLOSSARY

ATR-FTIR	attenuated total reflection Fourier transform infrared (spectroscopy)
AQ	anthraquinone
BC	black carbon
BrC	brown carbon
CDOM	chromophoric dissolved organic matter
CIMS	chemical ionization mass spectrometry
CRDS	cavity ring-down spectroscopy
DBK	dibenzyl ketone
DMA	<i>N,N</i> -dimethylaniline
2,4-DNP	2,4-dinitrophenol
DOM	dissolved organic matter
GC	gas chromatography
HULIS	humic-like substances
IC	imidazole-2-carboxaldehyde
ISC	intersystem crossing
MeDBK	4-methyldibenzyl ketone
OPPC	1-oleoyl-2-palmitoyl- <i>sn</i> -glycero-3-phosphocholine
PAH	polycyclic aromatic hydrocarbon
PCB	poly-chlorinated biphenyl
PM	particulate matter
POA	primary organic aerosol
POP	persistent organic pollutant
RH	relative humidity
SOA	secondary organic aerosol
SAM	self-assembled monolayer
SOM	secondary organic material
VOC	volatile organic compound

## REFERENCES

- (1) (a) Schmauss, A. W. A. *Die Atmosphäre als Kolloid*; F. Vieweg & Sohn akt.-ges.: Braunschweig, 1929. (b) Schmauß, A. *Meteorol. Z.* **1920**, *37*, 1.
- (2) Jacobson, M. Z. *Atmospheric Pollution History, Science, and Regulation*; Cambridge University Press: Cambridge, 2002.
- (3) Finlayson-Pitts, B. J.; Pitts, J. N. *Chemistry of the Upper and Lower Atmosphere: Theory, Experiments, and Applications*; Academic Press: San Diego, CA, 2000.

- (4) Chang, W. L.; Bhawe, P. V.; Brown, S. S.; Riemer, N.; Stutz, J.; Dabdub, D. *Aerosol Sci. Technol.* **2011**, *45*, 665.
- (5) WHO, 2015.
- (6) Sigman, R.; et al. *Health and Environment*; OECD Publishing: Paris.
- (7) Goldstein, A. H.; Galbally, I. E. *Environ. Sci. Technol.* **2007**, *41*, 1514.
- (8) Domine, F.; Shepson, P. B. *Science* **2002**, *297*, 1506.
- (9) Kerbrat, M.; Pinzer, B.; Huthwelker, T.; Gäggeler, H. W.; Ammann, M.; Schneebeli, M. *Atmos. Chem. Phys.* **2008**, *8*, 1261.
- (10) Diamond, M. L.; Priemer, D. A.; Law, N. L. *Chemosphere* **2001**, *44*, 1655.
- (11) Schulze, E.; Kelliher, F. M.; Korner, C.; Lloyd, J.; Leuning, R. *Annu. Rev. Ecol. Syst.* **1994**, *25*, 629.
- (12) Calvert, J. G.; Pitts, J. N. *Photochemistry*; Wiley: New York, 1966.
- (13) Herrmann, H.; Schaefer, T.; Tilgner, A.; Weller, C.; Teich, M.; Styler, S. A. *Chem. Rev.* **2014**, submitted.
- (14) Vione, D.; Maurino, V.; Minero, C.; Pelizzetti, E.; Harrison, M. A. J.; Olariu, R. I.; Arsene, C. *Chem. Soc. Rev.* **2006**, *35*, 441.
- (15) (a) Canonica, S.; Jans, U.; Stemmler, K.; Hoigne, J. *Environ. Sci. Technol.* **1995**, *29*, 1822. (b) Smith, J. D.; Sio, V.; Yu, L.; Zhang, Q.; Anastasio, C. *Environ. Sci. Technol.* **2013**, *48*, 1049. (c) Maurino, V.; Bedini, A.; Borghesi, D.; Vione, D.; Minero, C. *Phys. Chem. Chem. Phys.* **2011**, *13*, 11213.
- (16) (a) Atkinson, R.; Baulch, D. L.; Cox, R. A.; Crowley, J. N.; Hampson, R. F.; Hynes, R. G.; Jenkin, M. E.; Rossi, M. J.; Troe, J. *Atmos. Chem. Phys.* **2004**, *4*, 1461. (b) Sander, S. P. J.; Abbatt, J. P. D.; Burkholder, J. B.; Friedl, D.; Golden, D. M.; Huie, R. E.; Kolb, C. E.; Kurylo, M. J.; Moortgat, G. K.; Orkin, V. L.; Wine, P. H. *Chemical Kinetics and Photochemical Data for Use in Atmospheric Studies, Evaluation No. 17*; Jet Propulsion Laboratory: Pasadena, CA, 2011.
- (17) Ervens, B.; Turpin, B. J.; Weber, R. J. *Atmos. Chem. Phys.* **2011**, *11*, 11069.
- (18) (a) Reeser, D. I.; George, C.; Donaldson, D. J. *J. Phys. Chem. A* **2009**, *113*, 8591. (b) Reeser, D. I.; Jammoul, A.; Clifford, D.; Brigante, M.; D'Anna, B.; George, C.; Donaldson, D. J. *J. Phys. Chem. C* **2009**, *113*, 2071.
- (19) Donaldson, D. J.; Tuck, A. F.; Vaida, V. *Chem. Rev.* **2003**, *103*, 4717.
- (20) Crowley, J. N.; Ammann, M.; Cox, R. A.; Hynes, R. G.; Jenkin, M. E.; Mellouki, A.; Rossi, M. J.; Troe, J.; Wallington, T. J. *Atmos. Chem. Phys.* **2010**, *10*, 9059.
- (21) Ammann, M.; Cox, R. A.; Crowley, J. N.; Jenkin, M. E.; Mellouki, A.; Rossi, M. J.; Troe, J.; Wallington, T. J. *Atmos. Chem. Phys.* **2013**, *13*, 8045.
- (22) Ammann, M.; Poschl, U.; Rudich, Y. *Phys. Chem. Chem. Phys.* **2003**, *5*, 351.
- (23) Minero, C. *Catal. Today* **1999**, *54*, 205.
- (24) (a) Romanias, M. N.; El Zein, A.; Bedjanian, Y. *J. Phys. Chem. A* **2012**, *116*, 8191. (b) Stemmler, K.; Ammann, M.; Donders, C.; Kleffmann, J.; George, C. *Nature* **2006**, *440*, 195.
- (25) (a) Laß, K.; Friedrichs, G. *J. Geophys. Res.* **2011**, *116*, C08042. (b) Liss, P. S.; Duce, R. A. *The Sea Surface and Global Change*, 1st ed.; Cambridge University Press: Cambridge; New York, 2005. (c) Laß, K.; Friedrichs, G. *J. Geophys. Res.: Oceans* **2011**, *116*, C08042. (d) Donaldson, D. J.; George, C. *Environ. Sci. Technol.* **2012**, *46*, 10385.
- (26) Jang, M. S.; Czoschke, N. M.; Lee, S.; Kamens, R. M. *Science* **2002**, *298*, 814.
- (27) Hallquist, M.; Wenger, J. C.; Baltensperger, U.; Rudich, Y.; Simpson, D.; Claeys, M.; Dommen, J.; Donahue, N. M.; George, C.; Goldstein, A. H.; Hamilton, J. F.; Herrmann, H.; Hoffmann, T.; Iinuma, Y.; Jang, M.; Jenkin, M. E.; Jimenez, J. L.; Kiendler-Scharr, A.; Maenhaut, W.; McFiggans, G.; Mentel, T. F.; Monod, A.; Prevot, A. S. H.; Seinfeld, J. H.; Surratt, J. D.; Szmigielski, R.; Wildt, J. *Atmos. Chem. Phys.* **2009**, *9*, 5155.
- (28) Clegg, S. L.; Seinfeld, J. H.; Brimblecombe, P. *J. Aerosol Sci.* **2001**, *32*, 713.
- (29) Peng, C.; Chan, M. N.; Chan, C. K. *Environ. Sci. Technol.* **2001**, *35*, 4495.
- (30) Tsigaridis, K.; Kanakidou, M. *Atmos. Chem. Phys.* **2003**, *3*, 1849.
- (31) Volkamer, R.; Martini, F. S.; Molina, L. T.; Salcedo, D.; Jimenez, J. L.; Molina, M. J. *Geophys. Res. Lett.* **2007**, *34*, 5.
- (32) Nissenon, P.; Dabdub, D.; Das, R.; Maurino, V.; Minero, C.; Vione, D. *Atmos. Environ.* **2010**, *44*, 4859.
- (33) Zhou, S. M.; Shiraiwa, M.; McWhinney, R. D.; Poschl, U.; Abbatt, J. P. D. *Faraday Discuss.* **2013**, *165*, 391.
- (34) Virtanen, A.; Joutsensaari, J.; Koop, T.; Kannosto, J.; Yli-Pirila, P.; Leskinen, J.; Makela, J. M.; Holopainen, J. K.; Poschl, U.; Kulmala, M.; Worsnop, D. R.; Laaksonen, A. *Nature* **2010**, *467*, 824.
- (35) Koop, T.; Bookhold, J.; Shiraiwa, M.; Poschl, U. *Phys. Chem. Chem. Phys.* **2011**, *13*, 19238.
- (36) Vaden, T. D.; Song, C.; Zaveri, R. A.; Imre, D.; Zelenyuk, A. *Proc. Natl. Acad. Sci. U.S.A.* **2010**, *107*, 6658.
- (37) You, Y.; Renbaum-Wolff, L.; Carreras-Sospedra, M.; Hanna, S. J.; Hiranuma, N.; Kamal, S.; Smith, M. L.; Zhang, X.; Weber, R. J.; Shilling, J. E.; Dabdub, D.; Martin, S. T.; Bertram, A. K. *Proc. Natl. Acad. Sci. U.S.A.* **2012**, *109*, 13188.
- (38) O'Brien, R. E.; Neu, A.; Epstein, S. A.; MacMillan, A. C.; Wang, B.; Kelly, S. T.; Nizkorodov, S. A.; Laskin, A.; Moffet, R. C.; Gilles, M. K. *Geophys. Res. Lett.* **2014**, *41*, 4347.
- (39) Bones, D. L.; Reid, J. P.; Lienhard, D. M.; Krieger, U. K. *Proc. Natl. Acad. Sci. U.S.A.* **2012**, *109*, 11613.
- (40) (a) Eiseenthal, K. B. *Acc. Chem. Res.* **1993**, *26*, 636. (b) Eiseenthal, K. B. *Chem. Rev.* **1996**, *96*, 1343.
- (41) Somasundaram, T.; Lynden-Bell, R.; Patterson, C. *Phys. Chem. Chem. Phys.* **1999**, *1*, 143.
- (42) Adamson, A. W. *Physical Chemistry of Surfaces*, 4th ed.; J. Wiley: New York, 1982.
- (43) Jungwirth, P.; Tobias, D. J. *Chem. Rev.* **2006**, *106*, 1259.
- (44) (a) Pegram, L. M.; Record, M. T., Jr. *Proc. Natl. Acad. Sci. U.S.A.* **2006**, *103*, 14278. (b) Roeselová, M.; Jungwirth, P.; Tobias, D. J.; Gerber, R. B. *J. Phys. Chem. B* **2003**, *107*, 12690. (c) Tobias, D. J.; Jungwirth, P.; Parrinello, M. *J. Chem. Phys.* **2001**, *114*, 7036. (d) Jungwirth, P.; Tobias, D. J. *J. Phys. Chem. B* **2002**, *106*, 6361. (e) Ghosal, S.; Hemminger, J. C.; Bluhm, H.; Mun, B. S.; Hebenstreit, E. L. D.; Ketteler, G.; Ogletree, D. F.; Requejo, F. G.; Salmeron, M. *Science* **2005**, *307*, 563.
- (45) (a) Knipping, E. M.; Lakin, M. J.; Foster, K. L.; Jungwirth, P.; Tobias, D. J.; Gerber, R. B.; Dabdub, D.; Finlayson-Pitts, B. J. *Science* **2000**, *288*, 301. (b) Clifford, D.; Donaldson, D. J. *J. Phys. Chem. A* **2007**, *111*, 9809. (c) Hunt, S. W.; Roeselova, M.; Wang, W.; Wingen, L. M.; Knipping, E. M.; Tobias, D. J.; Dabdub, D.; Finlayson-Pitts, B. J. *J. Phys. Chem. A* **2004**, *108*, 11559. (d) Oldridge, N. W.; Abbatt, J. P. D. *J. Phys. Chem. A* **2011**, *115*, 2590.
- (46) Taraniuk, I.; Graber, E. R.; Kostinski, A.; Rudich, Y. *Geophys. Res. Lett.* **2007**, *34*, 5.
- (47) Kolb, C. E.; Cox, R. A.; Abbatt, J. P. D.; Ammann, M.; Davis, E. J.; Donaldson, D. J.; Garrett, B. C.; George, C.; Griffiths, P. T.; Hanson, D. R.; Kulmala, M.; McFiggans, G.; Pöschl, U.; Riipinen, I.; Rossi, M. J.; Rudich, Y.; Wagner, P. E.; Winkler, P. M.; Worsnop, D. R.; O'Dowd, C. D. *Atmos. Chem. Phys.* **2010**, *10*, 10561.
- (48) Bartels-Rausch, T.; Bergeron, V.; Cartwright, J. H. E.; Escribano, R.; Finney, J. L.; Grothe, H.; Gutiérrez, P. J.; Haapala, J.; Kuhs, W. F.; Pettersson, J. B. C.; Price, S. D.; Sainz-Díaz, C. I.; Stokes, D. J.; Strazzulla, G.; Thomson, E. S.; Trinks, H.; Uras-Aytemiz, N. *Rev. Mod. Phys.* **2012**, *84*, 885.
- (49) Henson, B. F.; Robinson, J. M. *Phys. Rev. Lett.* **2004**, *92*.
- (50) Wei, X.; Miranda, P. B.; Shen, Y. R. *Phys. Rev. Lett.* **2001**, *86*, 1554.
- (51) (a) Bartels-Rausch, T.; Jacobi, H. W.; Kahan, T. F.; Thomas, J. L.; Thomson, E. S.; Abbatt, J. P. D.; Ammann, M.; Blackford, J. R.; Bluhm, H.; Boxe, C.; Domine, F.; Frey, M. M.; Gladich, I.; Guzmán, M. I.; Heger, D.; Huthwelker, T.; Klán, P.; Kuhs, W. F.; Kuo, M. H.; Maus, S.; Moussa, S. G.; McNeill, V. F.; Newberg, J. T.; Pettersson, J. B. C.; Roeselová, M.; Sodeau, J. R. *Atmos. Chem. Phys.* **2014**, *14*, 1587. (b) Domine, F.; Albert, M.; Huthwelker, T.; Jacobi, H. W.;

- Kokhanovsky, A. A.; Lehning, M.; Picard, G.; Simpson, W. R. *Atmos. Chem. Phys.* **2008**, *8*, 171.
- (52) Kania, R.; Malongwe, J. K. E.; Nachtigallová, D.; Krausko, J.; Gladich, I.; Roeselová, M.; Heger, D.; Klán, P. *J. Phys. Chem. A* **2014**, *118*, 7535.
- (53) (a) Heger, D.; Nachtigallová, D.; Surman, F.; Krausko, J.; Magyarova, B.; Brumovsky, M.; Rubes, M.; Gladich, I.; Klan, P. *J. Phys. Chem. A* **2011**, *115*, 11412. (b) Kahan, T. F.; Donaldson, D. J. *J. Phys. Chem. A* **2007**, *111*, 1277.
- (54) Usher, C. R.; Michel, A. E.; Grassian, V. H. *Chem. Rev.* **2003**, *103*, 4883.
- (55) Desboeufs, K. V.; Losno, R.; Colin, J. L. *J. Atmos. Chem.* **2003**, *46*, 159.
- (56) Li, P.; Perreau, K. A.; Covington, E.; Song, C. H.; Carmichael, G. R.; Grassian, V. H. *J. Geophys. Res.: Atmos.* **2001**, *106*, 5517.
- (57) (a) Cho, H.; Shepson, P. B.; Barrie, L. A.; Cowin, J. P.; Zaveri, R. *J. Phys. Chem. B* **2002**, *106*, 11226. (b) Guzman, M. I.; Athalye, R. R.; Rodriguez, J. M. *J. Phys. Chem. A* **2012**, *116*, 5428. (c) Robinson, C.; Boxe, C.; Guzman, M.; Colussi, A.; Hoffmann, M. *J. Phys. Chem. B* **2006**, *110*, 7613.
- (58) Tegen, I.; Lacis, A. A. *J. Geophys. Res.: Atmos.* **1996**, *101*, 19237.
- (59) (a) Sassen, K.; DeMott, P. J.; Prospero, J. M.; Poellot, M. R. *Geophys. Res. Lett.* **2003**, *30*. (b) Ansmann, A.; Mattis, I.; Müller, D.; Wandinger, U.; Radlach, M.; Althausen, D.; Damoah, R. *J. Geophys. Res.: Atmos.* **2005**, *110*.
- (60) Twomey, S. A.; Piepgrass, M.; Wolfe, T. L. *Tellus, Ser. B* **1984**, *36*, 356.
- (61) (a) Krinner, G.; Boucher, O.; Balkanski, Y. *Clim. Dyn.* **2006**, *27*, 613. (b) Lambert, F.; Kug, J. S.; Park, R. J.; Mahowald, N.; Winckler, G.; Abe-Ouchi, A.; O'ishi, R.; Takemura, T.; Lee, J. H. *Nat. Clim. Change* **2013**, *3*, 487.
- (62) (a) Alfaro, S. C.; Lafon, S.; Rajot, J. L.; Formenti, P.; Gaudichet, A.; Maille, M. *J. Geophys. Res.: Atmos.* **2004**, *109*, 9. (b) Lafon, S.; Sokolik, I. N.; Rajot, J. L.; Caqueneau, S.; Gaudichet, A. *J. Geophys. Res.: Atmos.* **2006**, *111*, 19. (c) Linke, C.; Mohler, O.; Veres, A.; Mohacsi, A.; Bozoki, Z.; Szabo, G.; Schnaiter, M. *Atmos. Chem. Phys.* **2006**, *6*, 3315.
- (63) Linke, C.; Möhler, O.; Veres, A.; Mohácsi, Á.; Bozoki, Z.; Szabó, G.; Schnaiter, M. *Atmos. Chem. Phys.* **2006**, *6*, 3315.
- (64) (a) Herrmann, J. M. *Catal. Today* **1999**, *53*, 115. (b) Hoffmann, M. R.; Martin, S. T.; Choi, W.; Bahnemann, D. W. *Chem. Rev.* **1995**, *95*, 69.
- (65) Chen, H.; Nanayakkara, C. E.; Grassian, V. H. *Chem. Rev.* **2012**, *112*, 5919.
- (66) George, C.; D'Anna, B.; Herrmann, H.; Weller, C.; Vaida, V.; Donaldson, D. J.; Bartels-Rausch, T.; Ammann, M. In *Atmospheric and Aerosol Chemistry*; McNeill, V. F., Ariya, P. A., Eds.; Springer: New York, 2014; Vol. 339.
- (67) (a) Geng, L.; Alexander, B.; Cole-Dai, J.; Steig, E. J.; Savarino, J.; Sofen, E. D.; Schauer, A. J. *Proc. Natl. Acad. Sci. U.S.A.* **2014**, *111*, 5808. (b) Buffen, A. M.; Hastings, M. G.; Thompson, L. G.; Mosley-Thompson, E. *J. Geophys. Res.: Atmos.* **2014**, *119*, 2674. (c) Röthlisberger, R.; Hutterli, M. A.; Sommer, S.; Wolff, E. W.; Mulvaney, R. *J. Geophys. Res.: Atmos.* **2000**, *105*, 20565.
- (68) Grannas, A. M.; Jones, A. E.; Dibb, J.; Ammann, M.; Anastasio, C.; Beine, H. J.; Bergin, M.; Bottenheim, J.; Boxe, C. S.; Carver, G.; Chen, G.; Crawford, J. H.; Domine, F.; Frey, M. M.; Guzman, M. I.; Heard, D. E.; Helmig, D.; Hoffmann, M. R.; Honrath, R. E.; Huey, L. G.; Hutterli, M.; Jacobi, H. W.; Klan, P.; Lefer, B.; McConnell, J.; Plane, J.; Sander, R.; Savarino, J.; Shepson, P. B.; Simpson, W. R.; Sodeau, J. R.; von Glasow, R.; Weller, R.; Wolff, E. W.; Zhu, T. *Atmos. Chem. Phys.* **2007**, *7*, 4329.
- (69) Mack, J.; Bolton, J. R. *J. Photochem. Photobiol., A: Chem.* **1999**, *128*, 1.
- (70) Goldstein, S.; Rabani, J. *J. Am. Chem. Soc.* **2007**, *129*, 10597.
- (71) Herrmann, H. *Phys. Chem. Chem. Phys.* **2007**, *9*, 3935.
- (72) Zellner, R.; Exner, M.; Herrmann, H. *J. Atmos. Chem.* **1990**, *10*, 411.
- (73) Anastasio, C.; Robles, T. *J. Geophys. Res.* **2007**, *112*, D24304.
- (74) (a) Andreae, M. O.; Gelencser, A. *Atmos. Chem. Phys.* **2006**, *6*, 3131. (b) Sun, H.; Biedermann, L.; Bond, T. C. *Geophys. Res. Lett.* **2007**, *34*, L17813.
- (75) Simoneit, B. R. T. *Appl. Geochem.* **2002**, *17*, 129.
- (76) (a) Robinson, A. L.; Donahue, N. M.; Shrivastava, M. K.; Weitkamp, E. A.; Sage, A. M.; Grieshop, A. P.; Lane, T. E.; Pierce, J. R.; Pandis, S. N. *Science* **2007**, *315*, 1259. (b) Rogge, W. F.; Hildemann, L. M.; Mazurek, M. A.; Cass, G. R.; Simoneit, B. R. T. *Environ. Sci. Technol.* **1993**, *27*, 636. (c) Schauer, J. J.; Rogge, W. F.; Hildemann, L. M.; Mazurek, M. A.; Cass, G. R.; Simoneit, B. R. T. *Atmos. Environ.* **1996**, *30*, 3837. (d) Yunker, M. B.; Macdonald, R. W.; Vingarzan, R.; Mitchell, R. H.; Goyette, D.; Sylvestre, S. *Org. Geochem.* **2002**, *33*, 489. (e) Zhang, Q.; Jimenez, J. L.; Canagaratna, M. R.; Allan, J. D.; Coe, H.; Ulbrich, I.; Alfarra, M. R.; Takami, A.; Middlebrook, A. M.; Sun, Y. L.; Dzepina, K.; Dunlea, E.; Docherty, K.; DeCarlo, P. F.; Salcedo, D.; Onasch, T.; Jayne, J. T.; Miyoshi, T.; Shimojo, A.; Hatakeyama, S.; Takegawa, N.; Kondo, Y.; Schneider, J.; Drewnick, F.; Borrmann, S.; Weimer, S.; Demerjian, K.; Williams, P.; Bower, K.; Bahreini, R.; Cottrell, L.; Griffin, R. J.; Rautiainen, J.; Sun, J. Y.; Zhang, Y. M.; Worsnop, D. R. *Geophys. Res. Lett.* **2007**, *34*, 6.
- (77) Flanner, M. G.; Liu, X.; Zhou, C.; Penner, J. E. *Atmos. Chem. Phys. Discuss.* **2012**, *12*, 2057.
- (78) (a) Gehlinger, W.; Dellinger, B. *Environ. Sci. Technol.* **2013**, *47*, 8172. (b) Li, Q.; Shang, J.; Zhu, T. *Atmos. Environ.* **2013**, *81*, 68.
- (79) Monge, M. E.; D'Anna, B.; Mazri, L.; Giroir-Fendler, A.; Ammann, M.; Donaldson, D. J.; George, C. *Proc. Natl. Acad. Sci. U.S.A.* **2010**, DOI: 10.1073/pnas.0908341107.
- (80) Zelenay, V.; Monge, M. E.; D'Anna, B.; George, C.; Styler, S. A.; Huthwelker, T.; Ammann, M. *J. Geophys. Res.* **2011**, *116*, D11301.
- (81) Han, C.; Liu, Y.; Ma, J.; He, H. *J. Chem. Phys.* **2012**, *137*, 084507.
- (82) (a) Decesari, S.; Facchini, M. C.; Matta, E.; Mircea, M.; Fuzzi, S.; Chughtai, A. R.; Smith, D. M. *Atmos. Environ.* **2002**, *36*, 1827. (b) Chughtai, A. R.; Jassim, J. A.; Peterson, J. H.; Stedman, D. H.; Smith, D. M. *Aerosol Sci. Technol.* **1991**, *15*, 112.
- (83) Han, C.; Liu, Y.; He, H. *Atmos. Environ.* **2013**, *64*, 270.
- (84) (a) Gabrieli, J.; Vallelonga, P.; Cozzi, G.; Gabrieli, P.; Gambaro, A.; Sigl, M.; Decet, F.; Schwikowski, M.; Gaeggeler, H.; Boutron, C.; Cescon, P.; Barbante, C. *Environ. Sci. Technol.* **2010**, *44*, 3260. (b) McNeill, V. F.; Grannas, A. M.; Abbatt, J. P. D.; Ammann, M.; Ariya, P.; Bartels-Rausch, T.; Domine, F.; Donaldson, D. J.; Guzman, M. I.; Heger, D.; Kahan, T. F.; Klán, P.; Masclin, S.; Toubin, C.; Voisin, D. *Atmos. Chem. Phys.* **2012**, *12*, 9653.
- (85) Gu, X.; Ma, X.; Li, L.; Liu, C.; Cheng, K.; Li, Z. *J. Anal. Appl. Pyrolysis* **2013**, *102*, 16.
- (86) (a) Fine, P. M.; Cass, G. R.; Simoneit, B. R. T. *Environ. Sci. Technol.* **2001**, *35*, 2665. (b) Fine, P. M.; Cass, G. R.; Simoneit, B. R. T. *Environ. Sci. Technol.* **2002**, *36*, 1442. (c) Graham, B.; Mayol-Bracero, O. L.; Guyon, P.; Roberts, G. C.; Decesari, S.; Facchini, M. C.; Artaxo, P.; Maenhaut, W.; Koll, P.; Andreae, M. O. *J. Geophys. Res.: Atmos.* **2002**, *107*, 16. (d) Oros, D. R.; Simoneit, B. R. T. *Appl. Geochem.* **2001**, *16*, 1513. (e) Simoneit, B. R. T.; Schauer, J. J.; Nolte, C. G.; Oros, D. R.; Elias, V. O.; Fraser, M. P.; Rogge, W. F.; Cass, G. R. *Atmos. Environ.* **1999**, *33*, 173.
- (87) Canonica, S.; Hellrung, B.; Wirz, J. *J. Phys. Chem. A* **2000**, *104*, 1226.
- (88) (a) Leigh, W. J.; Lathioor, E. C.; StPierre, M. J. *J. Am. Chem. Soc.* **1996**, *118*, 12339. (b) Canonica, S. *Chimia* **2007**, *61*, 641.
- (89) Guenther, A. B.; Jiang, X.; Heald, C. L.; Sakulyanontvittaya, T.; Duhl, T.; Emmons, L. K.; Wang, X. *Geosci. Model Dev.* **2012**, *5*, 1471.
- (90) (a) Griffith, E. C.; Carpenter, B. K.; Shoemaker, R. K.; Vaida, V. *Proc. Natl. Acad. Sci. U.S.A.* **2013**, *110*, 11714. (b) Griffith, E. C.; Shoemaker, R. K.; Vaida, V. *Origins Life Evol. Biospheres* **2013**, *43*, 341. (c) Larsen, M. C.; Vaida, V. *J. Phys. Chem. A* **2012**, *116*, 5840. (d) Vaida, V. *J. Phys. Chem. A* **2009**, *113*, 5.
- (91) (a) Ervens, B.; Feingold, G.; Frost, G. J.; Kreidenweis, S. M. *J. Geophys. Res.: Atmos.* **2004**, *109*, 20. (b) Limbeck, A.; Puxbaum, H. *Atmos. Environ.* **1999**, *33*, 1847. (c) Talbot, R. W.; Andreae, M. O.;

- Berresheim, H.; Jacob, D. J.; Beecher, K. M. *J. Geophys. Res.: Atmos.* **1990**, *95*, 16799. (d) Yu, S. *Atmos. Res.* **2000**, *53*, 185.
- (92) Kawamura, K.; Yokoyama, K.; Fujii, Y.; Watanabe, O. *J. Geophys. Res.: Atmos.* **2001**, *106*, 1331.
- (93) Talbot, R. W.; Mosher, B. W.; Heikes, B. G.; Jacob, D. J.; Munger, J. W.; Daube, B. C.; Keene, W. C.; Maben, J. R.; Artz, R. S. *J. Geophys. Res.: Atmos.* **1995**, *100*, 9335.
- (94) Andino, J. M.; Smith, J. N.; Flagan, R. C.; Goddard, W. A.; Seinfeld, J. H. *J. Phys. Chem.* **1996**, *100*, 10967.
- (95) Epstein, S. A.; Tapavicza, E.; Furche, F.; Nizkorodov, S. A. *Atmos. Chem. Phys.* **2013**, *13*, 9461.
- (96) Grgic, I.; Nieto-Gligorovski, L. I.; Net, S.; Temime-Roussel, B.; Gligorovski, S.; Wortham, H. *Phys. Chem. Chem. Phys.* **2010**, *12*, 698.
- (97) (a) Altieri, K. E.; Seitzinger, S. P.; Carlton, A. G.; Turpin, B. J.; Klein, G. C.; Marshall, A. G. *Atmos. Environ.* **2008**, *42*, 1476. (b) Carlton, A. G.; Turpin, B. J.; Altieri, K. E.; Seitzinger, S.; Reff, A.; Lim, H. J.; Ervens, B. *Atmos. Environ.* **2007**, *41*, 7588. (c) Ervens, B.; Volkamer, R. *Atmos. Chem. Phys.* **2010**, *10*, 8219. (d) Galloway, M. M.; Chhabra, P. S.; Chan, A. W. H.; Surratt, J. D.; Flagan, R. C.; Seinfeld, J. H.; Keutsch, F. N. *Atmos. Chem. Phys.* **2009**, *9*, 3331. (e) Hastings, W. P.; Koehler, C. A.; Bailey, E. L.; De Haan, D. O. *Environ. Sci. Technol.* **2005**, *39*, 8728. (f) Lim, Y. B.; Tan, Y.; Perri, M. J.; Seitzinger, S. P.; Turpin, B. J. *Atmos. Chem. Phys.* **2010**, *10*, 10521. (g) Volkamer, R.; Ziemann, P. J.; Molina, M. J. *Atmos. Chem. Phys.* **2009**, *9*, 1907.
- (98) Tan, Y.; Perri, M. J.; Seitzinger, S. P.; Turpin, B. J. *Environ. Sci. Technol.* **2009**, *43*, 8105.
- (99) (a) Argirova, M.; Breipohl, W. *J. Biochem. Mol. Toxicol.* **2002**, *16*, 140. (b) De Haan, D. O.; Hawkins, L. N.; Kononenko, J. A.; Turley, J. J.; Corrigan, A. L.; Tolbert, M. A.; Jimenez, J. L. *Environ. Sci. Technol.* **2011**, *45*, 984. (c) De Haan, D. O.; Tolbert, M. A.; Jimenez, J. L. *Geophys. Res. Lett.* **2009**, *36*, 5. (d) Douglas, T. A.; Domine, F.; Barret, M.; Anastasio, C.; Beine, H. J.; Bottenheim, J.; Grannas, A.; Houdier, S.; Netcheva, S.; Rowland, G.; Staebler, R.; Steffen, A. *J. Geophys. Res.: Atmos.* **2012**, *117*, 15. (e) Drozd, G. T.; McNeill, V. F. *Environ. Sci.: Processes Impacts* **2014**, *16*, 741. (f) Hamilton, J. F.; Baeza-Romero, M. T.; Finessi, E.; Rickard, A. R.; Healy, R. M.; Peppe, S.; Adams, T. J.; Daniels, M. J. S.; Ball, S. M.; Goodall, I. C. A.; Monks, P. S.; Borrás, E.; Munoz, A. *Faraday Discuss.* **2013**, *165*, 447. (g) Hecobian, A.; Zhang, X.; Zheng, M.; Frank, N.; Edgerton, E. S.; Weber, R. *J. Atmos. Chem. Phys.* **2010**, *10*, 5965. (h) Kampf, C. J.; Jakob, R.; Hoffmann, T. *Atmos. Chem. Phys.* **2012**, *12*, 6323. (i) Lee, A. K. Y.; Zhao, R.; Li, R.; Liggio, J.; Li, S. M.; Abbatt, J. P. D. *Environ. Sci. Technol.* **2013**, *47*, 12819. (j) Noziere, B.; Dziedzic, P.; Cordova, A. *Phys. Chem. Chem. Phys.* **2010**, *12*, 3864. (k) Powelson, M. H.; Espelien, B. M.; Hawkins, L. N.; Galloway, M. M.; De Haan, D. O. *Environ. Sci. Technol.* **2014**, *48*, 985. (l) Rossignol, S.; Aregahegn, K. Z.; Tinell, L.; Fine, L.; Noziere, B.; George, C. *Environ. Sci. Technol.* **2014**, *48*, 3218. (m) Sareen, N.; Moussa, S. G.; McNeill, V. F. *J. Phys. Chem. A* **2013**, *117*, 2987. (n) Schwier, A. N.; Sareen, N.; Mitroo, D.; Shapiro, E. L.; McNeill, V. F. *Environ. Sci. Technol.* **2010**, *44*, 6174. (o) Shapiro, E. L.; Szprengiel, J.; Sareen, N.; Jen, C. N.; Giordano, M. R.; McNeill, V. F. *Atmos. Chem. Phys.* **2009**, *9*, 2289. (p) Trainic, M.; Riziq, A. A.; Lavi, A.; Rudich, Y. *J. Phys. Chem. A* **2012**, *116*, 5948. (q) Updyke, K. M.; Nguyen, T. B.; Nizkorodov, S. A. *Atmos. Environ.* **2012**, *63*, 22. (r) Utry, N.; Ajtai, T.; Filep, A.; Pinter, M. D.; Hoffer, A.; Bozoki, Z.; Szabo, G. *Atmos. Environ.* **2013**, *69*, 321. (s) Woo, J. L.; Kim, D. D.; Schwier, A. N.; Li, R. Z.; McNeill, V. F. *Faraday Discuss.* **2013**, *165*, 357. (t) Yu, G.; Bayer, A. R.; Galloway, M. M.; Korshavn, K. J.; Fry, C. G.; Keutsch, F. N. *Environ. Sci. Technol.* **2011**, *45*, 6336. (u) Zarzana, K. J.; De Haan, D. O.; Freedman, M. A.; Hasenkopf, C. A.; Tolbert, M. A. *Environ. Sci. Technol.* **2012**, *46*, 4845.
- (100) Aregahegn, K. Z.; Noziere, B.; George, C. *Faraday Discuss.* **2013**, *165*, 123.
- (101) Krivacsy, Z.; Kiss, G.; Varga, B.; Galambos, I.; Sarvari, Z.; Gelencser, A.; Molnar, A.; Fuzzi, S.; Facchini, M. C.; Zappoli, S.; Andracchio, A.; Alsberg, T.; Hansson, H. C.; Persson, L. *Atmos. Environ.* **2000**, *34*, 4273.
- (102) Facchini, M. C.; Decesari, S.; Mircea, M.; Fuzzi, S.; Loggion, G. *Atmos. Environ.* **2000**, *34*, 4853.
- (103) Santos, P. S. M.; Otero, M.; Filipe, O. M. S.; Santos, E. B. H.; Duarte, A. C. *Talanta* **2010**, *83*, 505.
- (104) Havers, N.; Burba, P.; Lambert, J.; Klockow, D. *J. Atmos. Chem.* **1998**, *29*, 45.
- (105) Voisin, D.; Jaffrezo, J.-L.; Houdier, S.; Barret, M.; Cozic, J.; King, M. D.; France, J. L.; Reay, H. J.; Grannas, A.; Kos, G.; Ariya, P. A.; Beine, H. J.; Domine, F. *J. Geophys. Res.* **2012**, *117*, D00R19.
- (106) (a) Graber, E. R.; Rudich, Y. *Atmos. Chem. Phys.* **2006**, *6*, 729. (b) Zheng, G. J.; He, K. B.; Duan, F. K.; Cheng, Y.; Ma, Y. L. *Environ. Pollut.* **2013**, *181*, 301.
- (107) Cavalli, F.; Facchini, M. C.; Decesari, S.; Mircea, M.; Emblico, L.; Fuzzi, S.; Ceburnis, D.; Yoon, Y. J.; O'Dowd, C. D.; Putaud, J. P.; Dell'Acqua, A. *J. Geophys. Res.: Atmos.* **2004**, *109*, 16.
- (108) Sun, J. M.; Ariya, P. A. *Atmos. Environ.* **2006**, *40*, 795.
- (109) Wang, B. B.; Knopf, D. A. *J. Geophys. Res.: Atmos.* **2011**, *116*, 14.
- (110) Hoffer, A.; Gelencser, A.; Guyon, P.; Kiss, G.; Schmid, O.; Frank, G. P.; Artaxo, P.; Andreae, M. O. *Atmos. Chem. Phys.* **2006**, *6*, 3563.
- (111) Baduel, C.; Monge, M. E.; Voisin, D.; Jaffrezo, J. L.; George, C.; El Haddad, I.; Marchand, N.; D'Anna, B. *Environ. Sci. Technol.* **2011**, *45*, 5238.
- (112) (a) Beine, H.; Anastasio, C.; Domine, F.; Douglas, T.; Barret, M.; France, J.; King, M.; Hall, S.; Ullmann, K. *J. Geophys. Res.* **2012**, *117*, D00R15. (b) Beine, H.; Anastasio, C.; Esposito, G.; Patten, K.; Wilkenings, E.; Domine, F.; Voisin, D.; Barret, M.; Houdier, S.; Hall, S. *J. Geophys. Res.* **2011**, *116*, D00R05.
- (113) Remucal, C. K. *Environ. Sci.: Processes Impacts* **2014**, *16*, 628.
- (114) (a) Nebbioso, A.; Piccolo, A. *Anal. Bioanal. Chem.* **2013**, *405*, 109. (b) Sulzberger, B.; Durisch-Kaiser, E. *Aquat. Sci.* **2009**, *71*, 104.
- (115) Sharpless, C. M.; Blough, N. V. *Environ. Sci.: Processes Impacts* **2014**, *16*, 654.
- (116) Phillips, S. M.; Smith, G. D. *Environ. Sci. Technol.* **2014**, *1*, 382.
- (117) Zepp, R. G.; Baughman, G. L.; Schlotzhauer, P. F. *Chemosphere* **1981**, *10*, 119.
- (118) Cooper, W. J.; Zika, R. G. *Science* **1983**, *220*, 711.
- (119) Fischer, A. M.; Kliger, D. S.; Winterle, J. S.; Mill, T. *Chemosphere* **1985**, *14*, 1299.
- (120) Zafriou, O. C.; Jousset-Dubien, J.; Zepp, R. G.; Zika, R. G. *Environ. Sci. Technol.* **1984**, *18*, 358A.
- (121) (a) Mopper, K.; Zhou, X. *Science* **1990**, *250*, 661. (b) Albinet, A.; Minero, C.; Vione, D. *Sci. Total Environ.* **2010**, *408*, 3367.
- (122) Chen, H. H.; Navea, J. G.; Young, M. A.; Grassian, V. H. *J. Phys. Chem. A* **2011**, *115*, 490.
- (123) Parmon, V. N.; Zakharenko, V. S. *CATTECH* **2001**, *5*, 96.
- (124) Vlasenko, A.; Huthwelker, T.; Gaggeler, H. W.; Ammann, M. *Phys. Chem. Chem. Phys.* **2009**, *11*, 7921.
- (125) (a) Ndour, M.; D'Anna, B.; George, C.; Ka, O.; Balkanski, Y.; Kleffmann, J.; Stemmler, K.; Ammann, M. *Geophys. Res. Lett.* **2008**, *35*, 5. (b) Ndour, M.; Nicolas, M.; D'Anna, B.; Ka, O.; George, C. *Phys. Chem. Chem. Phys.* **2009**, *11*, 1312. (c) Gustafsson, R. J.; Orlov, A.; Griffiths, P. T.; Cox, R. A.; Lambert, R. M. *Chem. Commun.* **2006**, 3936. (d) El Zein, A.; Bedjanian, Y. *Atmos. Chem. Phys.* **2012**, *12*, 1013.
- (126) Monge, M. E.; D'Anna, B.; George, C. *Phys. Chem. Chem. Phys.* **2010**, *12*, 8992.
- (127) (a) Ohko, Y.; Nakamura, Y.; Fukuda, A.; Matsuzawa, S.; Takeuchi, K. *J. Phys. Chem. C* **2008**, *112*, 10502. (b) Bedjanian, Y.; El Zein, A. *J. Phys. Chem. A* **2012**, *116*, 1758. (c) Goodman, A. L.; Underwood, G. M.; Grassian, V. H. *J. Phys. Chem. A* **1999**, *103*, 7217. (d) Ramazan, K. A.; Syomin, D.; Finlayson-Pitts, B. J. *Phys. Chem. Chem. Phys.* **2004**, *6*, 3836.
- (128) (a) Hashimoto, K.; Wasada, K.; Toukai, N.; Kominami, H.; Kera, Y. *J. Photochem. Photobiol., A: Chem.* **2000**, *136*, 103. (b) Hoffmann, M. R.; Martin, S. T.; Choi, W. Y.; Bahnemann, D. W. *Chem. Rev.* **1995**, *95*, 69. (c) Shang, J.; Du, Y.; Xu, Z. *Chemosphere* **2002**, *46*, 93.
- (129) Beaumont, S. K.; Gustafsson, R. J.; Lambert, R. M. *ChemPhysChem* **2009**, *10*, 331.
- (130) Gerischer, H.; Heller, A. *J. Electrochem. Soc.* **1992**, *139*, 113.

- (131) Hirakawa, T.; Daimon, T.; Kitazawa, M.; Ohguri, N.; Koga, C.; Negishi, N.; Matsuzawa, S.; Nosaka, Y. *J. Photochem. Photobiol., A: Chem.* **2007**, *190*, 58.
- (132) Dentener, F. J.; Carmichael, G. R.; Zhang, Y.; Lelieveld, J.; Crutzen, P. J. *J. Geophys. Res.: Atmos.* **1996**, *101*, 22869.
- (133) (a) Ndour, M.; Conchon, P.; D'Anna, B.; Ka, O.; George, C. *Geophys. Res. Lett.* **2009**, *36*. (b) Rubasinghege, G.; Elzey, S.; Baltrusaitis, J.; Jayaweera, P. M.; Grassian, V. H. *J. Chem. Phys. Lett.* **2010**, *1*, 1729. (c) Rubasinghege, G.; Grassian, V. H. *J. Phys. Chem. A* **2009**, *113*, 7818.
- (134) (a) Chen, H. H.; Stanier, C. O.; Young, M. A.; Grassian, V. H. *J. Phys. Chem. A* **2011**, *115*, 11979. (b) Meland, B.; Kleiber, P. D.; Grassian, V. H.; Young, M. A. *J. Quant. Spectrosc. Radiat. Transfer* **2011**, *112*, 1108.
- (135) Nanayakkara, C. E.; Jayaweera, P. M.; Rubasinghege, G.; Baltrusaitis, J.; Grassian, V. H. *J. Phys. Chem. A* **2014**, *118*, 158.
- (136) Rosseler, O.; Sleiman, M.; Montesinos, V. N.; Shavorskiy, A.; Keller, V.; Keller, N.; Litter, M. I.; Bluhm, H.; Salmeron, M.; Destailats, H. *J. Chem. Phys. Lett.* **2013**, 536.
- (137) Gankanda, A.; Grassian, V. H. *J. Phys. Chem. C* **2014**, *118*, 29117.
- (138) Boonstra, A. H.; Mutsaers, C. A. H. A. *J. Phys. Chem.* **1975**, *79*, 1940.
- (139) Pradhan, M.; Kalberer, M.; Griffiths, P. T.; Braban, C. F.; Pope, F. D.; Cox, R. A.; Lambert, R. M. *Environ. Sci. Technol.* **2010**, *44*, 1360.
- (140) Yi, J.; Bahrini, C.; Schoemaeker, C.; Fittschen, C.; Choi, W. J. *Phys. Chem. C* **2012**, *116*, 10090.
- (141) Vincent, G.; Aluculesei, A.; Parker, A.; Fittschen, C.; Zahraa, O.; Marquaire, P.-M. *J. Phys. Chem. C* **2008**, *112*, 9115.
- (142) Bedjanian, Y.; Romanias, M. N.; El Zein, A. *Atmos. Chem. Phys.* **2013**, *13*, 6461.
- (143) Dupart, Y.; King, S. M.; Nekat, B.; Nowak, A.; Wiedensohler, A.; Herrmann, H.; David, G.; Thomas, B.; Miffre, A.; Rairoux, P.; D'Anna, B.; George, C. *Proc. Natl. Acad. Sci. U.S.A.* **2012**, *109*, 20842.
- (144) Hanisch, F.; Crowley, J. N. *Atmos. Chem. Phys.* **2003**, *3*, 119.
- (145) Lampimäki, M.; Zelenay, V.; Křepelová, A.; Liu, Z.; Chang, R.; Bluhm, H.; Ammann, M. *ChemPhysChem* **2013**, *14*, 2419.
- (146) Roscoe, J. M.; Abbatt, J. P. D. *J. Phys. Chem. A* **2005**, *109*, 9028.
- (147) (a) Chen, H.; Stanier, C. O.; Young, M. A.; Grassian, V. H. *J. Phys. Chem. A* **2011**, *115*, 11979. (b) Nicolas, M.; Ndour, M.; Ka, O.; D'Anna, B.; George, C. *Environ. Sci. Technol.* **2009**, *43*, 7437. (c) Ohtani, B.; Zhang, S.-W.; Nishimoto, S.-i.; Kagiya, T. *J. Chem. Soc., Faraday Trans.* **1992**, *88*, 1049. (d) Mills, A.; Lee, S.-K.; Lepre, A. *J. Photochem. Photobiol., A: Chem.* **2003**, *155*, 199.
- (148) Styler, S. A.; Donaldson, D. J. *Environ. Sci. Technol.* **2012**, *46*, 8756.
- (149) Styler, S. A.; Myers, A. L.; Donaldson, D. J. *Environ. Sci. Technol.* **2013**, *47*, 6358.
- (150) Wentworth, G. R.; Al-Abadleh, H. A. *Phys. Chem. Chem. Phys.* **2011**, *13*, 6507.
- (151) Tofan-Lazar, J.; Al-Abadleh, H. A. *Environ. Sci. Technol.* **2014**, *48*, 394.
- (152) Bossan, D.; Wortham, H.; Masclat, P. *Chemosphere* **1995**, *30*, 21.
- (153) Lackhoff, M.; Niessner, R. *Environ. Sci. Technol.* **2002**, *36*, 5342.
- (154) (a) Karagulian, F.; Dilbeck, C. W.; Finlayson-Pitts, B. J. *J. Phys. Chem. A* **2009**, *113*, 7205. (b) Karagulian, F.; Dilbeck, C. W.; Finlayson-Pitts, B. J. *J. Am. Chem. Soc.* **2008**, *130*, 11272.
- (155) Nie, W.; Wang, T.; Xue, L. K.; Ding, A. J.; Wang, X. F.; Gao, X. M.; Xu, Z.; Yu, Y. C.; Yuan, C.; Zhou, Z. S.; Gao, R.; Liu, X. H.; Wang, Y.; Fan, S. J.; Poon, S.; Zhang, Q. Z.; Wang, W. X. *Atmos. Chem. Phys.* **2012**, *12*, 11985.
- (156) Nie, W.; Ding, A.; Wang, T.; Kerminen, V.-M.; George, C.; Xue, L.; Wang, W.; Zhang, Q.; Petaja, T.; Qi, X.; Gao, X.; Wang, X.; Yang, X.; Fu, C.; Kulmala, M. *Sci. Rep.* **2014**, *4*.
- (157) Benjamin, I. *Chem. Rev.* **1996**, *96*, 1449.
- (158) Richert, S.; Fedoseeva, M.; Vauthey, E. *J. Chem. Phys. Lett.* **2012**, *3*, 1635.
- (159) McArthur, E. A.; Eisenthal, K. B. *J. Am. Chem. Soc.* **2006**, *128*, 1068.
- (160) Fita, P.; Fedoseeva, M.; Vauthey, E. *J. Phys. Chem. A* **2011**, *115*, 2465.
- (161) Fita, P.; Fedoseeva, M.; Vauthey, E. *Langmuir* **2011**, *27*, 4645.
- (162) Clifford, D.; Donaldson, D. J.; Brigante, M.; D'Anna, B.; George, C. *Environ. Sci. Technol.* **2008**, *42*, 1138.
- (163) Henderson, E. A.; Donaldson, D. J. *J. Phys. Chem. A* **2012**, *116*, 423.
- (164) Styler, S. A.; Brigante, M.; D'Anna, B.; George, C.; Donaldson, D. J. *Phys. Chem. Chem. Phys.* **2009**, *11*, 7876.
- (165) Sitzmann, E. V.; Eisenthal, K. B. *J. Chem. Phys.* **1989**, *90*, 2831.
- (166) (a) Brown, A. R.; Yellowlees, L. J.; Girault, H. H. *J. Chem. Soc., Faraday Trans.* **1993**, *89*, 207. (b) Kott, K. L.; Higgins, D. A.; McMahon, R. J.; Corn, R. M. *J. Am. Chem. Soc.* **1993**, *115*, 5342.
- (167) Finlayson-Pitts, B. J. *Phys. Chem. Chem. Phys.* **2009**, *11*, 7760.
- (168) (a) Richards, N. K.; Finlayson-Pitts, B. J. *Environ. Sci. Technol.* **2012**, *46*, 10447. (b) Richards, N. K.; Wingen, L. M.; Callahan, K. M.; Nishino, N.; Kleinman, M. T.; Tobias, D. J.; Finlayson-Pitts, B. J. *J. Phys. Chem. A* **2011**, *115*, 5810. (c) Richards-Henderson, N. K.; Callahan, K. M.; Nissenson, P.; Nishino, N.; Tobias, D. J.; Finlayson-Pitts, B. J. *Phys. Chem. Chem. Phys.* **2013**, *15*, 17636. (d) Wingen, L. M.; Moskun, A. C.; Johnson, S. N.; Thomas, J. L.; Roeselova, M.; Tobias, D. J.; Kleinman, M. T.; Finlayson-Pitts, B. J. *Phys. Chem. Chem. Phys.* **2008**, *10*, 5668.
- (169) Das, R.; Dutta, B.; Maurino, V.; Vione, D.; Minero, C. *Environ. Chem. Lett.* **2009**, *7*, 337.
- (170) Hong, A. C.; Wren, S. N.; Donaldson, D. J. *J. Chem. Phys. Lett.* **2013**, *4*, 2994.
- (171) Yu, Y.; Ezell, M. J.; Zelenyuk, A.; Imre, D.; Alexander, L.; Ortega, J.; D'Anna, B.; Harmon, C. W.; Johnson, S. N.; Finlayson-Pitts, B. J. *Atmos. Environ.* **2008**, *42*, 5044.
- (172) Yang, W. T.; Ranby, B. J. *Appl. Polym. Sci.* **1996**, *62*, 545.
- (173) de Samaniego, M. S. S.; Miller, A. F. *Colloids Surf., A* **2008**, *321*, 271.
- (174) Posfai, M.; Gelencser, A.; Simonics, R.; Arato, K.; Li, J.; Hobbs, P. V.; Buseck, P. R. *J. Geophys. Res.* **2004**, *109*, D06213.
- (175) Liu, P.; Zhang, Y.; Martin, S. T. *Environ. Sci. Technol.* **2013**, *47*, 13594.
- (176) Nizkorodov, S. A.; Laskin, J.; Laskin, A. *Phys. Chem. Chem. Phys.* **2011**, *13*, 3612.
- (177) (a) Jimenez, J. L.; Canagaratna, M. R.; Donahue, N. M.; Prevot, A. S. H.; Zhang, Q.; Kroll, J. H.; DeCarlo, P. F.; Allan, J. D.; Coe, H.; Ng, N. L.; Aiken, A. C.; Docherty, K. S.; Ulbrich, I. M.; Grieshop, A. P.; Robinson, A. L.; Duplissy, J.; Smith, J. D.; Wilson, K. R.; Lanz, V. A.; Hueglin, C.; Sun, Y. L.; Tian, J.; Laaksonen, A.; Raatikainen, T.; Rautiainen, J.; Vaattovaara, P.; Ehn, M.; Kulmala, M.; Tomlinson, J. M.; Collins, D. R.; Cubison, M. J.; Dunlea, J.; Huffman, J. A.; Onasch, T. B.; Alfarra, M. R.; Williams, P. I.; Bower, K.; Kondo, Y.; Schneider, J.; Drewnick, F.; Borrmann, S.; Weimer, S.; Demerjian, K.; Salcedo, D.; Cottrell, L.; Griffin, R.; Takami, A.; Miyoshi, T.; Hatakeyama, S.; Shimono, A.; Sun, J. Y.; Zhang, Y. M.; Dzepina, K.; Kimmel, J. R.; Sueper, D.; Jayne, J. T.; Herndon, S. C.; Trimborn, A. M.; Williams, L. R.; Wood, E. C.; Middlebrook, A. M.; Kolb, C. E.; Baltensperger, U.; Worsnop, D. R. *Science* **2009**, *326*, 1525. (b) Rudich, Y.; Donahue, N. M.; Mentel, T. F. *Annu. Rev. Phys. Chem.* **2007**, *58*, 321. (c) Petters, M. D.; Prenni, A. J.; Kreidenweis, S. M.; DeMott, P. J.; Matsunaga, A.; Lim, Y. B.; Ziemann, P. *J. Geophys. Res. Lett.* **2006**, *33*, L24806. (d) Kanakidou, M.; Seinfeld, J. H.; Pandis, S. N.; Barnes, I.; Dentener, F. J.; Facchini, M. C.; Van Dingenen, R.; Ervens, B.; Nenes, A.; Nielsen, C. J.; Swietlicki, E.; Putaud, J. P.; Balkanski, Y.; Fuzzi, S.; Horth, J.; Moortgat, G. K.; Winterhalter, R.; Myhre, C. E. L.; Tsigaridis, K.; Vignati, E.; Stephanou, E. G.; Wilson, J. *Atmos. Chem. Phys.* **2005**, *5*, 1053. (e) Ng, N. L.; Canagaratna, M. R.; Jimenez, J. L.; Chhabra, P. S.; Seinfeld, J. H.; Worsnop, D. R. *Atmos. Chem. Phys.* **2011**, *11*, 6465.
- (178) (a) Nieto-Gligorovski, L. I.; Net, S.; Gligorovski, S.; Wortham, H.; Grothe, H.; Zetzsch, C. *Atmos. Environ.* **2010**, *44*, 5451. (b) Net, S.; Gligorovski, S.; Wortham, H. *Atmos. Environ.* **2010**, *44*, 3286.

- (c) Vione, D.; Maurino, V.; Minero, C.; Pelizzetti, E.; Harrison, M. A. J.; Olariu, R.-I.; Arsene, C. *Chem. Soc. Rev.* **2006**, *35*, 441.
- (d) Donaldson, D. J.; Valsaraj, K. T. *Environ. Sci. Technol.* **2010**, *44*, 865. (e) Parmon, V. N. *Colloids Surf., A* **1999**, *151*, 351. (f) Isidorov, V.; Klokova, E.; Povarov, V.; Kolkova, S. *Catal. Today* **1997**, *39*, 233. (g) Isidorov, V. A.; Klokova, E. M.; Kozubenko, S. G.; Ivanova, A. R. *Vestn. S.-Peterb. Univ., Ser. 4: Fiz., Khim.* **1992**, *97*. (h) Monge, M. E.; Rosenørn, T.; Favez, O.; Müller, M.; Adler, G.; Abo Riziq, A.; Rudich, Y.; Herrmann, H.; George, C.; D'Anna, B. *Proc. Natl. Acad. Sci. U.S.A.* **2012**, *109*, 6840.
- (179) (a) Fan, Z.; Kamens, R. M.; Hu, J.; Zhang, J.; McDow, S. *Environ. Sci. Technol.* **1996**, *30*, 1358. (b) McDow, S. R.; Jang, M.; Hong, Y.; Kamens, R. M. *J. Geophys. Res.* **1996**, *101*, 19593. (c) McDow, S. R.; Sun, Q. R.; Vartiainen, M.; Hong, Y. S.; Yao, Y. L.; Hayes, E. A.; Kamens, R. M. *Polycyclic Aromat. Compd.* **1993**, *3*, 111. (d) Feilberg, A.; Nielsen, T. *Environ. Sci. Technol.* **2001**, *35*, 108. (e) Feilberg, A.; Nielsen, T. *Environ. Sci. Technol.* **2000**, *34*, 789.
- (180) (a) Pan, X.; Underwood, J. S.; Xing, J.-H.; Mang, S. A.; Nizkorodov, S. A. *Atmos. Chem. Phys.* **2009**, *9*, 3851. (b) Mang, S. A.; Henricksen, D. K.; Bateman, A. P.; Andersen, M. P. S.; Blake, D. R.; Nizkorodov, S. A. *J. Phys. Chem. A* **2008**, *112*, 8337. (c) Walser, M. L.; Park, J.; Gomez, A. L.; Russell, A. R.; Nizkorodov, S. A. *J. Phys. Chem. A* **2007**, *111*, 1907. (d) Mang, S. A.; Walser, M. L.; Pan, X.; Xing, J.-H.; Bateman, A. P.; Underwood, J. S.; Gomez, A. L.; Park, J.; Nizkorodov, S. A. In *Atmospheric Aerosols: Characterization, Chemistry, and Modeling (ACS Symposium Series)*; Valsaraj, K. T., Kommalapati, R. R., Eds.; American Chemical Society: Washington, DC, 2009; Vol. 1005 (Atmospheric Aerosols). (e) Hung, H.-M.; Chen, Y.-Q.; Martin, S. T. *J. Phys. Chem. A* **2013**, *117*, 108.
- (181) Kwan, A. J.; Crouse, J. D.; Clarke, A. D.; Shinozuka, Y.; Anderson, B. E.; Crawford, J. H.; Avery, M. A.; McNaughton, C. S.; Brune, W. H.; Singh, H. B.; Wennberg, P. O. *Geophys. Res. Lett.* **2006**, *33*, L15815.
- (182) Turro, N. J.; Ramamurthy, V.; Scaiano, J. C. *Modern Molecular Photochemistry of Organic Molecules*; University Science Books: Sausalito, CA, 2010.
- (183) Klán, P.; Wirz, J. *Photochemistry of Organic Compounds: From Concepts to Practice*; John Wiley & Sons Ltd.: Chichester, UK, 2009.
- (184) Haagen-Smit, A. J. *J. Ind. Eng. Chem. (Washington, D. C.)* **1952**, *44*, 1342.
- (185) (a) Presto, A. A.; Donahue, N. M. *Environ. Sci. Technol.* **2006**, *40*, 3536. (b) Presto, A. A.; Huff Hartz, K. E.; Donahue, N. M. *Environ. Sci. Technol.* **2005**, *39*, 7036.
- (186) Zhang, J.; Huff Hartz, K. E.; Pandis, S. N.; Donahue, N. M. *J. Phys. Chem. A* **2006**, *110*, 11053.
- (187) Henry, K. M.; Donahue, N. M. *J. Phys. Chem. A* **2012**, *116*, 5932.
- (188) Kroll, J. H.; Ng, N. L.; Murphy, S. M.; Flagan, R. C.; Seinfeld, J. H. *Environ. Sci. Technol.* **2006**, *40*, 1869.
- (189) Surratt, J. D.; Murphy, S. M.; Kroll, J. H.; Ng, N. L.; Hildebrandt, L.; Sorooshian, A.; Szmigielski, R.; Vermeylen, R.; Maenhaut, W.; Claeys, M.; Flagan, R. C.; Seinfeld, J. H. *J. Phys. Chem. A* **2006**, *110*, 9665.
- (190) Kroll, J. H.; Ng, N. L.; Murphy, S. M.; Flagan, R. C.; Seinfeld, J. H. *Geophys. Res. Lett.* **2005**, *32*, L18808.
- (191) Leskinen, A. P.; Jokiniemi, J. K.; Lehtinen, K. E. *J. Atmos. Environ.* **2007**, *41*, 3713.
- (192) Zhong, M.; Jang, M. *Atmos. Chem. Phys.* **2014**, *14*, 1517.
- (193) Wong, J.; Zhou, S.; Abbatt, J. *J. Phys. Chem. A* **2015**, DOI: 10.1021/jp506898c.
- (194) Epstein, S. A.; Blair, S. L.; Nizkorodov, S. A. *Environ. Sci. Technol.* **2014**.
- (195) Laskin, A.; Laskin, J.; Nizkorodov, S. A. *Chem. Rev.* **2015**, DOI: 10.1021/cr5006167.
- (196) Bahadur, R.; Praveen, P. S.; Xu, Y.; Ramanathan, V. *Proc. Natl. Acad. Sci. U.S.A.* **2012**, *109*, 17366.
- (197) Lee, H. J.; Aiona, P. K.; Laskin, A.; Laskin, J.; Nizkorodov, S. A. *Environ. Sci. Technol.* **2014**, *48*, 10217.
- (198) Bones, D. L.; Phillips, L. F. *Phys. Chem. Chem. Phys.* **2009**, *11*, 5392.
- (199) (a) Jang, M.; McDow, S. R. *Environ. Sci. Technol.* **1997**, *31*, 1046. (b) Jang, M.; McDow, S. R. *Environ. Sci. Technol.* **1995**, *29*, 2654. (c) McDow, S. R.; Sun, Q.-r.; Vartiainen, M.; Hong, Y.-s.; Yao, Y.-l.; Fister, T.; Yao, R.-q.; Kamens, R. M. *Environ. Sci. Technol.* **1994**, *28*, 2147.
- (200) Sotero, P.; Arce, R. *J. Photochem. Photobiol., A* **2008**, *199*, 14.
- (201) Fioressi, S.; Arce, R. *Environ. Sci. Technol.* **2005**, *39*, 3646.
- (202) Reyes, C. A.; Medina, M.; Crespo-Hernandez, C.; Cedeno, M. Z.; Arce, R.; Rosario, O.; Steffenson, D. M.; Ivanov, I. N.; Sigman, M. E.; Dabestani, R. *Environ. Sci. Technol.* **1999**, *34*, 415.
- (203) (a) Hashimoto, S.; Kano, K. *Bull. Chem. Soc. Jpn.* **1972**, *45*, 549. (b) Barltrop, J. A.; Bunce, N. J. *J. Chem. Soc. C* **1968**, 1467.
- (204) Garcia-Berrios, Z. I.; Arce, R. *J. Phys. Chem. A* **2012**, *116*, 3652.
- (205) Dolinová, J.; Klánová, J.; Klán, P.; Holoubek, I. *Chemosphere* **2004**, *57*, 1399.
- (206) Pitts, J. N., Jr.; Wan, J. K. S.; Schuck, E. A. *J. Am. Chem. Soc.* **1964**, *86*, 3606.
- (207) Weiss, R. G.; Ramamurthy, V.; Hammond, G. S. *Acc. Chem. Res.* **1993**, *26*, 530.
- (208) Shiraiwa, M.; Ammann, M.; Koop, T.; Poschl, U. *Proc. Natl. Acad. Sci. U.S.A.* **2011**, *108*, 11003.
- (209) Lignell, H.; Hinks, M. L.; Nizkorodov, S. A. *Proc. Natl. Acad. Sci. U.S.A.* **2014**, *111*, 13780.
- (210) Renbaum-Wolff, L.; Grayson, J. W.; Bateman, A. P.; Kuwata, M.; Sellier, M.; Murray, B. J.; Shilling, J. E.; Martin, S. T.; Bertram, A. K. *Proc. Natl. Acad. Sci. U.S.A.* **2013**, *110*, 8014.
- (211) (a) Segal-Rosenheimer, M.; Dubowski, Y. *J. Photochem. Photobiol., A* **2010**, *209*, 193. (b) Segal-Rosenheimer, M.; Dubowski, Y. *J. Photochem. Photobiol., A* **2008**, *200*, 262. (c) Samsonov, Y. N. *J. Chem. Chem. Eng.* **2014**, *8*, 286.
- (212) Cowen, S.; Al-Abadleh, H. A. *Phys. Chem. Chem. Phys.* **2009**, *11*, 7838.
- (213) Stemmler, K.; Ndour, M.; Elshorbany, Y.; Kleffmann, J.; D'Anna, B.; George, C.; Bohn, B.; Ammann, M. *Atmos. Chem. Phys.* **2007**, *7*, 4237.
- (214) Sosedova, Y.; Rouviere, A.; Bartels-Rausch, T.; Ammann, M. *Photochem. Photobiol. Sci.* **2011**.
- (215) D'Anna, B.; Jammoul, A.; George, C.; Stemmler, K.; Fahrni, S.; Ammann, M.; Wisthaler, A. *J. Geophys. Res.* **2009**, *114*.
- (216) Staehelin, J.; Hoigné, J. *Vom Wasser* **1983**, *61*, 337.
- (217) Park, J.; Gomez, A. L.; Walser, M. L.; Lin, A.; Nizkorodov, S. A. *Phys. Chem. Chem. Phys.* **2006**, *8*, 2506.
- (218) Docherty, K. S.; Wu, W.; Lim, Y. B.; Ziemann, P. *J. Environ. Sci. Technol.* **2005**, *39*, 4049.
- (219) Shemesh, D.; Blair, S. L.; Nizkorodov, S. A.; Gerber, R. B. *Phys. Chem. Chem. Phys.* **2014**, *16*, 23861.
- (220) Gomez, A.; Park, J.; Walser, M.; Lin, A.; Nizkorodov, S. A. *J. Phys. Chem. A* **2006**, *110*, 3584.
- (221) De Laurentiis, E.; Socorro, J.; Vione, D.; Quivet, E.; Brigante, M.; Mailhot, G.; Wortham, H.; Gligorovski, S. *Atmos. Environ.* **2013**, *81*, 569.
- (222) (a) Jammoul, A.; Gligorovski, S.; George, C.; D'Anna, B. *J. Phys. Chem. A* **2008**, *112*, 1268. (b) Net, S.; Nieto-Gligorovski, L.; Gligorovski, S.; Wortham, H. *Atmos. Chem. Phys.* **2010**, *10*, 1545.
- (223) Net, S.; Nieto-Gligorovski, L.; Gligorovski, S.; Temime-Roussel, B.; Barbati, S.; Lazarou, Y. G.; Wortham, H. *Atmos. Environ.* **2009**, *43*, 1683.
- (224) Nieto-Gligorovski, L.; Net, S.; Gligorovski, S.; Zetzsch, C.; Jammoul, A.; D'Anna, B.; George, C. *Phys. Chem. Chem. Phys.* **2008**, *10*, 2964.
- (225) Forrester, S. M.; Knopf, D. A. *Atmos. Chem. Phys.* **2013**, *13*, 6507.
- (226) Simpson, W. R.; von Glasow, R.; Riedel, K.; Anderson, P.; Ariya, P.; Bottenheim, J.; Burrows, J.; Carpenter, L. J.; Frieß, U.; Goodsite, M. E.; Heard, D.; Hutterli, M.; Jacobi, H. W.; Kaleschke, L.; Neff, B.; Plane, J.; Platt, U.; Richter, A.; Roscoe, H.; Sander, R.;

- Shepson, P.; Sodeau, J.; Steffen, A.; Wagner, T.; Wolff, E. *Atmos. Chem. Phys.* **2007**, *7*, 4375.
- (227) Steffen, A.; Douglas, T.; Amyot, M.; Ariya, P.; Aspmo, K.; Berg, T.; Bottenheim, J.; Brooks, S.; Cobbett, F.; Dastoor, A.; Dommergue, A.; Ebinghaus, R.; Ferrari, C.; Gardfeldt, K.; Goodsite, M. E.; Lean, D.; Poulain, A. J.; Scherz, C.; Skov, H.; Sommar, J.; Temme, C. *Atmos. Chem. Phys.* **2008**, *8*, 1445.
- (228) Morin, S.; Savarino, J.; Frey, M. M.; Yan, N.; Bekki, S.; Bottenheim, J. W.; Martins, J. M. F. *Science* **2008**, *322*, 730.
- (229) McNeill, V. F.; Wolff, E.; Bartels-Rausch, T.; Pfeiffenberger, H. *Copernic* **2014**.
- (230) Pinzer, B. R.; Schneebeili, M. *Geophys. Res. Lett.* **2009**, *36*.
- (231) Maus, S.; Muller, S.; Buttner, J.; Brutsch, S.; Huthwelker, T.; Schwikowski, M.; Enzmann, F.; Vahatolo, A. *Ann. Glaciol.* **2011**, *52*, 301.
- (232) Guimbaud, C.; Grannas, A. M.; Shepson, P. B.; Fuentes, J.; Boudries, H.; Bottenheim, J.; Domine, F.; Houdier, S.; Perrier, S.; Biesenthal, T.; Splawn, B. *Atmos. Environ.* **2002**, *36*, 2743.
- (233) Popp, P. J.; Gao, R. S.; Marcy, T. P.; Fahey, D. W.; Hudson, P. K.; Thompson, T. L.; Karcher, B.; Ridley, B. A.; Weinheimer, A. J.; Knapp, D. J.; Montzka, D. D.; Baumgardner, D.; Garrett, T. J.; Weinstock, E. M.; Smith, J. B.; Sayres, D. S.; Pittman, J. V.; Dhaniyala, S.; Bui, T. P.; Mahoney, M. J. *J. Geophys. Res.: Atmos.* **2004**, *109*, art. no.
- (234) Huthwelker, T.; Ammann, M.; Peter, T. *Chem. Rev.* **2006**, *106*, 1375.
- (235) (a) Bartels-Rausch, T.; Wren, S. N.; Schreiber, S.; Riche, F.; Schneebeili, M.; Ammann, M. *Atmos. Chem. Phys. Discuss.* **2013**, *13*, 6131. (b) Pinzer, B. R.; Kerbrat, M.; Huthwelker, T.; Gäggeler, H. W.; Schneebeili, M.; Ammann, M. *J. Geophys. Res.* **2010**, *115*, D03304.
- (236) (a) Barret, M.; Domine, F.; Houdier, S.; Gallet, J.-C.; Weibring, P.; Walega, J.; Fried, A.; Richter, D. *J. Geophys. Res.* **2011**, *116*, D00R03. (b) Barret, M.; Houdier, S.; Domine, F. *J. Phys. Chem. A* **2011**, *115*, 307.
- (237) Warren, S. G.; Brandt, R. E.; Grenfell, T. C. *Appl. Opt.* **2006**, *45*, 5320.
- (238) (a) Chu, L.; Anastasio, C. *J. Phys. Chem. A* **2003**, *107*, 9594. (b) Chu, L.; Anastasio, C. *J. Phys. Chem. A* **2005**, *109*, 6264. (c) Chu, L.; Anastasio, C. *Environ. Sci. Technol.* **2007**, *41*, 3626.
- (239) Hutterli, M. A.; Bales, R. C.; McConnell, J. R.; Stewart, R. W. *Geophys. Res. Lett.* **2002**, *29*.
- (240) Beine, H.; Anastasio, C. *J. Geophys. Res.* **2011**, *116*.
- (241) Dubowski, Y.; Colussi, A. J.; Hoffmann, M. R. *J. Phys. Chem. A* **2001**, *105*, 4928.
- (242) Boxe, C. S.; Colussi, A. J.; Hoffmann, M. R.; Murphy, J.; Wooldridge, P. J.; Bertram, T.; Cohen, R. *J. Phys. Chem. A* **2005**, *109*, 8520.
- (243) Krepelova, A.; Newberg, J.; Huthwelker, T.; Bluhm, H.; Ammann, M. *Phys. Chem. Chem. Phys.* **2010**, *12*, 8870.
- (244) (a) Marchand, P.; Marcotte, G.; Ayotte, P. *J. Phys. Chem. A* **2012**, *116*, 12112. (b) Marcotte, G.; Ayotte, P.; Bendouan, A.; Sirotti, F.; Laffon, C.; Parent, P. *J. Chem. Phys. Lett.* **2013**, *4*, 2643.
- (245) Riikonen, S.; Parkkinen, P.; Halonen, L.; Gerber, R. B. *J. Phys. Chem. A* **2014**, *118*, 5029.
- (246) Zhu, C.; Xiang, B.; Chu, L.; Zhu, L. *J. Phys. Chem. A* **2010**, *114*, 2561.
- (247) Wren, S. N.; Donaldson, D. J. *J. Chem. Phys. Lett.* **2011**, *2*, 1967.
- (248) Meusinger, C.; Berhanu, T. A.; Erbland, J.; Savarino, J.; Johnson, M. S. *J. Chem. Phys.* **2014**, *140*.
- (249) Gillett, R. W.; van Ommen, T. D.; Jackson, A. V.; Ayers, G. P. *J. Glaciol.* **2000**, *46*, 15.
- (250) Epstein, S. A.; Shemesh, D.; Tran, V. T.; Nizkorodov, S. A.; Gerber, R. B. *J. Phys. Chem. A* **2012**, *116*, 6068.
- (251) Ignatov, S. K.; Gadzhiev, O. B.; Kulikov, M. Y.; Petrov, A. I.; Razuvaev, A. G.; Gand, M.; Feigin, A. M.; Schrems, O. *J. Phys. Chem. C* **2011**, *115*, 9081.
- (252) Shemesh, D.; Gerber, R. B. *Mol. Phys.* **2012**, *110*, 605.
- (253) Kamboures, M. A.; Nizkorodov, S. A.; Gerber, R. B. *Proc. Natl. Acad. Sci. U.S.A.* **2010**, *107*, 6600.
- (254) Hamer, P. D.; Shallcross, D. E.; Yabushita, A.; Kawasaki, M.; Marécal, V.; Boxe, C. S. *Environ. Chem.* **2014**, *11*, 459.
- (255) Matykiewiczova, N.; Kurkova, R.; Klanova, J.; Klan, P. *J. Photochem. Photobiol., A: Chem.* **2007**, *187*, 24.
- (256) Kahan, T. F.; Donaldson, D. J. *Environ. Sci. Technol.* **2010**, *44*, 3819.
- (257) Ardura, D.; Kahan, T. F.; Donaldson, D. J. *J. Phys. Chem. A* **2009**, *113*, 7353.
- (258) Kahan, T. F.; Zhao, R.; Jumaa, K. B.; Donaldson, D. J. *Environ. Sci. Technol.* **2010**, *44*, 1302.
- (259) Kurkova, R.; Ray, D.; Nachtigallova, D.; Klan, P. *Environ. Sci. Technol.* **2011**, *45*, 3430.
- (260) (a) Dolinova, J.; Ruzicka, R.; Kurkova, R.; Klanova, J.; Klan, P. *Environ. Sci. Technol.* **2006**, *40*, 7668. (b) Dubowski, Y.; Hoffmann, M. *Geophys. Res. Lett.* **2000**, *27*, 3321. (c) Klanova, J.; Klan, P.; Heger, D.; Holoubek, I. *Photochem. Photobiol. Sci.* **2003**, *2*, 1023. (d) Klanova, J.; Klan, P.; Nosek, J.; Holoubek, I. *Environ. Sci. Technol.* **2003**, *37*, 1568.
- (261) Kahan, T. F.; Kwamena, N. O. A.; Donaldson, D. J. *Atmos. Chem. Phys.* **2010**, *10*, 10917.
- (262) Ram, K.; Anastasio, C. *Atmos. Environ.* **2009**, *43*, 2252.
- (263) Weber, J.; Kurkova, R.; Klanova, J.; Klan, P.; Halsall, C. *Environ. Pollut.* **2009**, *157*, 3308.
- (264) Domine, F.; Bock, J.; Voisin, D.; Donaldson, D. J. *J. Phys. Chem. A* **2013**, *117*, 4733.
- (265) Malley, P. P. A.; Kahan, T. F. *J. Phys. Chem. A* **2014**, *118*, 1638.
- (266) (a) Klan, P.; Ansorgova, A.; del Favero, D.; Holoubek, I. *Tetrahedron Lett.* **2000**, *41*, 7785. (b) Klán, P.; del Favero, D.; Ansorgova, A.; Klanova, J.; Holoubek, I. *Environ. Sci. Pollut. Res.* **2001**, *8*, 195. (c) Klán, P.; Holoubek, I. *Chemosphere* **2002**, *46*, 1201.
- (267) Heger, D.; Klan, P. *J. Photochem. Photobiol., A: Chem.* **2007**, *187*, 275.
- (268) Matykiewiczova, N.; Klanova, J.; Klan, P. *Environ. Sci. Technol.* **2007**, *41*, 8308.
- (269) Rowland, G. A.; Bausch, A. R.; Grannas, A. M. *Environ. Pollut.* **2011**, *159*, 1076.
- (270) Guzman, M. I.; Colussi, A. J.; Hoffmann, M. R. *J. Phys. Chem. A* **2006**, *110*, 931.
- (271) Guzman, M. I.; Hoffmann, M. R.; Colussi, A. J. *J. Geophys. Res.: Atmos.* **2007**, *112*.
- (272) Ruzicka, R.; Baráková, L.; Klan, P. *J. Phys. Chem. B* **2005**, *109*, 9346.
- (273) Grannas, A. M.; Pagano, L. P.; Pierce, B. C.; Bobby, R.; Fede, A. *Environ. Sci. Technol.* **2014**.
- (274) Bower, J. P.; Anastasio, C. *J. Phys. Chem. A* **2013**, *117*, 6612.
- (275) Bartels-Rausch, T.; Brigante, M.; Elshorbany, Y. F.; Ammann, M.; D'Anna, B.; George, C.; Stemmler, K.; Ndour, M.; Kleffmann, J. *Atmos. Environ.* **2010**, *44*, 5443.
- (276) Bartels-Rausch, T.; Krysztofiak, G.; Bernhard, A.; Schläppi, M.; Schwikowski, M.; Ammann, M. *Chemosphere* **2011**, *82*, 199.
- (277) Jammoul, A.; Dumas, S.; D'Anna, B.; George, C. *Atmos. Chem. Phys.* **2009**, *9*, 4229.
- (278) Kim, K.; Choi, W.; Hoffmann, M. R.; Yoon, H.-I.; Park, B.-K. *Environ. Sci. Technol.* **2010**, *44*, 4142.
- (279) Kim, K.; Yoon, H.-I.; Choi, W. *Environ. Sci. Technol.* **2012**, *46*, 13160.
- (280) Kim, K.; Choi, W. *Environ. Sci. Technol.* **2011**, *45*, 2202.
- (281) (a) Law, N. L.; Diamond, M. L. *Chemosphere* **1998**, *36*, 2607. (b) Diamond, M. L.; Gingrich, S. E.; Fertuck, K.; McCarry, B. E.; Stern, G. A.; Billeck, B.; Grift, B.; Brooker, D.; Yager, T. D. *Environ. Sci. Technol.* **2000**, *34*, 2900. (c) Gingrich, S. E.; Diamond, M. L. *Environ. Sci. Technol.* **2001**, *35*, 4031.
- (282) Lam, B.; Diamond, M. L.; Simpson, A. J.; Makar, P. A.; Truong, J.; Hernandez-Martinez, N. A. *Atmos. Environ.* **2005**, *39*, 6578.
- (283) (a) Liu, Q. T.; Chen, R.; McCarry, B. E.; Diamond, M. L.; Bahavar, B. *Environ. Sci. Technol.* **2003**, *37*, 2340. (b) Simpson, A. J.; Lam, B.; Diamond, M. L.; Donaldson, D. J.; Lefebvre, B. A.; Moser, A.

Q.; Williams, A. J.; Larin, N. I.; Kvasha, M. P. *Chemosphere* **2006**, *63*, 142.

(284) (a) Favez, O.; Cachier, H.; Chabas, A.; Ausset, P.; Lefevre, R. *Atmos. Environ.* **2006**, *40*, 7192. (b) Ionescu, A.; Lefevre, R. A.; Chabas, A.; Lombardo, T.; Ausset, P.; Candau, Y.; Rosseman, L. *Sci. Total Environ.* **2006**, *369*, 246.

(285) Liu, Q. T.; Diamond, M. L.; Gingrich, S. E.; Ondov, J. M.; Maciejczyk, P.; Stern, G. A. *Environ. Pollut.* **2003**, *122*, 51.

(286) Baergen, A. M.; Donaldson, D. J. *Environ. Sci. Technol.* **2013**, *47*, 815.

(287) Butt, C. M.; Diamond, M. L.; Truong, J.; Ikononou, M. G.; Ter Schure, A. F. H. *Environ. Sci. Technol.* **2004**, *38*, 724.

(288) Wu, R. W.; Harner, T.; Diamond, M. L. *Atmos. Environ.* **2008**, *42*, 6131.

(289) Unger, M.; Gustafsson, O. *Atmos. Environ.* **2008**, *42*, 5550.

(290) Diamond, M. L.; Thibodeaux, L. J. In *Handbook of Chemical Mass Transport in the Environment*; Mackay, L. J. T. D., Ed.; CRC Press: Boca Raton, FL, 2011.

(291) (a) Wong, K. W.; Tsai, C.; Lefer, B.; Grossberg, N.; Stutz, J. *Atmos. Chem. Phys.* **2013**, *13*, 3587. (b) Wong, K. W.; Tsai, C.; Lefer, B.; Haman, C.; Grossberg, N.; Brune, W. H.; Ren, X.; Luke, W.; Stutz, J. *Atmos. Chem. Phys.* **2012**, *12*, 635.

(292) Michoud, V.; Colomb, A.; Borbon, A.; Miet, K.; Beekmann, M.; Camredon, M.; Aumont, B.; Perrier, S.; Zapf, P.; Siour, G.; Ait-Helal, W.; Afif, C.; Kukui, A.; Furger, M.; Dupont, J. C.; Haefelin, M.; Doussin, J. F. *Atmos. Chem. Phys.* **2014**, *14*, 2805.

(293) Spataro, F.; Ianniello, A.; Esposito, G.; Allegrini, I.; Zhu, T.; Hu, M. *Sci. Total Environ.* **2013**, *447*, 210.

(294) Handley, S. R.; Clifford, D.; Donaldson, D. J. *Environ. Sci. Technol.* **2007**, *41*, 3898.

(295) (a) Chabas, A.; Lombardo, T.; Cachier, H.; Pertuisot, M. H.; Oikonomou, K.; Falcone, R.; Verita, M.; Geotti-Bianchini, F. *Build. Environ.* **2008**, *43*, 2124. (b) Chabas, A.; Alfaro, S.; Lombardo, T.; Verney-Carron, A.; Da Silva, E.; Triquet, S.; Cachier, H.; Leroy, E. *Build. Environ.* **2014**, *79*, 57.

(296) Brigante, M.; Cazoir, D.; D'Anna, B.; George, C.; Donaldson, D. J. *J. Phys. Chem. A* **2008**, *112*, 9503.

(297) Cazoir, D.; Brigante, M.; Ammar, R.; D'Anna, B.; George, C. *J. Photochem. Photobiol., A: Chem.* **2014**, *273*, 23.

(298) Monge, M. E.; D'Anna, B.; George, C. *Geochim. Cosmochim. Acta* **2009**, *73*, A894.

(299) George, C.; Strekowski, R. S.; Kleffmann, J.; Stemmler, K.; Ammann, M. *Faraday Discuss.* **2005**, *130*, 195.

(300) Styler, S. A.; Loiseaux, M.-E.; Donaldson, D. J. *Atmos. Chem. Phys.* **2011**, *11*, 1243.

(301) Gligorovski, S.; Weschler, C. J. *Environ. Sci. Technol.* **2013**, *47*, 13905.

(302) Gómez Alvarez, E.; Amedro, D.; Afif, C.; Gligorovski, S.; Schoemacker, C.; Fittschen, C.; Doussin, J.-F.; Wortham, H. *Proc. Natl. Acad. Sci. U.S.A.* **2013**, *110*, 13294.

(303) Gómez Alvarez, E.; Sörgel, M.; Gligorovski, S.; Bassil, S.; Bartolomei, V.; Coulomb, B.; Zetzsch, C.; Wortham, H. *Atmos. Environ.* **2014**, *95*, 391.

(304) Shiraiwa, M.; Sosedova, Y.; Rouvière, A.; Yang, H.; Zhang, Y.; Abbatt, J. P. D.; Ammann, M.; Pöschl, U. *Nat. Chem.* **2011**, *3*, 291.